Technical Report Documentation Page

1. Report No.	2. Government Accession No.	3. Recipient's Catalog No.

4. Title and Subtitle	5. Report Date
Development of a Driver Model for Near/At-Limit Vehicle Handling	December 2001
	6. Performing Organization Code
	8. Performing Organization Report No.
7. Author(s)	UMTRI-2001-43
C. MacAdam	
9. Performing Organization Name and Address	10. Work Unit No. (TRAIS)
The University of Michigan Transportation Research Institute 2901 Baxter Road, Ann Arbor, Michigan 48109	11. Contract or Grant No. N001745
	13. Type of Report and Period Covered
12. Sponsoring Agency Name and Address	Final 6/1/00 - 11/30/01
General Motors Corporation Research and Development Center Warren, MI 48090-9055	14. Sponsoring Agency Code

15. Supplementary Notes

Technical Contacts: C. Liang, S. Chin, B. Lin, B. Repa

16. Abstract

The basic goal of this research was to develop a parametric driver model that can be used to help evaluate and predict representative driver/vehicle handling behavior at or near the limit of driving performance. The model includes provisions for representing a range of driver steering characteristics and vehicle dynamic properties so as to permit computer-based investigation of different combinations of vehicle chassis properties and driver abilities beyond the so-called "normal" driving regime. The focus of this initial stage of work was on driver-vehicle steering interactions under near-emergency or surprise conditions that can require substantial utilization of available tire/road friction. Accommodation of speed changes and alteration of vehicle dynamic properties with lateral and longitudinal acceleration operating conditions —within the driver model — is included in the model.

The nonlinear GM driver steering model developed under this work significantly extends analysis and predictive capabilities well into the nonlinear/near-limit handling regime of driver/vehicle systems.

In addition to the extended nonlinear performance, the development work has also added certain new model features that include variable driver preview, driver speed control preferences based on upcoming road curvature changes, sensory input processing of vehicle response signals, path selection/adjustment options, and a simplified situational awareness element.

17. Key Words	18. Distribution Statement
driver model, driver, nonlinear, vehicle, dynamics, steering, control, optimal, preview, human, path-following, modeling, limit, stability, directional, braking, path, handling	This document is available to the public through the National Technical Information Service, Springfield, VA 22161

19. Security Classif. (of this report)	20. Security Classif. (of this page)	21. No. of Pages	22. Price
None	None	120	

Development of a Driver Model for Near/At-Limit Vehicle Handling

Final Technical Report

UMTRI-2001-43

prepared for

The General Motors Corporation

by

The University of Michigan
Transportation Research Institute

C. MacAdam

December 2001

Acknowledgements

The author would like to acknowledge the helpful discussions and suggestions by a number of GM personnel that assisted in this work. These include members of the GM At/Near Limit Handling Driver Model Advisory Team and others listed below. Thanks to all.

Cwo Gee Liang (technical contact and project liaison)

Steve Chin

Bob Nisonger

Bill Lin

Brian Repa

Ian Lau

Narendra Kota

Ken Cameron

Elie Feit

Clark Robbins

Mark Hogle

blank page

Table of Contents

List of Figures

List of Tables

1.0 Introduction

This document constitutes the final technical report for the GM project entitled "Development of a Driver Model for Near/At-Limit Vehicle Handling" under UM Project No. DRDA 00-2040 and GM Purchase Order TCS78135 with the University of Michigan. The report contains a technical description and discussion of the work performed.

The basic goal of this research was to develop a parametric driver model that can be used to help evaluate and predict representative driver/vehicle handling behavior at or near the limit of driving performance. The model includes provisions for representing a range of driver steering characteristics and vehicle dynamic properties so as to permit computer-based investigation of different combinations of vehicle chassis properties and driver abilities beyond the so-called "normal" driving regime. The focus of this initial stage of work was on driver-vehicle steering interactions under near-emergency or surprise conditions that can require substantial utilization of available tire/road friction. Accommodation of speed changes and alteration of vehicle dynamic properties with lateral and longitudinal acceleration operating conditions —within the driver model — is included in the model.

As noted in the original proposal for this work, little, if any, experimental data covering closed-loop, driver/vehicle handling behavior under near-limit operating conditions exist in the technical literature. A key element of this work was therefore to gather such data by conducting driver/vehicle test maneuvers under these types of conditions. These resulting data would then be used to evaluate and pass ultimate judgment on the predictive capability and accuracy of the developed model. During the course of the project work it was determined by GM that full-scale road test data would not be available during this initial phase of work but that driving simulator test data provided by a third party would be substituted in its place.

The driving simulator tests were intended to cover a range of driver skill levels, tire/road friction conditions, and vehicle dynamic properties. The driver model validation process then utilized these data, in place of full-scale test track data, to validate and refine the driver model. The validation process included the identification of different sets of driver model parameters corresponding to the different simulator subjects.

The new GM driver model was based on a driver model previously developed and validated by UMTRI for primarily linear-range operating conditions. The GM model extends the basic characteristics of that initial modeling effort to nonlinear or near-limit operating conditions, while retaining the same important human-machine characteristics exhibited by the original linear model when operating under linear or "normal" driving conditions. In addition, the new model adds several new features not present in the original model such as variable driver preview, speed control, and various elements related to human factors concerns such as delays, filtering, and thresholding of input/output signals processed by the model.

Validation of the new model utilizes driving simulator data collected under this initial project work, but should not be considered necessarily complete, particularly for predicting actual driver/vehicle responses with real vehicles, absent more extensive validation efforts that utilize full-scale test track results or on-road driver/vehicle test data. Nevertheless, the simulator data collected under this initial phase does provide a helpful start towards this eventual goal.

Table 1-1 summarizes the basic features and differences between the initial UMTRI linear driver model and the new GM nonlinear driver model following completion of this project work. Each of the noted features is described more fully in Section 3. Section 4 further discusses the key differences noted in Table 1-1 and provides several example comparison runs between the new model and its linear predecessor. Section 5 and 6 address the simulator tests and the associated model validation effort. Section 7 provides conclusions and recommendations.

The report is organized by the following sections:

1.0 Introduction

2.0 Project Task Summary

3.0 Driver Model Description

4.0 New Features / Capabilities of the GM Driver Model

5.0 Driving Simulator Tests

6.0 Driver Model Validation

7.0 Conclusions and Recommendations

Table 1-1. Comparison of the Original UMTRI Linear Driver Model vs. the GM Nonlinear Driver Model Developed Under This Project.

Model Feature	*UMTRI Linear Model*	*GM Nonlinear Model*
Previewed Scene Input Options	• Path Table	• Path Table, or • Left & Right Road Boundaries
Sensory Limitations	• None	• Time Delay • Filtering • Noise Addition • Signal Limiter • Thresholding
Internal Vehicle Dynamics	• 2 Degree-of-Freedom Linear Model (lateral and yaw motions)	• 4 Degree-of-Freedom Nonlinear Model (lateral, longitudinal, yaw, and roll motions)
Prediction Capability	• Linear Transition Matrix	• Numerical Integration
Steering Control Calculation	• Closed-Form Analytical Expression Based on Linear Analysis	• Numerical Optimization / Minimization of an Arbitrary Performance Index
Driver Physiological and Ergonomic Constraints	• Transport Time Delay	• Transport Time Delay • Neuromuscular Filter • Noise Addition • Magnitude / Rate Limiter • Threshold • Hysteresis
Path Planning	• None	• Center-line Smoothing • "Racing Line" Approximation
Variable Preview	• None	• Min/Max Preview Setting • Rate Control
Speed Control	• None	• Desired Speed Setting • Maximum Lateral Acceleration Preference
Situational Awareness	• None	• Delay Parameter • Lateral Acceleration Threshold Trigger

2.0 Project Task Summary

The project work summarized below involved eight tasks undertaken over a period of eighteen months. The first half of project work was primarily focused on model development and initiation of the driver/vehicle simulator test activities. The latter half of the project was concerned primarily with processing portions of the collected test data, model validation/refinement, and product delivery/reporting to GM.

Task 1 Literature Review

A review of existing technical literature was conducted and a Task 1 Summary Report was delivered to GM in August of 2000 covering this work. The literature review noted the dramatic increase in driver model publications occurring over the last several decades, particularly in the area related to artificial intelligence methods in the last decade. Most approaches fall into one of three basic categories: 1) classical linear control approaches, 2) optimal control methods, and 3) AI approaches such as neural net, fuzzy logic, or genetic algorithm methodologies.

Specific areas or concepts receiving more recent attention were recognized to be: 1) path planning behavior of drivers, 2) multi-level control aspects of driving behavior, 3) driver response to nonlinear or altered vehicle dynamic characteristics of the controlled vehicle, and 4) attention to speed control behavior by drivers when approaching curves or obstacles so as to facilitate their successful negotiation.

Each of these topics was given special attention under this work and is reflected by different components contained within the delivered driver model.

Task 2 Evaluation and Selection of a Candidate Driver Model

Different driver modeling approaches identified under the Task 1 activities were examined in more detail regarding their suitability for meeting the goals of the project. Key factors considered included the potential ability of the model to mimic common driver characteristics and limitations. Example characteristics include use of look-ahead or preview sight information, known driver abilities to adapt to different vehicle dynamic properties at varying adaptation rates, compensatory abilities of drivers to alter preview utilization, and anticipatory abilities based upon upcoming road geometry or path requirements. Example limitations included items such as basic driver reaction time delays, neuro-muscular dynamic lags, and corresponding frequency response characteristics.

The selection of a particular model as a starting point was made on the basis of (a) desirable features and fidelity present in the candidate model, (b) its likely ability to be further modified and extended under this proposed work, (c) its ultimate ease of use and capacity for being understood by the end-user, and (d) the level of effort required to adapt it to the new requirements and goals of this project. Based upon these considerations, an existing and widely used UMTRI driver model utilizing a linear preview control strategy was selected as the basis and starting point for the GM driver modeling work under this

project. Extension of the model to nonlinear operating conditions and addition of numerous features related to human factors issues (driver sensory delays, frequency response characteristics, rate limiting, etc.), as well as speed control, path planning, and variable preview modules were then undertaken during Task 3.

Task 3 Modification and Adaptation of the Selected Driver Model for Nonlinear Handling Conditions

The UMTRI linear driver model identified under Task 2 was modified and extended under this task work. The purpose of these modifications was to equip the model with new features and capabilities. Modifications included: 1) extension of the *internal vehicle model* (used by the driver model for predicting future path responses) to a form more applicable for the nonlinear operating regime, 2) additional degrees of freedom for roll motion and forward speed, 3) addition of adjustable on-the-fly preview capabilities, 4) provisions for time delays, frequency response characteristics, and signal limiting within a sensory input module receiving vehicle response information from the external controlled vehicle model, 5) neuromuscular filtering, time delay, and signal limiting treatment of the driver steering response output, 6) addition of a speed control feature for facilitating the negotiation of upcoming curves or obstacles, 7) extension of previewed path input information to permit variable levels of smoothing to approximate simple path selection strategies used by drivers, and 8) addition of a simplified situational awareness delay feature. The extended features allow for separate control and specification of the internal vehicle dynamics model parameters so as to allow "de-tuning" of the internal vehicle model away from the external vehicle model if desired. This latter detail can be used to study the effects of driver unfamiliarity or poor adaptation to different vehicles or operating conditions. (The original UMTRI driver model adopts a simple linear approximation of the external controlled vehicle as its reference vehicle for all drivers.)

The block diagram of Figure 2-1 shows the various components implemented in the GM driver model and the overall relationship to the external vehicle model (e.g., GM's VehSim or some other vehicle dynamics model). In this diagram, the block labeled "Internal Vehicle Dynamics" contains a simplified, though nonlinear, representation of the more complex external vehicle model labeled, "External Vehicle Simulation Program." Each of these blocks is described in more detail in the next Section 3.0.

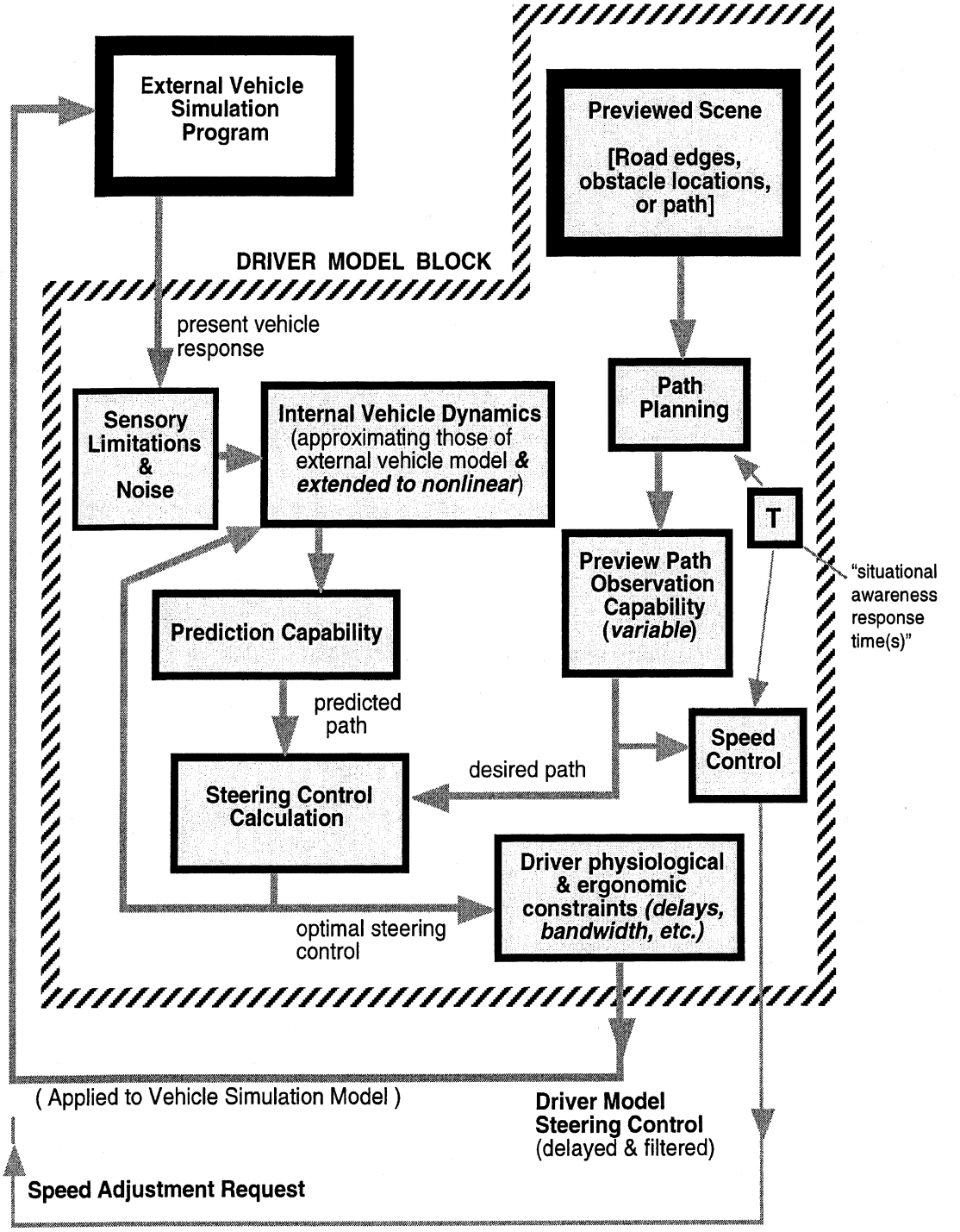

Figure 2-1. GM Driver Model Block Diagram.

Task 4 Driver/Vehicle Simulator Tests

Under Task 4, a variety of closed-loop handling tests were conducted with a third party driving simulator to provide data with which to validate the proposed driver model. A test matrix of handling maneuvers was executed to cover a representative range of three basic factors: a) driver skill level, b) vehicle dynamic properties (GVW and LVW

configurations), and c) operating conditions as represented by wet and dry surface friction conditions. Driver skill levels were initially categorized as 1) novice, 2) typical, and 3) expert. A 3/4 ton pickup served as the basic vehicle platform.

Test maneuvers included 1) a modified version of the ISO double lane-change maneuver ("moose test"), 2) a slalom course with non-uniform longitudinal cone placements, 3) a lane-change along a curve maneuver, and 4) a series of surprise obstacle avoidance maneuvers initiated by falling poles that required the driver to steer into adjacent lanes. Twelve test subjects took part in the tests and included two novice drivers (ages 15 and 16), four expert drivers (two of which were from GM), and 6 typical drivers. The driver ages ranged from 15 to 67. At the conclusion of simulator testing, data was delivered to GM and UMTRI in computer files that contained pertinent time histories for each simulator run.

Task 5 Analysis and Interpretation of the Driving Simulator Test Results

Under this task, the simulator test data were initially processed by UMTRI to obtain general information on overall average speed of travel and overall average cone strike performance for each driver. Test speeds and cone strikes for each maneuver were cumulatively averaged over each driver to obtain an approximate overall rating of driver skill represented by a combination of average cone strike activity and overall average test speed covering all test conditions/maneuvers. An initial plot of these results was then made to summarize the range of average travel speed and average cone strike performance (steering accuracy) for each of the twelve test drivers.

Figure 2-2 shows this plot with each driver designated with subject identification numbers and their respective skill level. In general, the plot shows a reasonable trend and grouping of expected and actual skill levels versus associated travel speeds. The highest skill level region on this plot is in the upper left corner where higher speeds and lower cone strike activity occurs. Correspondingly, the lowest skill level region is in the lower right corner where lower speeds and greater cone strike activity combine. Five simple clusters of overall skill are designated on the plot indicated by the ellipsoid regions and descriptive tags.

It should be noted that the indicated rankings here correspond to overall average performance and do not necessarily reflect individual achievement in every maneuver. That is, a particular test subject may have outperformed another test subject in three of the four tests by a small margin, but performed significantly poorer in the one remaining maneuver, thereby placing slightly lower in the overall ranking. Further discussion of these data and the associated model validation activities are contained in Sections 5 and 6.

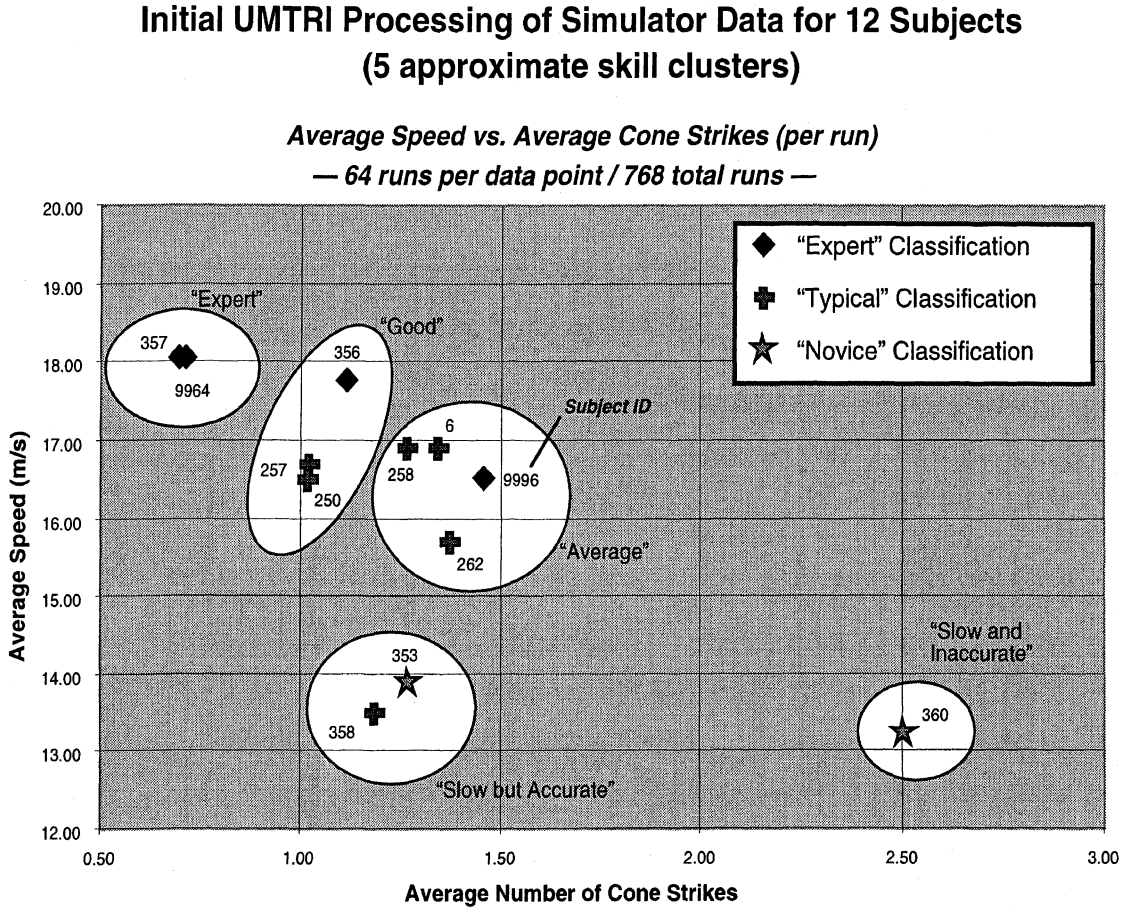

Figure 2-2. Speed vs. Cone Strike Plot for All Simulator Test Drivers.

Task 6 Refinement and Validation of the Model Using the Simulator Test Data

Under this task, direct comparisons were made between data from four of the twelve test subjects and predictions from the driver model. Two of the principal driver model parameters were adjusted by trial and error to obtain a reasonable matching to the key time history responses provided by the simulator test results. These comparisons appear in Section 6 and are discussed there in detail. In most cases, suitable representations were found using different values of the driver model *preview* ("look-ahead") parameter and the *transport delay* parameter.

An observation from this initial validation effort is that driver preview times and driver transport delays (Sections 3 and 6) appear to be correlated to some extent in most of these data. The analysis suggests that, for at least these four test subjects and regardless of skill level, an increased transport delay is associated with an increased preview time in order to successfully complete a particular test maneuver near the limit operating condition. The driver model parameters corresponding to these different validation runs seem to suggest an alignment of "preferred" closed-loop damping as discussed further in Section 6.

Previous validation work using the linear UMTRI predecessor driver model indicates a similar trend between driver preview time utilization and driver transport delay, but under more normal lower lateral acceleration operating conditions [1, 2, 3]. Additional

processing of other test subject data from the GM pool of data, as well as collection of similar test data from full-scale road test conditions, can help to further clarify these initial observations.

Task 7 Computer Model Implementation and Delivery to GM

The final version of the model was coded and implemented as a computer program for further applications. Technical details of the computer model appear in the next Section 3.

Task 8 Final Technical Report

This technical report constitutes the final report document for the project work.

3.0 Driver Model Description

This section of the report provides a technical description of the driver model components. The diagram in Figure 3-1 shows the overall content of the model with each block element numbered 1 to 10 for subsequent reference. More detailed information on each of the block elements is provided in the sub-sections that follow. The sub-section numbering seen below corresponds to the numbered blocks appearing in Figure 3-1.

Section **Topic**

3.1 - *Previewed Scene* - desired path or road input description

3.2 - *Sensory Limitations & Noise* - pertaining to incoming vehicle response signals

3.3 - *Internal Vehicle Dynamics*

3.4 - *Prediction Capability*

3.5 - *Steering Control Calculation*

3.6 - *Driver Physiological & Ergonomic Constraints* - associated with driver steering (output) control responses

3.7 - *Path Planning options* (center-line smoothing, or minimum curvature path)

3.8 - *Variable Driver Preview Capability* - based on upcoming vehicle-boundary constraints and projected interferences

3.9 - *Driver Speed Control* for accommodating upcoming lateral path requirements and estimated lateral acceleration demands

and

3.10 - *Situational Awareness Parameter(s)* – a simple delay that only affects the path input channel and only during the initial portion of a maneuver

A double lane-change "moose course" test maneuver is used to help illustrate the influence of different parameter settings in an example run in sub-section 3.11. ISO coordinates and metric measurement units are used in the examples and elsewhere in the report.

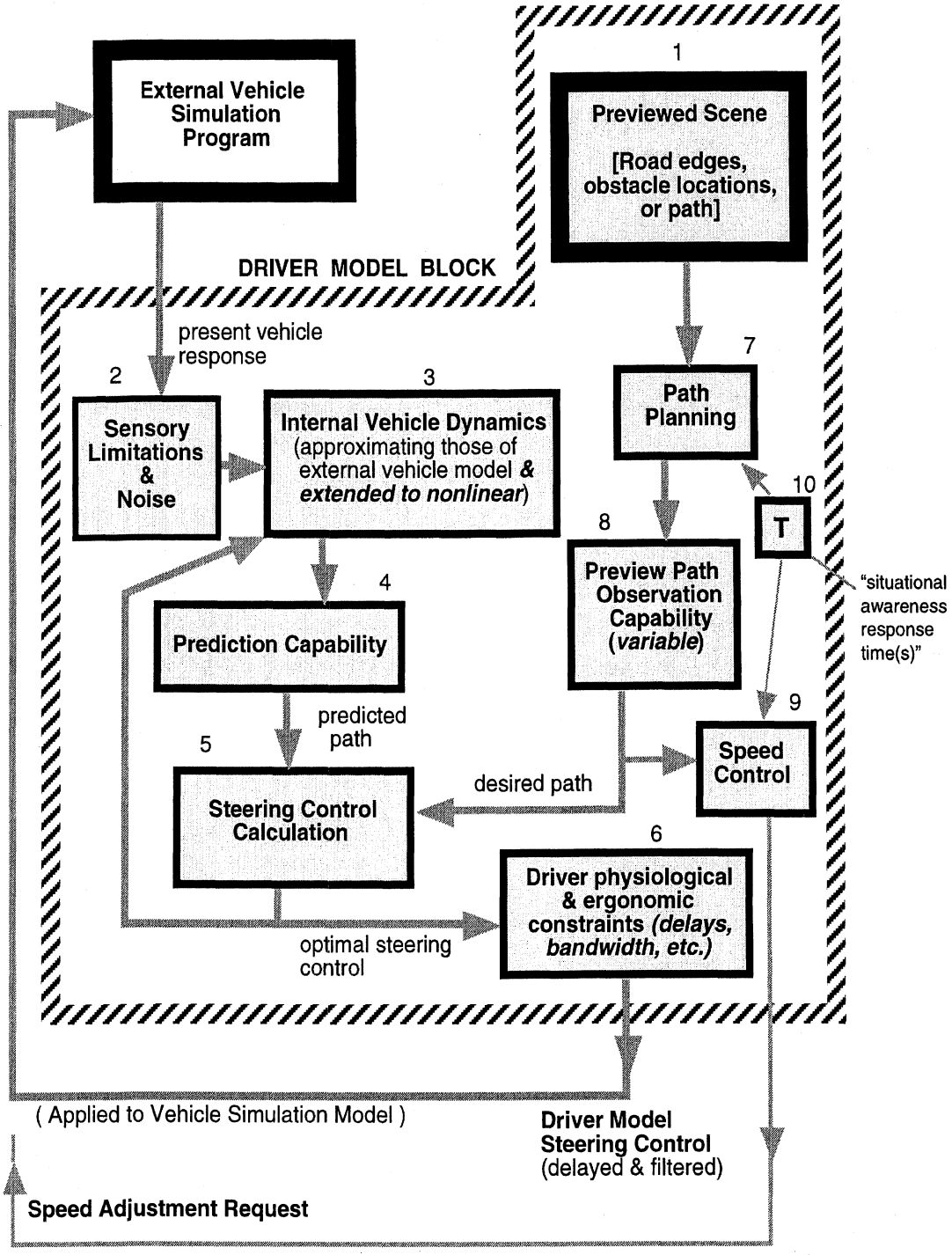

Figure 3-1. GM Driver Model with Reference Numbers for Each Element.

The following sections contain more detailed information on the feature elements of the driver model seen in the block diagram of Figure 3-1. Each topic is discussed in sequence and includes example diagrams for clarification.

3.1 Previewed Scene Element (desired path to follow) —

This model element allows the user to describe the desired path information in one of two forms. The user can define either (a) a set of x-y coordinate pairs describing a desired path trajectory to follow, or (b) a set of left and right road boundaries, as input. In the first case, specification of the desired path itself causes the model to internally generate a set of left and right boundary lane boundaries (default width: 3.7 meters) parallel to the desired path input. (As described later, the left and right road boundaries can be used by other model features to automatically adjust preview time or select minimum curvature paths through a designated course.) In the second option, entry of the left and right road boundaries, the model will internally generate the center-line of those two boundaries as the desired path to follow. In either case, the model will always have available internally a center line path and a corresponding set of left and right boundaries.

The center-line path obtained here can then be further modified by the *Path Planning* options available in the model and described in Section 3.7.

An example of the input path for the "moose test" double lane-change maneuver is seen in the following Table 3.1-1. The first line in the table is the number of left and right x-y pairs that immediately follow. (A negative entry for this number indicates left and right boundary information in the table; a positive value indicates the desired path itself.) The integer indicating the number of table lines is then followed by the table itself. The first two columns in this example are the x-y *left* boundary coordinates; the next two columns correspond to the *right* boundary. All coordinates are with respect to the vehicle inertial coordinate system.

If entry of just the path itself is desired, only one set of coordinate pairs corresponding to the desired center-line path itself would be entered, preceded by a positive integer indicating the number of x-y pairs that follow,

In either case of ***Previewed Scene*** data entered by the user, the model will always sub-sample this information to a finer fixed spacing interval of 1 meter. The higher resolution (1 meter spacing) boundaries and paths are then used *internally* by the model for all of its path-related calculations.

Table 3.1-1. Example of Left and Right Boundary Inputs for the "Moose Test."

```
-6     # of lines in following path/boundary table, <0 => L/R boundaries
0.00   1.35   0.00   -1.35
62.0   1.35   62.0   -1.35
89.0   5.30   89.0   2.02
100.0  5.30   100.0  2.02
125.0  1.35   125.0  -2.0
300.0  1.35   300.0  -2.0
```

Figure 3.1-2 shows a portion of the data from Table 3.1-1, along with the center-line path derived from the left and right boundaries. The derived center-line, or a smoothed version of it (see below under **Section 3.7 / *Path Planning***), is then used as the path to follow by the driver model steering control calculation.

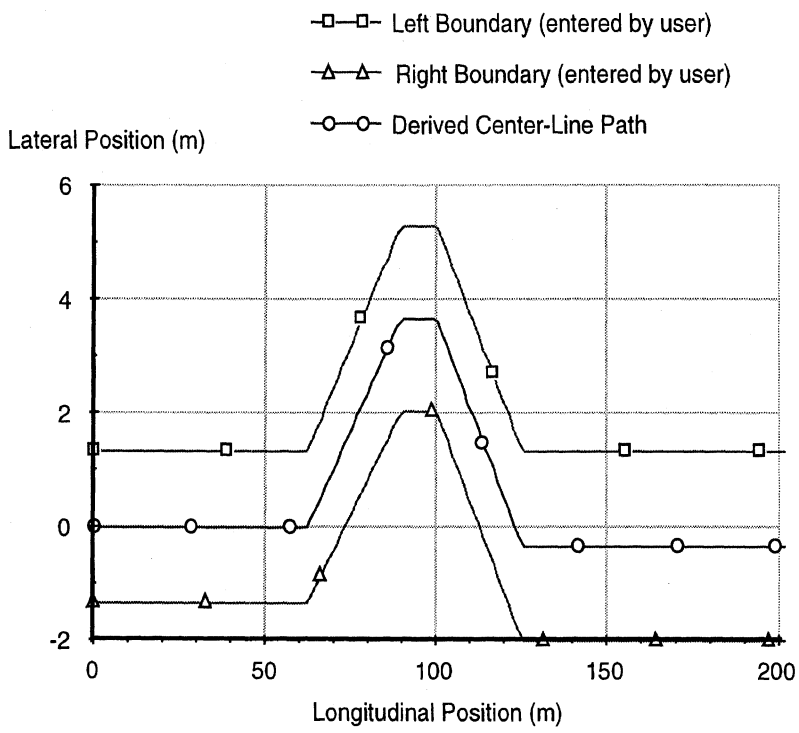

Figure 3.1-2. Moose Course Corresponding to Table 3.1-1 Entered Data.

3.2 Sensory Limitations & Noise —

This driver model element processes vehicle response information from the externally controlled vehicle. Its purpose is to provide a means by which the driver model can account for sensory delays, filtering, and signal limiting mechanisms that a user might wish to activate or study. In many cases, the features within this element might not be desired and so the vehicle response signals from the external model are then passed through to the driver model without modification. The default values within the driver model data files are set to that condition, but can be overridden by the user as described below.

The *Sensory Limitations & Noise* block contains a number of sub-elements that process vehicle response signals assumed to be sensed by the driver model for steering and speed control purposes. Theses signals include lateral acceleration plus the following vehicle states:

- lateral vehicle position
- vehicle heading angle
- vehicle lateral speed (sideslip velocity)
- vehicle roll angle
- longitudinal vehicle position
- vehicle forward speed
- vehicle yaw rate
- vehicle roll rate

Each of these signals can be independently processed by any or all of the following sub-elements, also depicted in Figure 3.2-1 and in the order shown below from 1 to 5:

- random noise addition
- signal threshold (below which the |signal| is assumed to be zero)
- signal amplitude limit (above which the |signal| saturates)
- a transport time delay
- first order filter specifications (gain and filter break-point frequency)

Each input signal has its own such data set and file for specifying the input processing associated with that channel. Certain parameter settings may essentially pass the input signals through un-touched (large limit value, large break-point, and small delay and noise specifications). However, in cases where human factor interests might wish to examine perceptual sensitivity issues related to driver-vehicle (or driving simulator) transmission delays or signal fidelity, these parameters and associated elements can provide this basic capability.

The eight vehicle response input signals (listed above) processed by this element are then passed to the *Internal Vehicle Dynamics* block (Section 3.3) as indicated in the overall block diagram of Figure 3-1. The vehicle response signals are then used as "initial conditions" by the *Internal Vehicle Dynamics* block and the *Prediction Capability* block (Section 3.4) to estimate the future vehicle path response over the current preview interval.

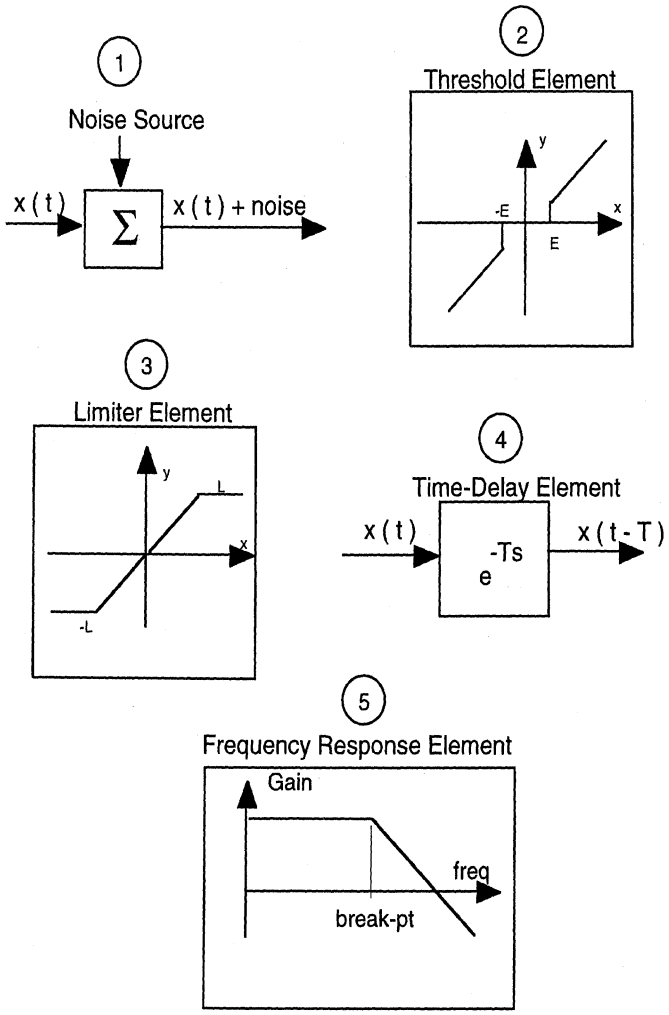

Figure 3.2-1. Signal Processing Elements for the Sensory Limitations & Noise Block.

3.3 Internal Vehicle Dynamics —

The driver model assumes that an actual driver has a basic "internal understanding" of the input/output relationship between steering and the expected vehicle response. This assumed capability allows drivers to predict with varying accuracy, depending on skill level and experience, how the vehicle will likely respond to steering inputs over any upcoming preview interval. In order to represent this assumed capability by drivers, the driver model incorporates an *internal* vehicle dynamics model that approximates the behavior of the externally controlled vehicle. By projecting forward the response of this internal model over the preview interval, an estimate of where and how the controlled vehicle will respond can be made by the driver model at any instant of time, given the current initial conditions of the external vehicle. These initial conditions are provided, as noted above in Section 3.2, by the output of the *Sensory Limitations and Noise* block.

Different levels of assumed driver skill and familiarity with the controlled vehicle can also be represented by "de-tuning" or modifying the internal vehicle model away from an accurate characterization of the external vehicle.

The internal vehicle model used by the driver model has four degrees of freedom that include longitudinal and lateral displacement as well as yaw and roll angular rotations. Figure 3.3-1 shows a simple diagram of the internal model.

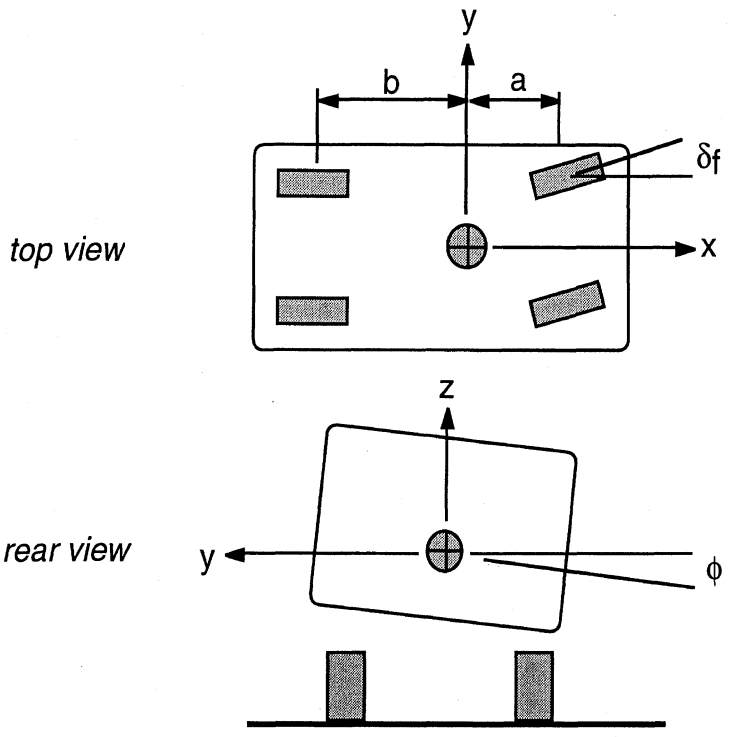

Figure 3.3-1. Four Degree of Freedom Internal Vehicle Model.

The dynamic equations for this model are given by,

$$
\begin{aligned}
&\dot{x} = u\cos\psi - v\sin\psi \\
&\dot{y} = v\cos\psi + u\sin\psi \\
&m\dot{v} = (Fy_{LF} + Fy_{RF})\cos(\delta_f) + (Fy_{LR} + Fy_{RR})\cos(\delta_r) - m \cdot u \cdot r \\
&I_z\dot{r} = a(Fy_{LF} + Fy_{RF})\cos(\delta_f) - b(Fy_{LR} + Fy_{RR})\cos(\delta_r) \\
&\dot{\psi} = r \\
&m\dot{u} = -(Fy_{LF} + Fy_{RF})\sin(\delta_f) - (Fy_{LR} + Fy_{RR})\sin(\delta_r) + m \cdot v \cdot r \\
&I_x\dot{p} = -cp - K_x\phi + ha_y mg = ha_y mg + (Fz_{LF} - Fz_{RF})\frac{t_f}{2} + (Fz_{LR} - Fz_{RR})\frac{t_r}{2} \\
&\dot{\phi} = p
\end{aligned}
\qquad (1)
$$

where,

x	is the longitudinal displacement of the vehicle mass center (inertial)
y	is the lateral displacement of the vehicle mass center (inertial)
v	is the vehicle sideslip velocity at the mass center (body axis))
u	is the forward speed component of the mass center (body axis)
r	is the vehicle yaw rate
ψ	is the heading (yaw) angle of the vehicle
p	is the roll rate
ϕ	is the vehicle roll angle
Fy_{LF}	is the left front tire lateral force
Fy_{RF}	is the right front tire lateral force
Fy_{LR}	is the left rear tire lateral force
Fy_{RR}	is the right rear tire lateral force
Fz_{LF}	is the left front tire vertical load
Fz_{RF}	is the right front tire vertical load
Fz_{LR}	is the left rear tire vertical load
Fz_{RR}	is the right rear tire vertical load
g	is the gravitational constant (9.8 m/s/s)

and

$a_y = \dot{v} + ur = (Fy_{LF} + Fy_{RF} + Fy_{LR} + Fy_{RR})/m$, or lateral acceleration.

The internal vehicle model parameters include,

a	the distance from the mass center to the front wheels
b	the distance from the mass center to the rear wheels
m	the vehicle mass
I_z	the vehicle yaw inertia
I_x	the vehicle roll inertia
c	the combined/lumped suspension and tire roll damping
K_x	the combined/lumped suspension and tire roll stiffness
h	the mass center height above ground

The tire model equations that generate the lateral tire forces, Fy, are given by,

$$Fy = \mu_y Fz \cdot tirefactor$$
$$\mu_y = -\tanh(\alpha')\mu_p(1 + k_z \Delta Fz)(1 + k_v \Delta V) \qquad (2)$$
$$\alpha' = 2\alpha/\alpha_{max}$$

where,

Fy	is the lateral tire force
Fz	is the vertical tire force
μ_y	is the normalized lateral force or friction
α	is the tire sideslip angle
ΔFz	is the variation in tire vertical load away from a nominal load, Fz_0
ΔV	is the variation in tire speed away from a nominal speed, V_0
tirefactor	is a scaling factor (normally 1.0) that allows tire force information to be passed to the driver model about the state of individual tire forces

and the tire model parameters include,

α_{max}	parameter affecting the rate of tire force build-up with tire sideslip angle
μ_p	the peak lateral tire/surface friction
k_z	vertical load sensitivity
k_v	speed sensitivity
Fz_0	nominal vertical tire load
V_0	nominal speed

The front and rear tire sideslip angles, α_f and α_r, are given by

$$\alpha_f = \tan^{-1}(v + a \cdot r)/u) - \delta_f$$
$$\alpha_r = \tan^{-1}(v - b \cdot r)/u) - \delta_r \qquad (3)$$

where,

δ_f is the front wheel steer angle
δ_r is the rear wheel steer angle = 0

and,

$$\delta_f = \delta_{DM} - \text{compliance}_f \cdot a_y + K_{\phi f} \cdot \phi$$
$$\delta_r = 0 - \text{compliance}_r \cdot a_y + K_{\phi r} \cdot \phi \qquad (4)$$

where,

δ_{DM}	is the front wheel steer angle calculated by the driver model
compliance_f	is the front steer compliance (to a_y)
compliance_r	is the rear steer compliance (to a_y)
a_y	is the vehicle lateral acceleration
$K_{\phi f}$	is the front roll steer
$K_{\phi r}$	is the rear roll steer

An example plot of lateral tire forces produced by the tire model is seen in Figure 3.3-2 corresponding to the model parameters given in Table 3.3-1.

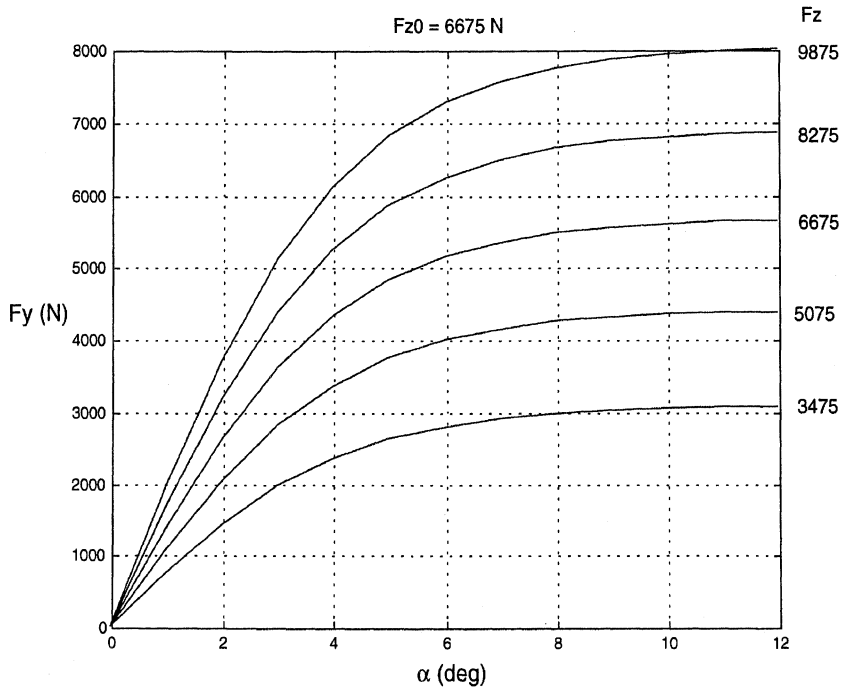

Figure 3.3-2. Example Tire Model Calculation.

Table 3.3-1. Tire Model Parameters Used in Figure 3.3-1.

α_{max}	=	8	degrees
μ_p	=	0.85	(-)
k_z	=	-0.0000135	(1/N)
k_v	=	0.0	(sec/m)
F_{z0}	=	6675	(N)
V_0	=	20	(m/s)

The front and rear vertical tire loads are determined from the quasi-static equations for roll moment and force equilibrium,

$$\begin{aligned}
&(Fz_{L_F} - Fz_{R_F})\frac{t_f}{2} + (Fz_{L_R} - Fz_{R_R})\frac{t_r}{2} = -K_r\phi - c\dot{\phi} \\
&Fz_{L_F} + Fz_{R_F} + Fz_{L_R} + Fz_{R_R} = W \\
&Fz_{L_F} + Fz_{R_F} = \frac{b}{L}W \\
&(Fz_{L_F} - Fz_{R_F})t_f = \eta(Fz_{L_R} - Fz_{R_R})t_r
\end{aligned} \tag{5a}$$

or,

$$\begin{bmatrix} t_f/2 & -t_f/2 & t_r/2 & -t_r/2 \\ 1 & 1 & 1 & 1 \\ 1 & 1 & 0 & 0 \\ t_f & -t_f & -\eta \cdot t_r & \eta \cdot t_r \end{bmatrix} \begin{Bmatrix} Fz_{L_F} \\ Fz_{R_F} \\ Fz_{L_R} \\ Fz_{R_R} \end{Bmatrix} = \begin{Bmatrix} -K_r - c\dot{\varphi} \\ W \\ \frac{b}{L}W \\ 0 \end{Bmatrix} \tag{5b}$$

where,

t_f	is the front wheel track distance
t_r	is the rear wheel track distance
K_r	is the lumped roll stiffness
c	is the lumped roll damping
W	is the vehicle weight
L	is the vehicle wheelbase = (a+b)
η	is the ratio of front-to-rear roll stiffnesses

The above matrix equation is then solved at each time step to obtain the four vertical tire loads used in the above tire force equations. Logical checks are included in the code to handle wheel lift-off conditions.

Communication Between the External Vehicle Model and the Driver Model

When the driver model is called from the main external vehicle model, each of the above tire and vehicle parameters is passed in as an element of an argument array in the driver model function. The program user can therefore control the characteristics of the internal vehicle model used by the driver model through values assigned to these parameters. By assigning values that reasonably approximate the properties of the external vehicle, the driver is assumed to have an accurate understanding of the dynamics of the external vehicle. By de-tuning or providing less accurate vehicle and tire information in this array argument, the driver model is characterized as having a poorer understanding of the directional control properties of the external vehicle. This therefore provides the

program user strong control over the "nature" of the driver model's internal vehicle properties. However, it also places some responsibility on the user insofar as requiring a basic familiarity with how these different parameters can affect the driver model steering response.

As an example, a sudden change in road friction (high mu to low mu occurring in the main vehicle model VehSim) may or may not be updated/communicated to the driver model in the parameter array as it occurs, depending on whether or not the program user wishes to represent the driver as having knowledge of the change in surface friction. By passing the same high friction tire model data continuously to the driver model, even after the low friction condition is encountered in VehSim, the user can represent an assumed driver who does not recognize or adapt to the surface friction change and thereby steers as though a high friction condition prevailed. In order to represent a driver who quickly recognizes the surface friction change and adapts accordingly, the model user can pass to the driver model tire data parameters that properly reflect the tire performance under the changed low mu condition.

Related examples can include the study of a sudden loss of tire pressure and the ensuing change in directional dynamics and whether or not that modification of directional dynamics is assumed to be sensed by the driver. In that case, tire properties associated with one of the tires would be altered during the course of a maneuver on the external vehicle model and then updated or not in the information passed to the driver model depending, as above, on the assumed adaptive capabilities of the driver. Examples such as these two appear in Section 4.

3.4 Prediction Capability —

This model element is used by the *Steering Control Calculation* to project forward the predicted response of the vehicle over the current preview time interval. It essentially amounts to a simple Euler numerical integration of the internal vehicle model's response from the current time, t, to an end time, t+T, where T is the driver preview time. The "initial condition" for the start of the integration is provided by the external vehicle model state information passed into the driver model as an argument array. As noted in Section 3.3, the state information for the internal vehicle model is comprised of 4 motion variables and their first derivatives. Integrations are performed at each driver model update time, typically at 0.01 or 0.02 second intervals.

3.5 Steering Control Calculation —

The basic goal of the steering control calculation itself is to minimize a performance index, J — largely dominated by preview path error terms — over the upcoming preview interval. See Figure 3.5-1. The path error terms appearing in the performance index represent differences between a desired path (input specification) and a projected vehicle path over the preview interval (Section 3.4 *Prediction Capability*), given the current dynamic state of the vehicle. The performance index, J, is then formed using the summation of the previewed path error quadratic terms seen in Figure 3.5-1. Minimization

of this performance index occurs at each driver model update interval, typically every 0.01 or 0.02 seconds during a simulation run.

The principal calculation involves identifying the optimal steering control value that will minimize the performance index over the current preview interval, given the "initial" condition (or state of the vehicle) at the current time. The "initial conditions" are provided to the *Internal Vehicle Dynamics* component by the *Sensory Limitations & Noise* processing element. The preview time is specified as either fixed, or allowed to automatically vary (Section 3.8), depending on the option selected by the user.

Prior work [2, 3, 4] with the linear model that uses this same basic concept has indicated good correlation with measured driver steering responses during routine driving maneuvers occurring largely in the linear driving regime. Since the current GM work involves extension of this approach to the nonlinear driver/vehicle operating regime, a numerical optimization approach is now necessary for identifying the optimal steering control. That is, in place of a closed-form analytical solution that can be used for the linear problem, a nonlinear numerical optimization method is instead required due to the non-linear/non-stationary tire and vehicle properties present in the nonlinear case.

The nonlinear numerical method, implemented in the computer model, involves calculating predicted responses of the vehicle (using the internal nonlinear model of the vehicle *within* the driver model itself) for estimating how the actual (external) vehicle will respond over the upcoming preview interval. This projected vehicle response estimation process occurs at each driver model time step and includes several vehicle response projections in order to obtain a field of predicted vehicle paths.

At each driver model update interval three numerical integrations are performed. The first integration corresponds to the predicted response using the fixed driver steering control value obtained from the last time step. The two additional integrations are performed with steering control values now incremented and decremented by a small amount from the value used in the first integration. These three integrations provide a field of trajectory response information about the current vehicle operating condition, corresponding to three steer input perturbations. Mean squared differences between each of these candidate paths and the desired input path are then fit with a quadratic curve from which the optimal steer value for that set of operating conditions is identified.

The optimal steer value obtained from this calculation is then passed to the *Driver Physiological & Ergonomic Constraints* block (Section 3.6) for filtering and transport time delay processing. This process is repeated at each driver model update interval of the simulation.

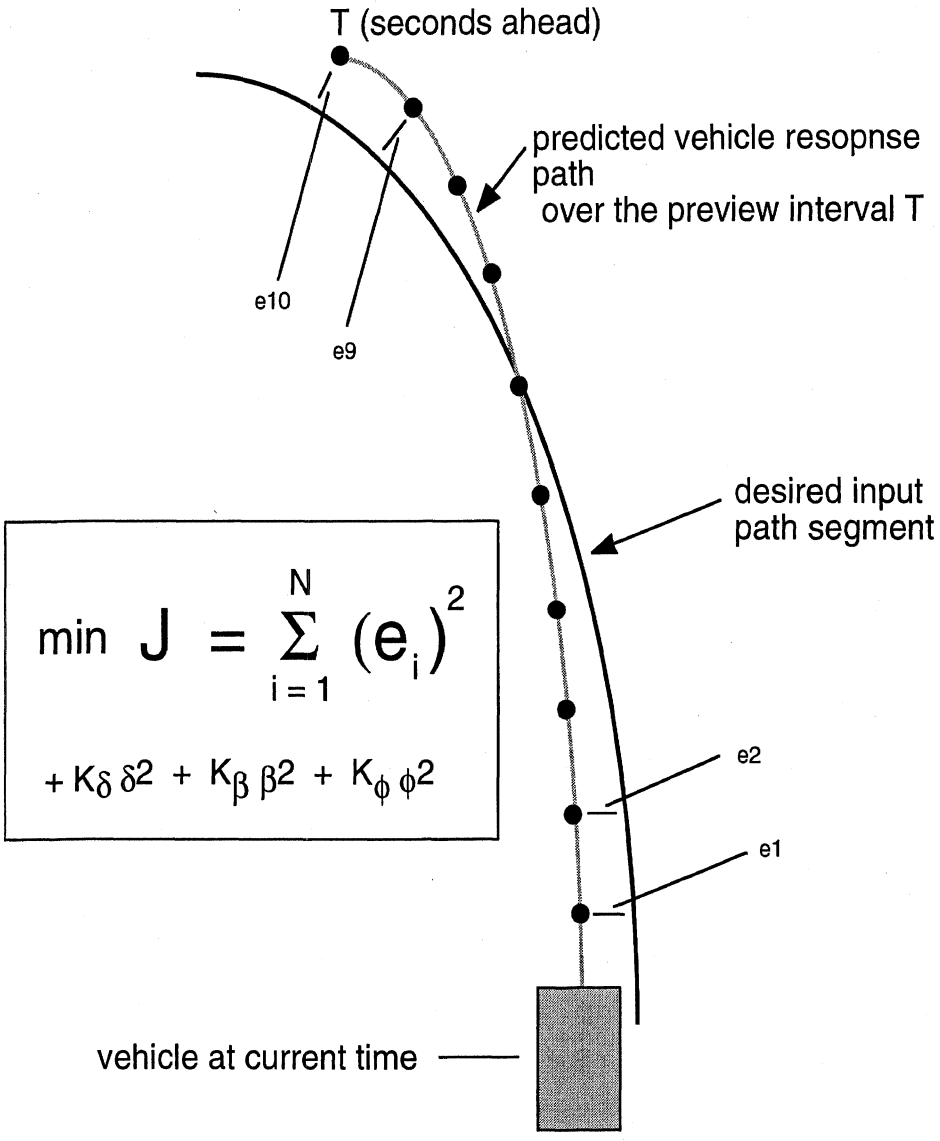

Figure 3.5-1. Preview Path Errors (e1, e2, ... e10) Minimized by Selection of an Optimal Steering Control Over the Upcoming Preview Interval, T.

Despite different implementations, the basic goal of the driver model — minimization of previewed path errors — is still present in the nonlinear formulation and, in fact, replicates the predicted linear model responses when the vehicle operates under identical linear driving regime conditions. This is, of course, desirable since the original model exhibits basic "cross-over model" traits present in most human/machine and driver/vehicle experimental data measured under these more common operating conditions [2, 3, 5, 6, 7].

Although the nonlinear calculation process may seem numerically intensive, the internal vehicle model calculation can utilize a fairly coarse time grid (typically 0.01 or 0.02 seconds) and is only projecting forward over the current preview interval, which in many cases may be less than one or two seconds. Current running time on a conventional

desktop workstation (500MHz PowerMac G4) is routinely several times faster than real time, depending on the specific options selected.

Future refinements of this calculation will allow for the program user to also include vehicle sideslip and/or roll angle terms in the performance index in order to help represent steering behavior related to a driver's aversion to large vehicle sideslip or roll responses under near-limit operating conditions. (That is, simulation of potential counter-steering or similar behavior by the driver in order to avert a vehicle roll-over or spin-out response that may be triggered by an emergency path-following or obstacle avoidance maneuver.) Roll angle and sideslip terms are shown present in the performance index of Figure 5.3-1, but are currently set to zero. Special simulator or on-road experiments are likely needed in order to obtain reliable settings for these parameters. A nonlinear threshold (or shaping function) feature should also be implemented with these types of terms in order to emphasize or weight roll and sideslip responses according to their magnitudes.

3.6 Driver Physiological & Ergonomic Constraints —

Once the optimal steer value is calculated, it is passed to the *Driver Physiological & Ergonomic Constraints* block. This element contains a set of sub-elements for processing this signal, similar to those contained in the *Sensory Limitations & Noise* block. The most important of these elements is the transport time delay, particularly for representing basic human steering control behavior. The processed steering control output from this block is returned to the external vehicle dynamics block (e.g., VehSim or other GM vehicle model) as the final output from the driver model and used to steer the external vehicle model.

The optimal steering control can be processed by any or all of the following sub-elements contained in the *Driver Physiological & Ergonomic Constraints* block. These are also shown in Figure 3.6-1. The order of operations is listed below and also by the numbered blocks seen in Figure 3.6-1.

- a transport time delay, T, applied to the optimal steer time history output
- steering hysteresis element (below which the |steer| is assumed to hold the +/- threshold value, E)
- threshold, E (below which the |steer| is assumed to be zero)
- random noise addition (remnant or other "noise" generated by the driver)
- first order filter specifications (gain and filter break-point frequency for steer output)
- steer rate limit, L (above which the |steering rate| saturates)
- steer amplitude limit, L (above which the |steer| saturates)

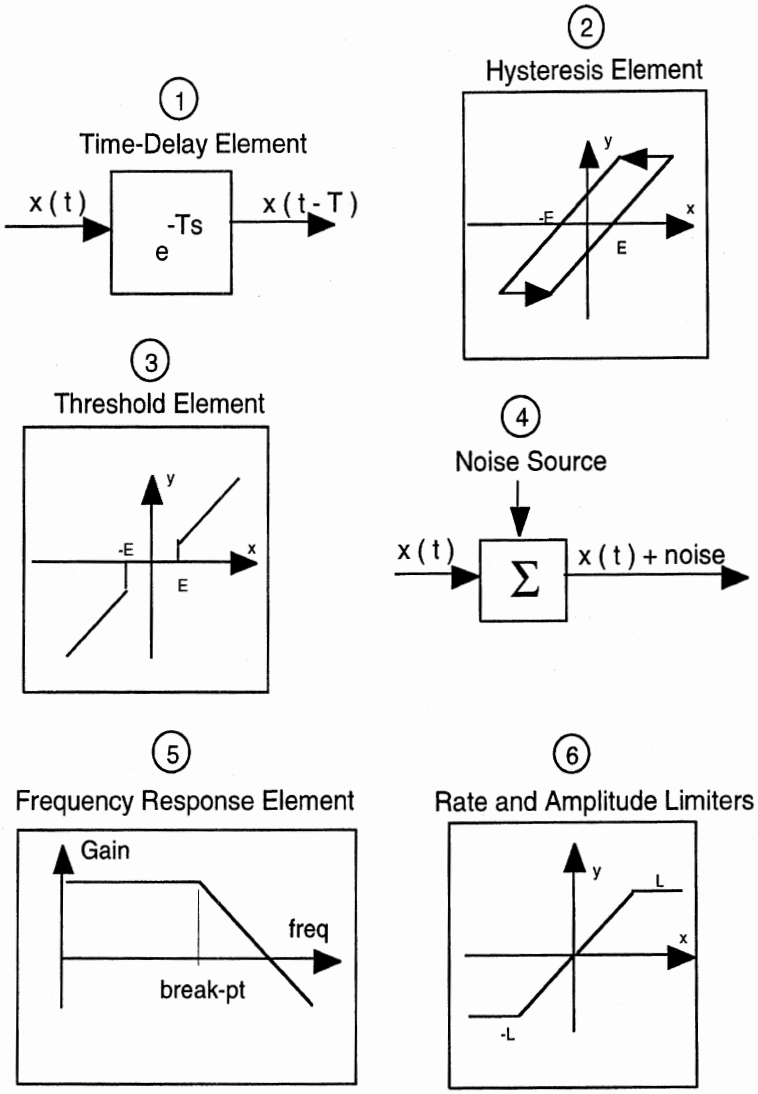

Figure 3.6-1. Processing Elements for the Driver Physiological & Ergonomic Constraints Block.

An example set of parameters for the *Physiological & Ergonomic Constraints* block is seen below in Table 3.6-1.

Table 3.6-1. Parameter Listing for the *Physiological & Ergonomic Constraints* Block.

0.10	Transport Delay	(sec)
0.00	Steer Noise	(rad)
0.00	Steer Hysteresis	(rad)
0.00	Steer Threshold	(rad)
1.0	Steer Gain	(-)
60.0	Steer Breakpoint	(rad/sec)
250.0	Steering Rate Limit	(deg/sec @ front wheel)
45.0	Steer Limit	(deg @ front wheel)

The example parameter settings seen here specify a 100 ms time delay applied to the optimal steering control and return the signal otherwise un-touched (large limit value, large break-point, zero noise and zero threshold specifications) to the external vehicle dynamics program. In cases where driver remnant noise addition or ergonomic limits on

driver steering control are desired, this set of parameters provides the means for enabling those properties.

3.7 Path Planning —

In addition to the road center-line path (input) specification and the left and right road boundary specifications described in Section 3.1, two other options exist under the *Path Planning* module that allow for further modification of the nominal center-line path entered by the user. These include either (a) smoothing of the basic center-line path over a user-specified moving average interval, or (b) using a derived "racing line" approximation calculated by the model using the left and right boundaries along with a vehicle width parameter (for determining vehicle-boundary interferences).

Option (a) allows the user to apply a uniform moving average filter to the initial center-line path. The output of this smoothing operation then replaces the initial center-line path as the desired path.

The approximate racing line algorithm, option (b), applies a simple moving average filter to each center line path point, in increasing filter widths, until vehicle contact is made with either road boundary (i.e., smoothed line + vehicle-width/2 produces contact with either boundary). The same process is repeated on the next center-line point. Consequently, each point on the resulting smoothed racing line curve will correspond to a varying level of smoothing, depending on the proximity of corners or curves present in the boundary data. An example of this type of calculation is seen in Figure 3.7-1 corresponding to the same "moose course" seen in Figure 3.1-2 and using an assumed vehicle width of 2 meters.

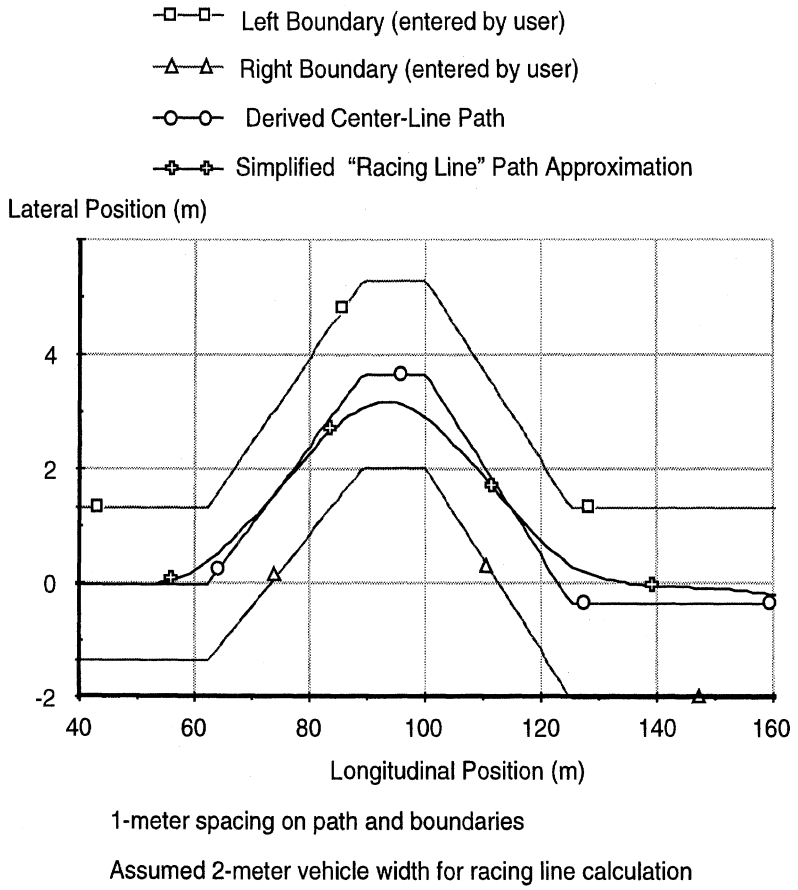

Figure 3.7-1. Derived Racing-Line Approximation for the Moose Course.

The following list of parameters in Table 3.7-1 define the properties of the *Path Planning* element:

Table 3.7-1. Path Planning Parameter Listing.

```
99     # of path smoothing points, >=99 => racing line calc
2.0    Vehicle Width for vehicle-boundary interference calculations (m)
99     Maximum limit for # of points to use in any smoothing calcs
```

The first parameter specifies the level of smoothing applied to the initial center-line path. It controls the length of the moving average window over which smoothing occurs. If this parameter is greater than or equal to 99, the racing line algorithm is used instead to obtain the desired path. The second parameter specifies the vehicle width parameter used for all path-related calculations involving vehicle-path conflicts with road boundaries (racing line algorithm, variable preview, etc.). The last parameter simply lets the user place an upper limit on the amount of maximum smoothing that can occur under either option (a) or (b) above.

While the "racing line" algorithm does not produce a true racing-line curve, it provides a simple method for approximating such trajectories without too much computational effort. The resulting racing line curve is further smoothed to some extent by the driver/vehicle response as the driver model attempts to follow the designated racing line trajectory. The fidelity of tracking will depend upon the quickness of the vehicle dynamics, the amount of driver preview, and the level of driver time delay. Greater skill level is assumed to correlate with faster driver reaction times, better adaptive preview behavior, and selection of racing-line (or minimum curvature paths) through most turns.

3.8 Preview Path Observation Capability (Variable Driver Preview) —

This element of the model allows for on-the-fly adjustment of driver preview during the course of a simulation run, as opposed to a fixed or constant preview interval. The most influential factor affecting how the driver model adjusts its preview is the geometry of the scene, and in particular, the nature of the left and right road edge boundaries. A more winding road with narrow lanes will cause the driver model, operating with variable preview, to reduce its preview down to shorter look-ahead times (or look-ahead distance) in order to avoid excessive corner-cutting. The preview adjustment algorithm is intended to mimic driver behavior which is assumed to utilize only that amount of path information that can be readily seen at any given time. For example, entry from a straight road section into a sharp corner will cause the model to shorten its preview down to its minimum value when entering the curve. When exiting a sharp curve on to a straight section, the associated geometry will permit the model to reach out to its maximum level of preview.

The use of variable preview or fixed preview is set by a flag (0 or 1) in the driver model data set. Upper and lower limits on how far the preview can be adjusted are also input parameters. Limits on how often preview can be adjusted (update rate) and how much it can be adjusted per update interval are also parameters that are under the control of the user whenever the adjustable preview option is selected.

The basic algorithm that controls how preview is adjusted works as follows. At any preview adjustment update time, the current path prediction provided by the internal vehicle model is interrogated along its length to check for interference between the projected path (plus half the vehicle width) and either of the two road boundaries. See Figure 3.8-1.

If a conflict exists, the current preview time is decremented downward (by a user-specified amount). If no conflict exists, the current preview is incremented upward. In either case, if the minimum or maximum allowable preview limits are reached, the preview is set to the respective limit value.

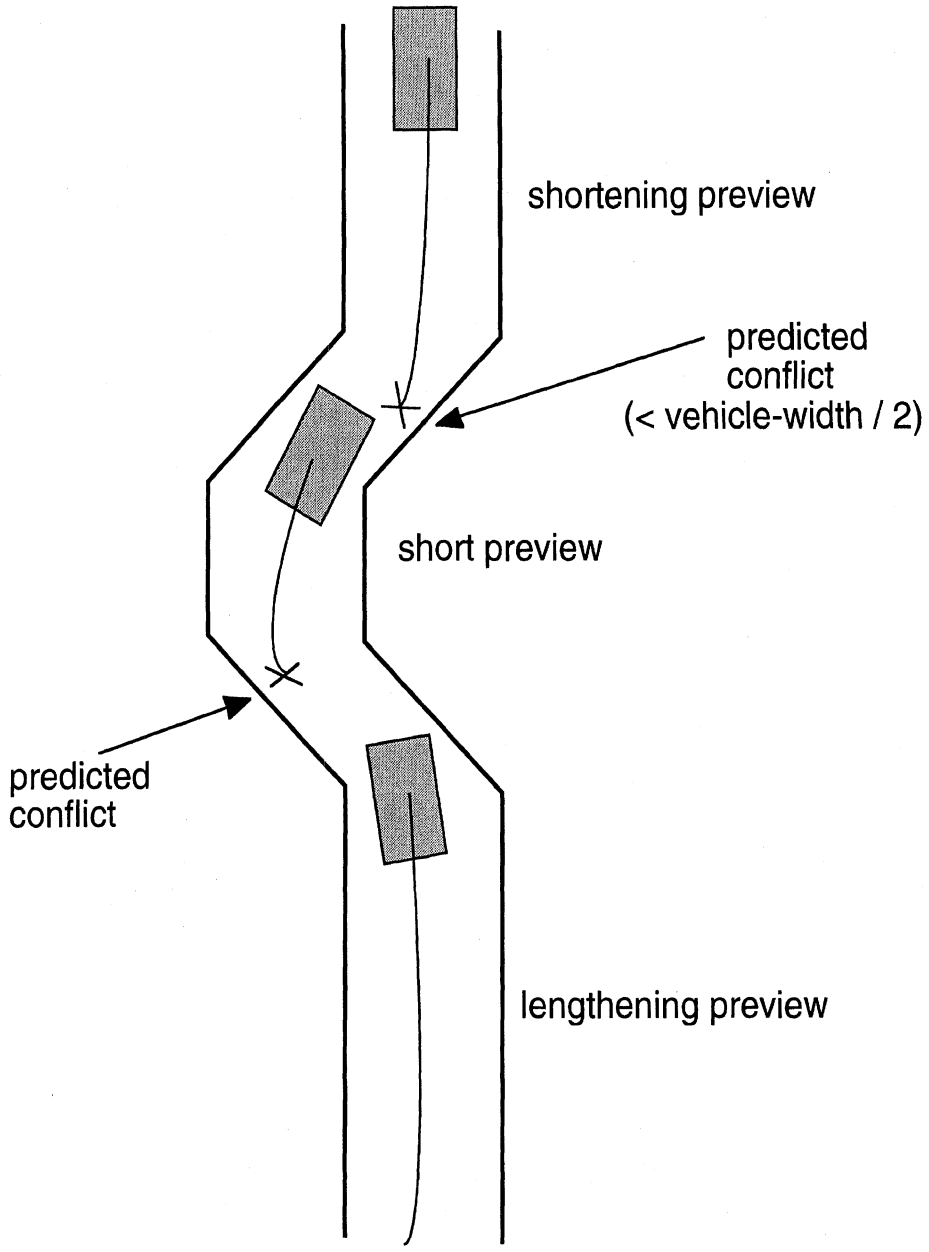

Figure 3.8-1. Variable Preview Feature Based Upon Conflicts Between Predicted Vehicle Path and Road Boundaries.

3.9 Speed Control —

The speed control element provides deceleration/acceleration requests to the external vehicle model in order to avoid excessive speed when entering an upcoming curve or for maintaining a desired speed. When activated, this element utilizes a "Desired Velocity" parameter. When vehicle speed falls below this level, the driver model will issue an acceleration request to the main vehicle model. This would likely occur during maneuvers in which forward speed is scrubbed off due to lateral maneuvering, or upon exit

from a tight turn during which the driver model previously requested deceleration to slow down.

When entering an upcoming curve or sequence of curves, the driver model attempts to evaluate the degree of turning likely required in the upcoming turns and will issue requests for deceleration to the main vehicle model if some designated level of lateral acceleration is likely to be exceeded at the current travel speed.

Three parameters listed in Table 3.9-1 are used by the speed control algorithm The first parameter is the Speed Control flag that activates or disables the speed control feature. The second parameter is the Desired Velocity, and the third parameter, Ay-max, is an upper limit on lateral acceleration for upcoming curves. More aggressive driving behavior would be represented with higher values of these latter two parameters.

Table 3.9-1. Speed Control Parameters.

```
1           Speed Control flag (= 0 => none, > 0 => active)
24.0        Desired Velocity for driver speed control algorithm (m/sec)
0.4         Ay-max for driver speed control algorithm  (g's)
```

The algorithm used by the driver model for estimating lateral acceleration demand in an upcoming curve utilizes information from the previewed path at the very end of the current preview interval. At each driver model time step, the angular heading of the road course T seconds ahead (at the end of the current preview interval) is estimated. This angle is then compared to the current heading angle of the vehicle. A difference in heading angles is then obtained. An estimate of road curvature is then made by dividing the current travel distance to that preview end-point, by the absolute change in heading angle obtained in the previous step. This provides a crude approximation of required turning radius (assuming the vehicle starts to turn immediately from its current position).

The resulting turn radius estimate is then used to compute a corresponding estimate of required lateral acceleration (V^2 / Radius) for that turning radius and the current vehicle speed. If the resulting lateral acceleration is above the Ay-max parameter entered by the user, a deceleration request is issued to the vehicle model. The level of deceleration requested is based on calculating the change in speed needed to reduce the upcoming lateral acceleration estimate to the Ay-max limit entered in the data set. The deceleration is assumed to take place uniformly over the next T seconds (preview interval).

- When activated, the model looks ahead to the very end of the current preview interval and estimates the angular heading of the desired path (in that region) and compares it to the current vehicle heading angle.
- Based on the relative difference in heading angles (path ahead vs. current vehicle), an estimate of upcoming path radius, R, is made. (See diagram below)
- Using the upcoming path radius estimate, R, and the current vehicle speed, V, an estimate of required lateral acceleration in the upcoming curve, Ay,is calculated as: V*V / R.
- If Ay > Ay-max, braking is requested to slow down. (Ay-max is an input parameter for the speed control feature.)
- The level of decel requested is based on linearly reducing the current speed (V) so as to produce Ay-max in a curve of radius (R), T seconds ahead.
- If the current vehicle speed falls below a desired speed (V-desired), and no braking is presently occurring, acceleration is requested to speed up. (V-desired is an input parameter for the speed control feature.)

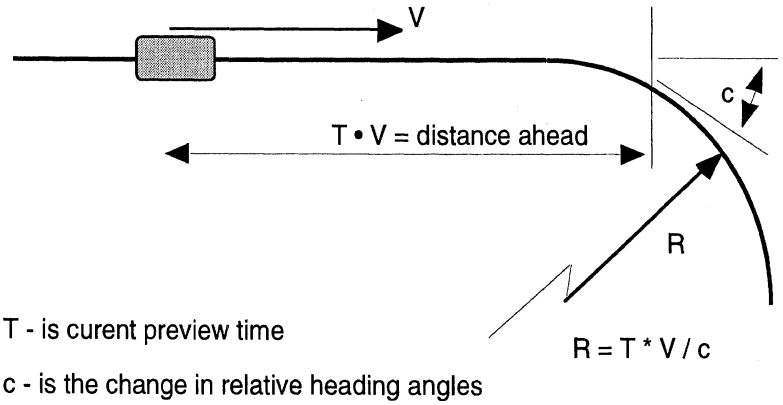

Figure 3.9-1. Driver Model Speed Control Algorithm.

Although the speed control algorithm has a tendency to underestimate the required turn radii for road courses containing sudden directional changes, it does still exhibit reasonable performance in many challenging scenarios. Further refinements to the speed control element can be always made after further usage and if driver/vehicle test data applicable to these types of driving scenarios become available.

3.10 Situational Awareness Parameter —

This driver model element provides a simple transport delay that only affects the desired path and only for the initial portion of a maneuver when lateral acceleration levels lie below a specified threshold. That is, the situational awareness element assumes an initial delay value that is applied to the path input until a certain lateral acceleration threshold is exceeded. Once that occurs, the delay is cancelled for the remainder of the run.

The intent here is to simulate an initial "casual" driver control behavior that is not particularly vigilant but then becomes highly involved in the control process once a specified lateral acceleration is exceeded during that initial period.

The basic idea is to apply a cognitive/recognition delay at the start of a developing conflict or sudden maneuvering condition. This is simulated by delaying the desired path information some amount (the amount determined by the parameter delay setting) and only at the very start of the conflict (as determined by when lateral acceleration exceeds an assumed threshold). Thus, the delay is transient in nature but can be sizeable in magnitude (a second or more, depending on the scenario). The lateral acceleration threshold value is used to define the maneuver severity level that is assumed to "get a driver's attention," after which point the driver is then fully engaged in the control activity.

Figures 3.10-1, 3.10-2, and 3.10-3 show example results for three different *Situational Awareness* delay values using the double lane change maneuver and a corresponding lateral acceleration threshold parameter value of 0.2 g's to then cancel the delay effect. The three delay values are 0.0, 0.6, and 1.2 seconds. Figure 3.10-1 shows the driver steering input result. Figures 3.10-2 and 3.10-3 show the corresponding lateral acceleration and path responses.

As seen in the figures, each additional 0.6 second of delay further amplifies the ensuing driver/vehicle response and produces significant path response delays at the start of the obstacle avoidance maneuver. Figure 3.10-3 shows the 1.2 second delay case encroaching well outside the right lane boundary at the start of the maneuver. In all cases, the driver/vehicle system recovers path and directional stability following the amplifying effects of the temporary initial delay.

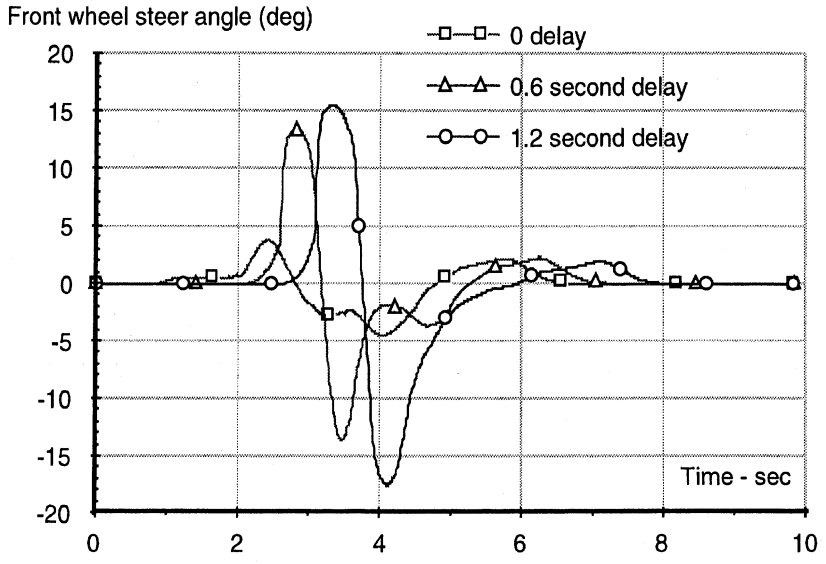

Figure 3.10-1. Driver Model Steer Response. Situational Awareness Example.

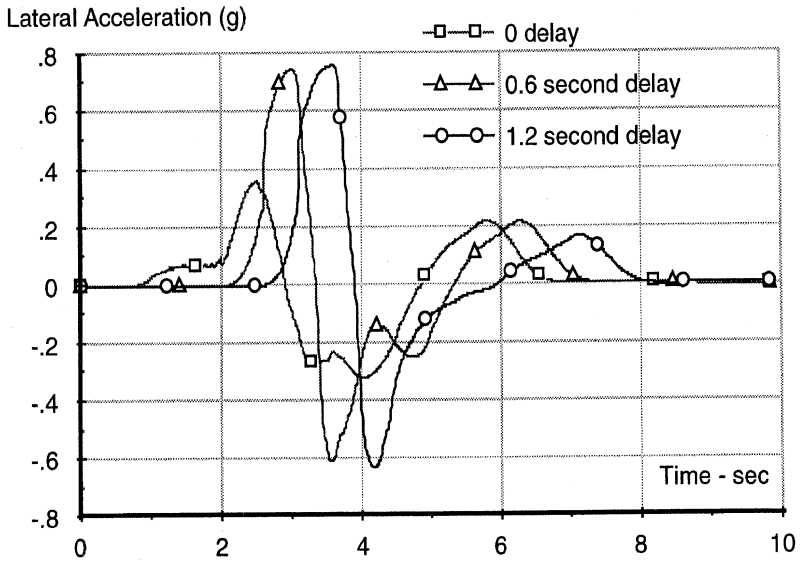

Figure 3.10-2. Lateral Acceleration Responses. Situational Awareness Example.

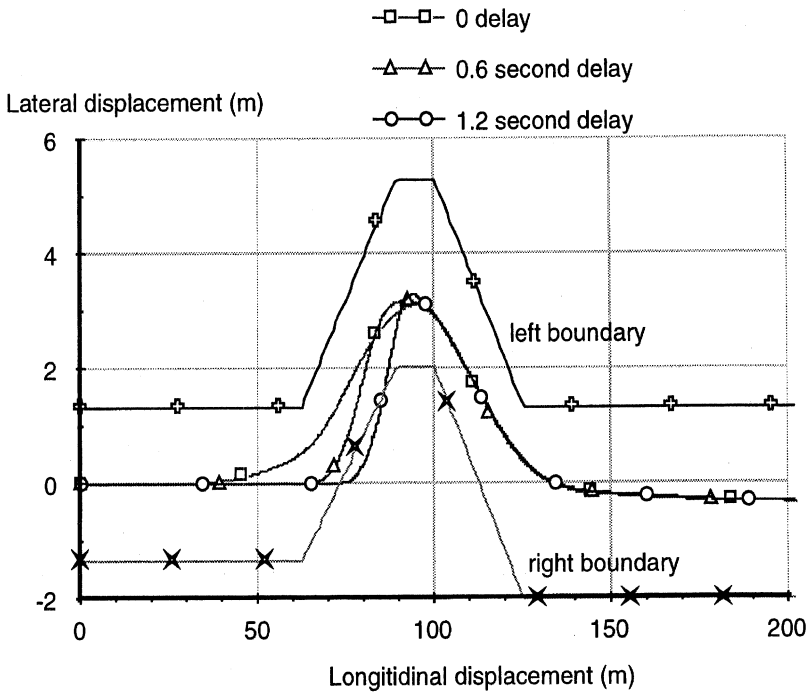

Figure 3.10-3. Path Responses. Situational Awareness Example.

3.11 Example Run Illustrating the Speed Control and Variable Preview Features for the Double Lane Change Maneuver.

This section uses an example run through the double lane change (moose course) maneuver to help illustrate the *Speed Control* and *Variable Preview* features present in the GM driver model.

Referring to Figures 3.11-1 to 3.11-6, the example run starts with the vehicle initially entering the moose course at a speed of 30 m/sec. However, the *Speed Control* parameters, Desired Velocity and Ay-max, are set to 26 m/sec and 0.4 g's respectively, indicating a desired travel speed of 26 m/sec and lateral acceleration levels less than 0.4 g's in any upcoming curves. Consequently, some braking is initially requested by the driver model (to the external vehicle dynamics program) in order to slow the vehicle down to at least 26 m/sec. Additional braking then occurs as the vehicle enters the upcoming course in order to avoid lateral acceleration levels larger than 0.4 g's. Upon exit from the moose course, where vehicle speed is less than 26 m/sec, acceleration requests are generated by the driver model in order to speed up to the desired 26 m/sec travel speed. During traversal of the course, acceleration and deceleration requests are periodically generated by the model, depending on the course geometry ahead of the vehicle and its current speed. Figures 3.11-1 and 3.11-2 show the corresponding speed profile and longitudinal acceleration responses through the course.

The driver model *Variable Preview* feature is also active in the example run. The parameter settings for this feature specify a minimum preview time of 0.6 seconds and a maximum preview time of 2.0 seconds. In addition, the preview control sampling rate is set at 0.1 seconds and the maximum rate of change of preview at any sampling time is set to 0.1 seconds, thereby indicating a limit on the rate of preview time adjustment of 0.1/0.1 or 1 second change of preview per 1 second of simulation time.

Figure 3.11-3 shows the driver preview time being continuously adjusted as it enters, traverses, and exits the moose course. The preview time is ratcheted downward as sharp turns approach and is ramped upward as straight sections of the course are encountered - per the descriptive behavior depicted in the earlier Figure 3.8-1. The initial preview setting is 0.7 seconds. As the simulation run begins, the model attempts to lengthen its preview. As the first lane-change becomes sensed by the model, the preview is then shortened down to its minimum setting (0.6 seconds) due to vehicle-boundary conflicts sensed by the model at longer preview times. The preview time varies up and down during the two lane-change traversals and then increases upon exit from the last turn up to its maximum value of 2 seconds.

Figures 3.11-4 and 3.11-5 contain the corresponding driver steering and lateral acceleration waveforms. The peak values of lateral acceleration are seen to lie just below the 0.4 g preference parameter setting for Ay-max. Figure 3.11-6 shows the vehicle trajectory through the double lane-change course. Figure 3.11-7 contains a simple animation sequence for the example run seen above.

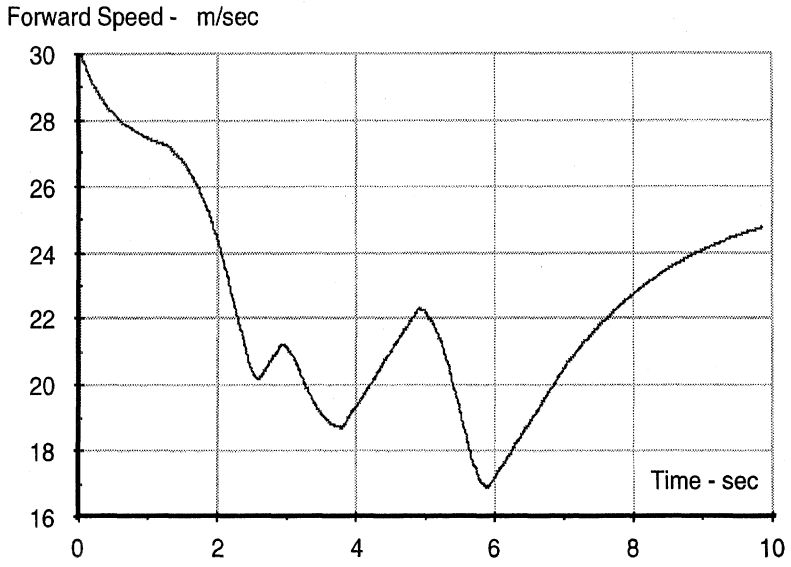

Figure 3.11-1. Example Speed Profile Produced by the Driver Model Speed Control Feature During Entry and Exit from the DLC "Moose Course."

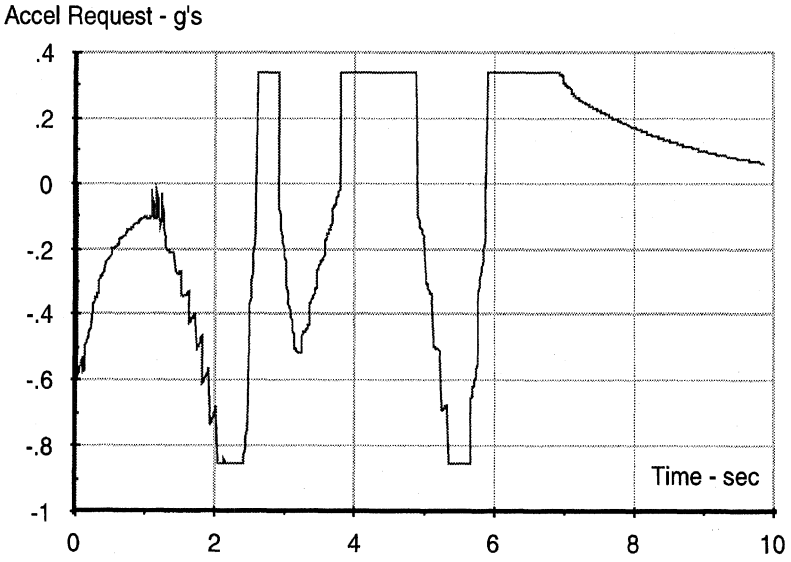

Figure 3.11-2. Corresponding Acceleration Profile Produced by the Driver Model Speed Control Feature During Entry and Exit from the Moose Course.

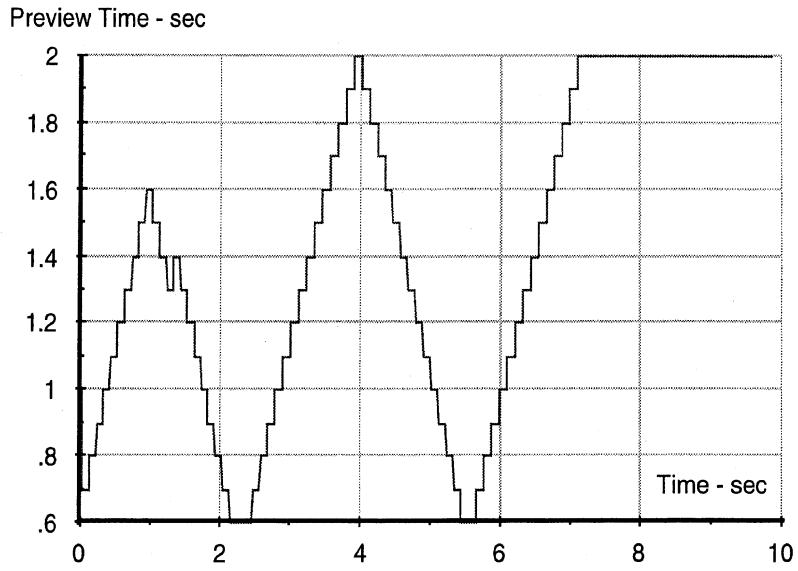

Figure 3.11-3. Corresponding Preview Adjustment Produced by the Driver Model During Entry and Exit from the Moose Course.

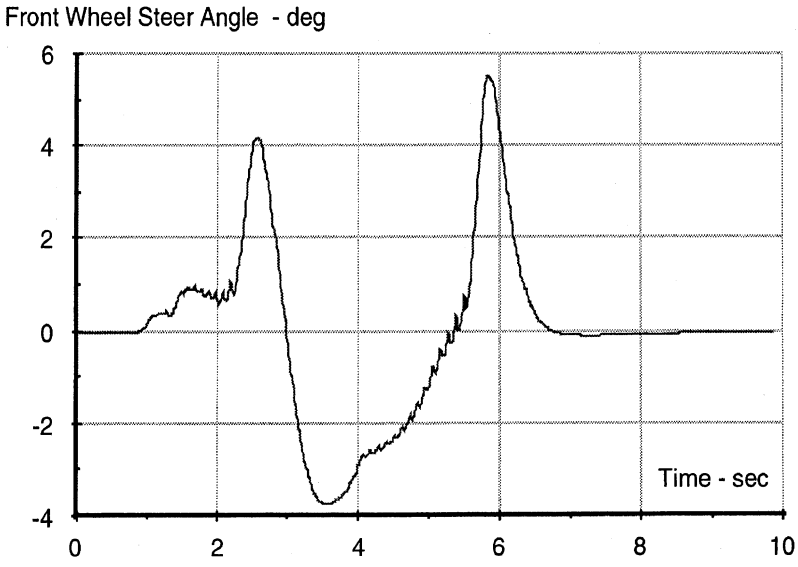

Figure 3.11-4. Corresponding Driver Steering During Entry and Exit from the Moose Course.

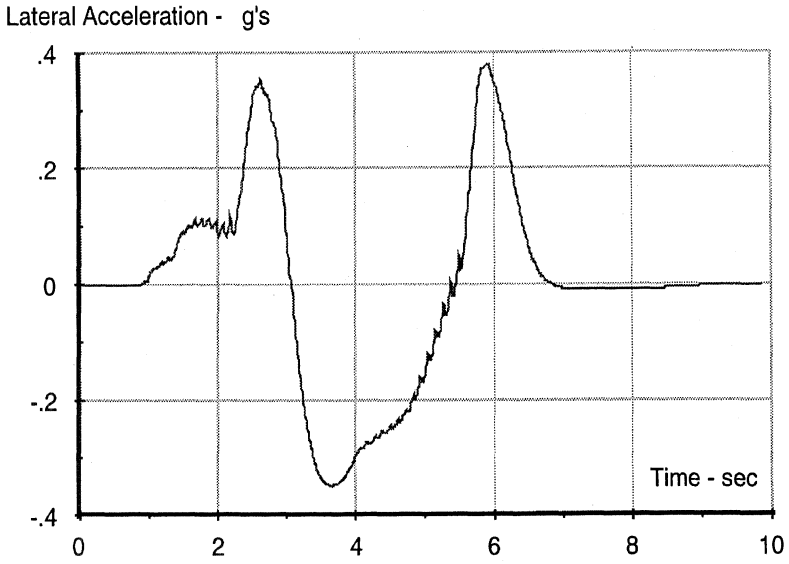

Figure 3.11-5. Corresponding Lateral Acceleration — Moose Course.

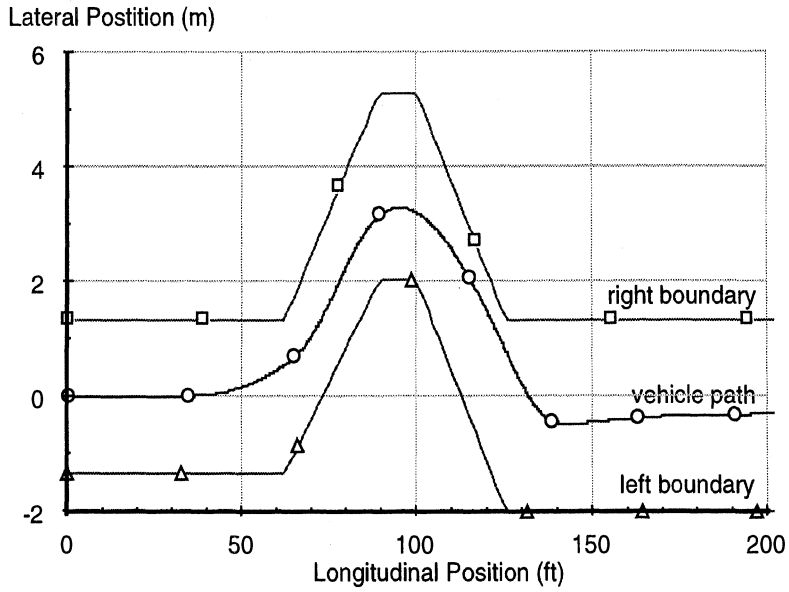

Figure 3.11-6. Vehicle Trajectory Through the Moose Course.

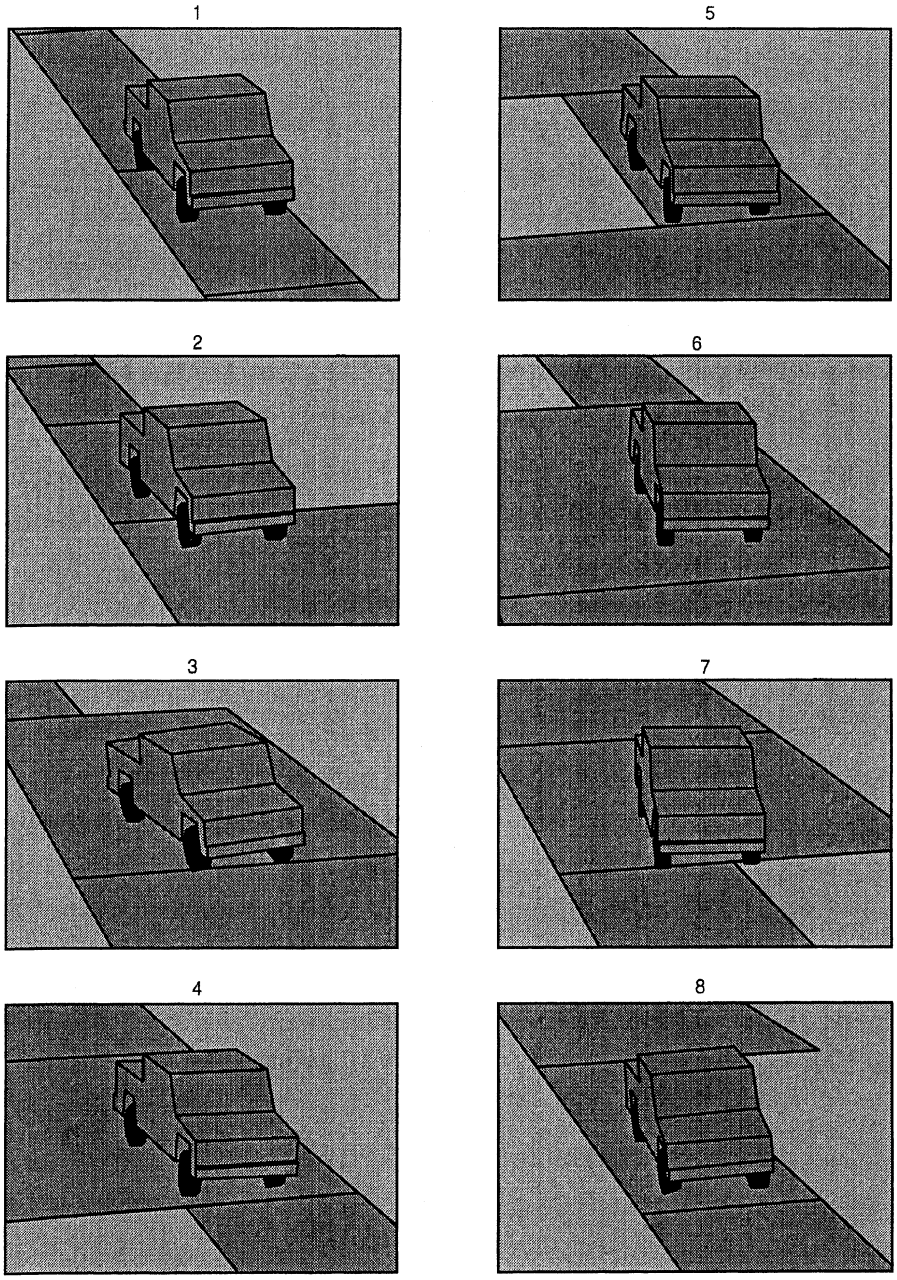

Figure 3.11-7. Animation Sequence Corresponding to the Example Run.

4.0 New Features / Capabilities of the GM Driver Model

As noted in previous sections, the GM nonlinear driver model developed under this work was derived from a linear UMTRI model initially developed in the 1980's [1, 2] and subsequently refined and used in a number of later research studies [3, 4, 8, 9]. This section of the report serves to delineate new features present in the GM model from those of the preceding model, and to illustrate, by way of two examples, how the GM model extends the analysis capabilities beyond that present in the initial and more recent versions of the UMTRI model.

4.1 Model Comparison Overview

As noted in the Introduction by way of Table 1-1, and repeated below as Table 4.1-1 for convenience, several new features have been added to the GM model. Some of these, such as the *variable preview*, *speed control*, and *situational awareness* features were explained and demonstrated in the previous Section 3.0.

The following list of sub-sections summarize each of the new features and also note the differences between the new and original models listed in Table 4.1-1.

4.1.1 Previewed Scene Input — The new model accepts either 1) a path table input or 2) a set of left and right path boundary tables as the scene input for path-following purposes. In the latter case, the centerline of the left and right boundaries is used as the desired path. The left and right boundaries are used by the *variable preview* and *speed control* modules for their respective calculations. The original linear model only utilized a path table input.

4.1.2 Sensory Limitations — Sensory limitations are now provided as an intermediary processing block between the external vehicle model (i.e., VehSim) and the driver model. The primary purpose of this block is to allow optional processing of vehicle response signals assumed to be sensed by the driver such as vehicle position, yaw rate, sideslip, etc. and used by a driver for steering control purposes. Processing that can occur here include time delays, limiting, and other items listed in Section 3.2. The linear model contained no such provision.

4.1.3 Internal Vehicle Dynamics — The new GM driver model includes a nonlinear four degree-of-freedom internal vehicle dynamics model as described in Section 3.3. The original UMTRI driver model contained a linear two degree-of-freedom constant velocity internal vehicle model. The extension of the internal model includes nonlinear tire properties, roll motion influences affecting lateral tire load transfer, suspension steer influences, and speed changes. The example runs in the next two Sections 4.3 and 4.4 illustrate many of these effects and the resulting differences with the original linear model.

4.1.4 Prediction Capability — The new model utilizes numerical integration of the above internal vehicle dynamical equations of motion to predict future vehicle responses over the preview interval. The original model used a linear transition matrix formulation to accomplish the same task for its linear internal vehicle model.

4.1.5 Steering Control Calculation — Numerical minimization of a performance index, based primarily on previewed path errors, is utilized as the basic steering control calculation. At each driver model update interval, several predicted vehicle responses over the preview interval are first generated to provide a family of mean square preview path errors. A quadratic curve fit is then used to identify the minimum path error from this family, and thereby, the corresponding optimal steering control for the next time step. The original linear driver model used the closed form solution to the idealized linear preview minimization problem documented in its derivation references [1, 2].

4.1.6 Driver Physiological and Ergonomic Constraints — The optimal steering control identified above is passed through several optional processing stages prior to its output from the overall driver model block. The most common and characteristic human-centered process involves a pure transport time delay applied to the optimal steering control. Other processing options within this output block include provisions for neuromuscular filtering, limiting, rate limiting, noise addition, hysteresis, and thresholding effects as described more fully in Section 3.6. The original linear model contained only the transport delay option.

4.1.7 Path Planning — This feature provides for modification of the desired input path specified in the previewed scene input to the model. The assumption here is that a driver can elect to follow a variety of different paths in the general vicinity of a nominally designated path or road boundary input. Two options exist with the new model: 1) simple smoothing of the nominal path input to provide a lower curvature path input, or 2) a "racing-line" approximation path along the specified path input. The original linear model contained no such path planning/modification provision.

4.1.8 Variable Preview — The new model now contains an option for incorporating variable driver preview in addition to the original fixed preview assumption. This feature allows the model to vary driver preview on-the-fly based upon the upcoming road geometry at any point in the maneuver. It is described in more detail within Section 3.8 and within the example run seen in Section 3.11. The original linear model only provided a fixed driver preview parameter.

4.1.9 Speed Control — A speed control feature is now present in the GM driver model primarily for the purpose of facilitating handling through upcoming curves or steering around obstacles. The intent is to help anticipate and limit excessive speed in upcoming turning maneuvers based upon the available tire/road friction limit or driver preferences for maximum lateral acceleration. The feature is described further in Section 3.9 and in the example run of Section 3.11. The original linear model had no speed control feature.

Table 4.1-1. Comparison of the Original UMTRI Linear Driver Model vs. the GM Nonlinear Driver Model Developed Under This Project.

Model Feature	*UMTRI Linear Model*	*GM Nonlinear Model*
Previewed Scene Input Options	• Path Table	• Path Table, or • Left & Right Road Boundaries
Sensory Limitations	• None	• Time Delay • Filtering • Noise Addition • Signal Limiter • Thresholding
Internal Vehicle Dynamics	• 2 Degree-of-Freedom Linear Model (lateral and yaw motions)	• 4 Degree-of-Freedom Nonlinear Model (lateral, longitudinal, yaw, and roll motions)
Prediction Capability	• Linear Transition Matrix	• Numerical Integration
Steering Control Calculation	• Closed-Form Analytical Expression Based on Linear Analysis	• Numerical Optimization / Minimization of an Arbitrary Performance Index
Driver Physiological and Ergonomic Constraints	• Transport Time Delay	• Transport Time Delay • Neuromuscular Filter • Noise Addition • Magnitude / Rate Limiter • Threshold • Hysteresis
Path Planning	• None	• Center-line Smoothing • "Racing Line" Approximation
Variable Preview	• None	• Min/Max Preview Setting • Rate Control
Speed Control	• None	• Desired Speed Setting • Maximum Lateral Acceleration Preference
Situational Awareness	• None	• Delay Parameter • Lateral Acceleration Threshold Trigger

4.1.10 Situational Awareness — This feature in the new model provides a simple initial delayed response to the first turning maneuver encountered in a maneuver. The delay only affects the first portion of the maneuver. A designated lateral acceleration threshold parameter is used to trigger cancellation of the specified delay for the remainder of the maneuver whenever the vehicle response first exceeds the threshold setting. The intent is to approximate an initial "casual" driver steering control behavior that then becomes vigilant and responsive once exposed to a certain level of lateral acceleration. This feature is described and demonstrated further in Section 3.10. The initial linear model provided no situational awareness feature.

4.2 Example Runs Illustrating Linear Model vs. Nonlinear Model Differences

As noted above, certain features present in the original UMTRI driver model, particularly its internal vehicle model, have been extended under this work to cover a broader range of operating conditions, up to and including the limit of tire/road adhesion. The remainder of this section focuses primarily on that issue. Namely, the ability of the new GM model to better predict vehicle performance under near-limit conditions and to correspondingly provide improved steering control predictions for path-following under those more demanding conditions. Adaptation of the driver model to sense sudden changes in operating conditions and to respond more quickly and accurately to those sudden changes is demonstrated by two example simulation scenarios. The first example involves encounter with a low friction patch of pavement midway through a double lane change obstacle avoidance maneuver. The second example simulates a tire blowout midway through the same double lane-change geometry on a uniform high friction surface.

To set the stage for the two example maneuvers — where sudden changes in operating conditions occur during the most demanding portion of the maneuver — the two models are first compared side-by-side for no change in operating conditions in order to provide a set of baseline or reference results. This also provides an opportunity to examine very basic differences between the two models, absent any additional unusual influences that may cloud the basic comparison. The baseline reference results will also be used to measure changes induced in subsequent runs when the slippery pavement patch and tire blow-out events are introduced.

To begin, the double lane-change maneuver used in the simulator tests (the modified ISO "moose test") serves as the nominal maneuver for these example runs. See Figure 4.2-1. As seen in the figure, the exit lane width is different from the entry lane width and is also further displaced center-to-center (3.99 m vs. 3.66 m). The initial vehicle speed is 22 m/sec and no speed control, variable preview or other special features are active in these comparison runs

The nominal tire/road friction limit is 0.85 for the nonlinear vehicle model with tire lateral force characteristics equal to those seen in the previous Figure 3.3-2. The nonlinear driver model uses the same internal vehicle and tire model characteristics as described in Section 3.3.

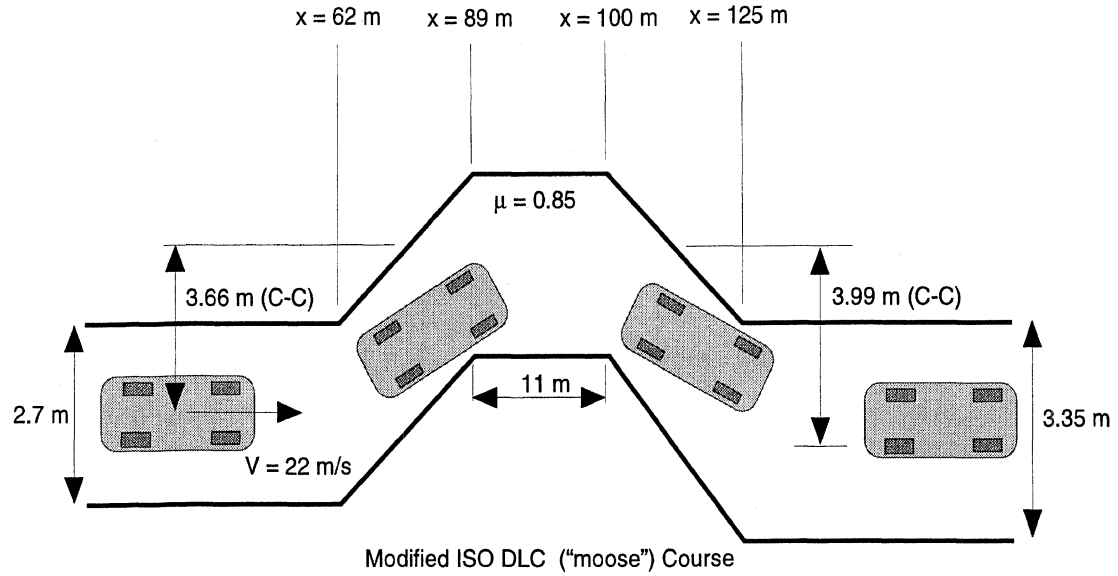

Figure 4.2-1. Double Lane-Change Geometry Used in Example Runs.

The linear driver model interacts with the same nonlinear vehicle model but utilizes a two degree of freedom (internal) linear vehicle model with linear tire properties. The linear tire characteristics of this internal vehicle model are set to fixed cornering stiffness values of 1600 N/deg and 1400 N/deg for the front and rear tires respectively. Consequently, no friction limit is assumed by the linear driver. The roll degree of freedom and suspension compliance effects in the internal vehicle model have also been eliminated for the linear driver model case.

Both driver models use the same fixed level of preview time of 1.25 seconds and a transport time delay value of 0.25 seconds. All other filtering, delay, and thresholding elements are set to values rendering them inoperative.

Figure 4.2-2 shows a direct comparison of the GM nonlinear driver model result with that obtained using the linear driver model. As seen, the nonlinear model stays uniformly within the two lane boundaries and exhibits good tracking performance. On the other hand, the linear model starts turning at about the same time but fails to achieve sufficient lateral displacement at the beginning of the initial turn, causing it to brush the right boundary at about the 90 meter location. The linear model then fails to turn sharply back to the recovery lane, thereby traversing the left boundary between the 120 to 135 meter locations. In general the linear model is too sluggish and damped under these elevated lateral acceleration conditions to provide adequate path tracking performance.

Figure 4.2-3 shows a comparison of the corresponding steering control waveforms generated by the two models. As seen, the nonlinear model is more aggressive and quicker to generate sufficient steer angle inputs in order to maintain proper lane control. The linear model appears sluggish and over-damped by comparison.

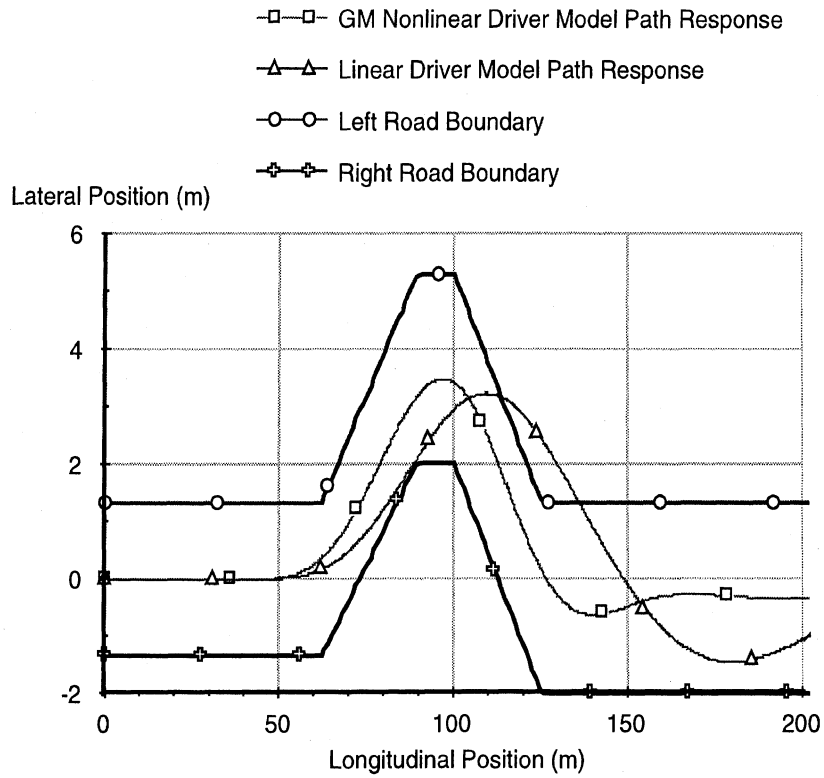

Figure 4.2-2. Path Responses for the Linear and Nonlinear Driver Models.

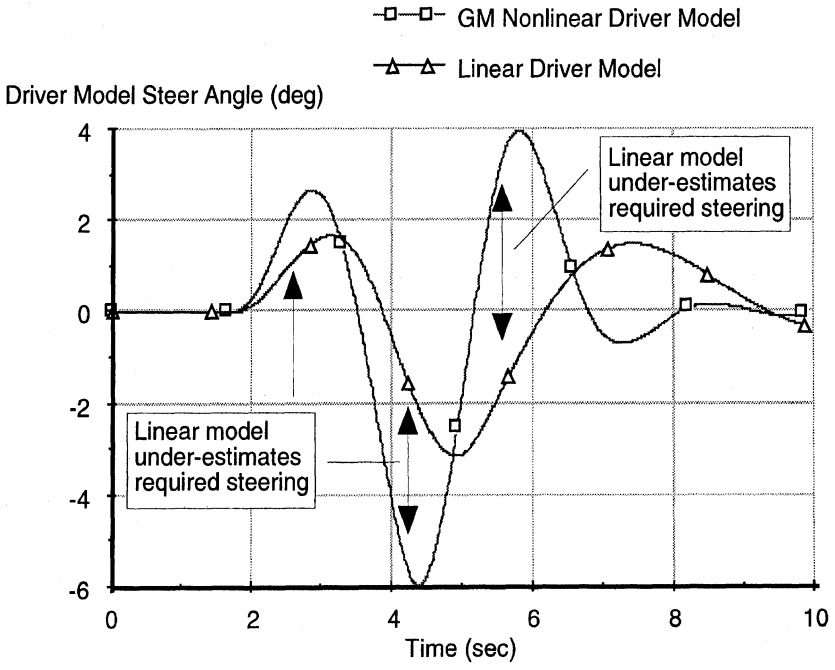

Figure 4.2-3. Comparison of Driver Model Steering Responses (Road Wheel).

The reason for this relates directly to the nature of the internal vehicle dynamics model employed by each respective driver model. The linear driver model employs linear

tires that do not saturate and know no limit for tire/road adhesion, even though the external vehicle model being controlled includes this tire force "reality" as part of its tire model. Consequently the linear model will under-utilize the amount of steering required to accomplish a turning maneuver at intermediate and elevated levels of lateral acceleration where the actual tire begins to lose effectiveness and eventually saturate. In contrast, the nonlinear driver model "knows" about this tire property since it employs a more accurate nonlinear tire characterization within its internal vehicle model and therefore steers more aggressively under those same elevated lateral accelerations conditions in order to properly compensate for the saturating tire force characteristics. The net result is that the linear model is always trying to play "catch-up" because it under-predicts the projected path response of the controlled vehicle. Figures 4.2-4 and 4.2-5 show the corresponding lateral acceleration and vehicle sideslip responses.

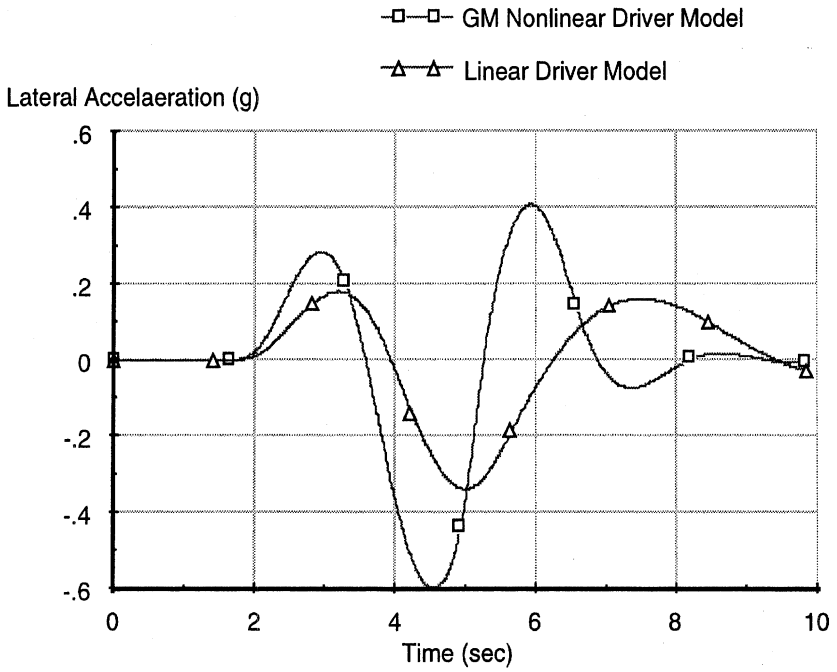

Figure 4.2-4. Comparison of Lateral Acceleration Responses.

This very basic difference between the linear and nonlinear driver model formulations — well illustrated by this initial example — is a fundamental under-pinning of the research proposed and conducted for GM under this work. Without this internal model nonlinear capability, the original linear driver model behaves as though the external world is simply linear, and thereby behaves accordingly, not recognizing the vehicle performance degradations imposed by friction transitions and tire force saturations present under real world nonlinear operating conditions.

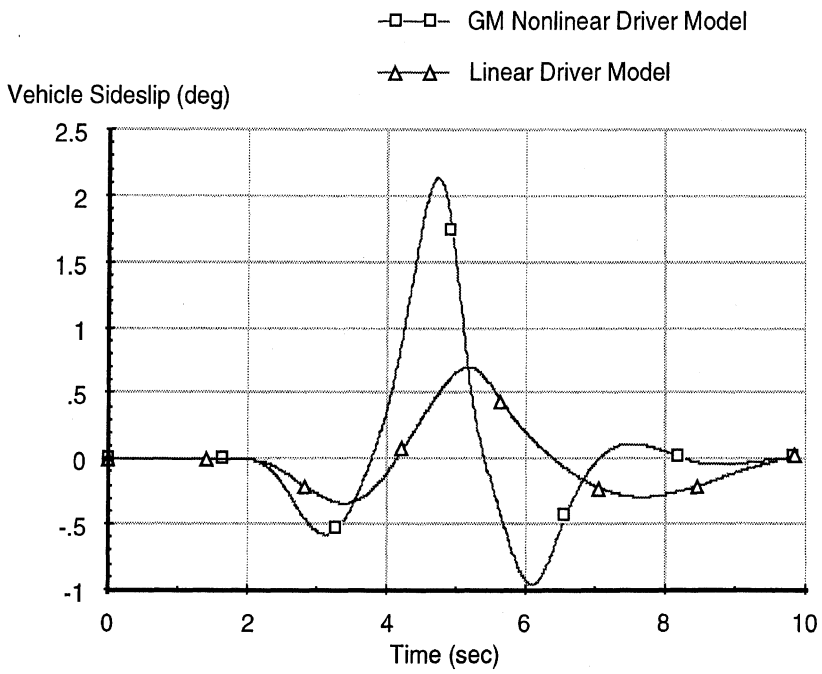

Figure 4.2-5. Comparison of Vehicle Sideslip Responses (mass center location).

It should be noted, that these steering behavior and path tracking performance differences exist only under elevated lateral acceleration conditions and that the two models behave nearly identically within the linear driving regime where tire force properties are linear and where compliance-steer and body roll influences play much smaller roles. This is desirable since the original UMTRI linear driver model has been shown to properly predict and represent driver vehicle steering control behavior under those more normal driving conditions [2, 3, 6]. In effect, the GM driver model "collapses" to the behavioral properties exhibited by the original UMTRI model under low-level linear driving conditions.

Figure 4.2-6 and 4.2-7 contain simple animation sequences corresponding to the linear driver model and nonlinear driver model baseline responses described above. The frame interval is 0.5 seconds. The first frame corresponds to time equal to 2.9 seconds.

The next two sections expand upon this baseline example by introducing two separate nonlinear effects — encounter with a slippery patch of pavement midway through the same maneuver (Section 4.3), and a left front tire blow-out event also midway through the maneuver (Section 4.4).

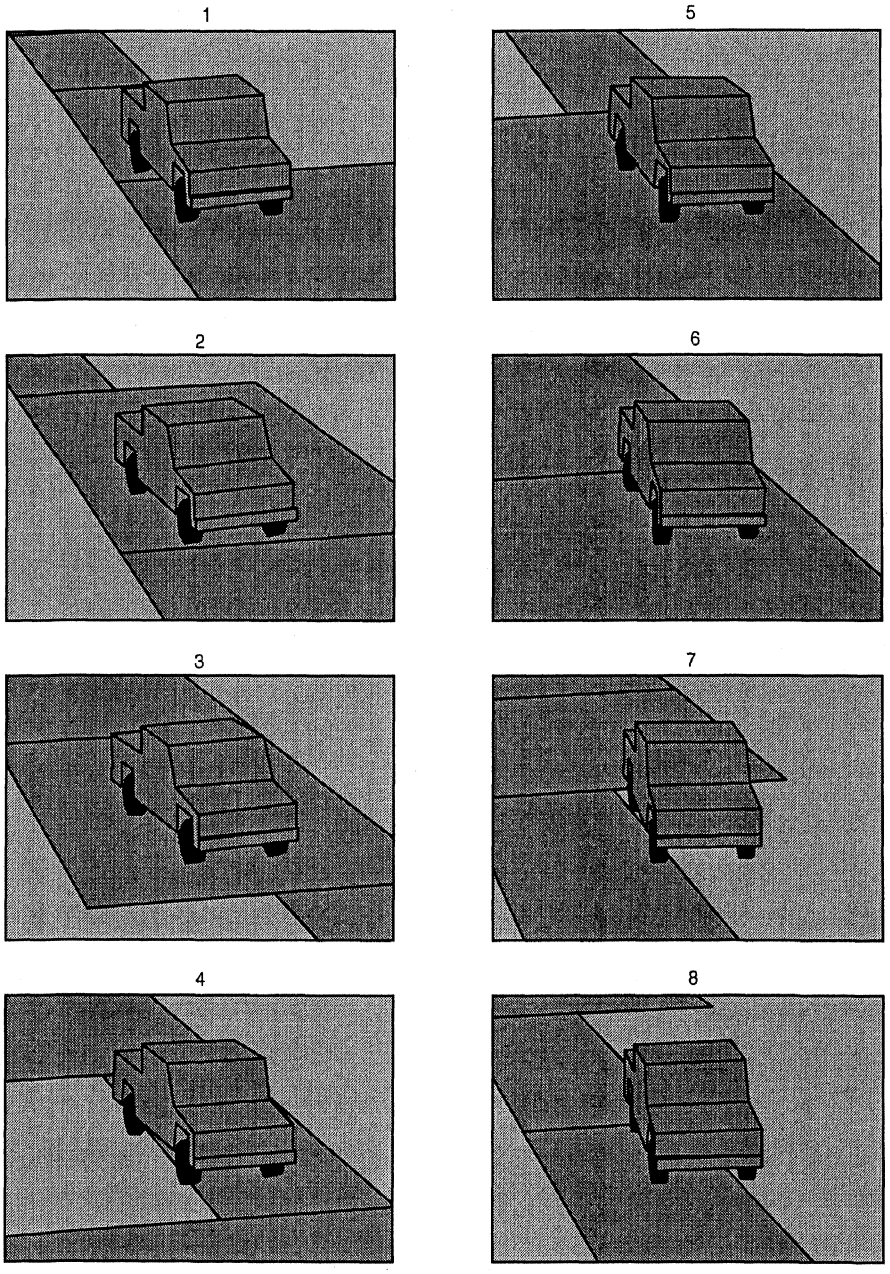

Figure 4.2-6. Animation Sequence for the Baseline Linear Driver Model Response.

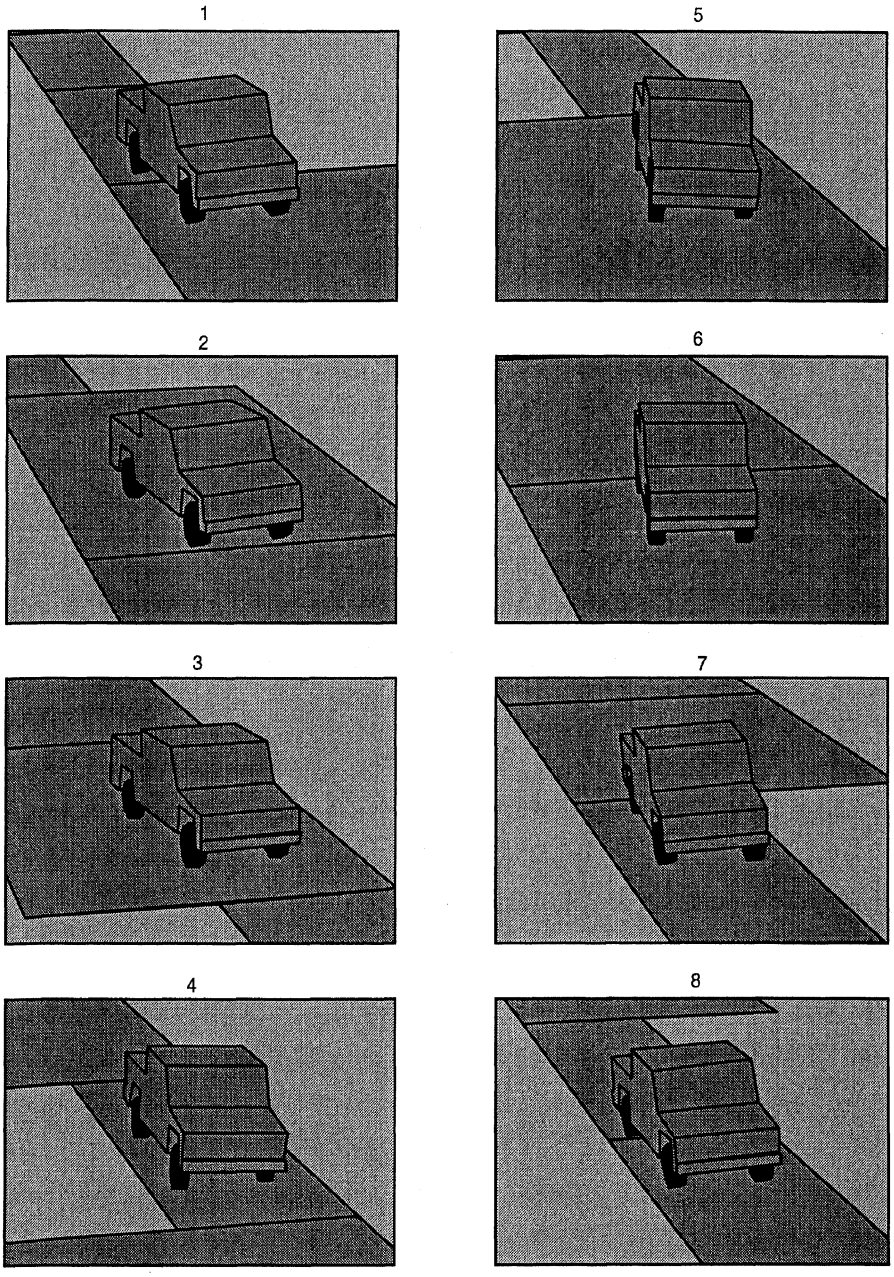

Figure 4.2-7. Animation Sequence for the Baseline Nonlinear Driver Model Response.

4.3 Double Lane-Change Example Run With a Slippery Patch of Pavement

Figure 4.3-1 shows the basic double lane change maneuver again but now with an 11 meter section of low friction pavement inserted into the mid-portion of the maneuver where the vehicle is at its highest level of lateral acceleration. The peak friction of the tire/road interface starts at 0.85, drops to 0.40 in the 11 meter patch, and then returns to 0.85 for the remainder of the maneuver. As before, the initial speed of the vehicle is 22 m/sec and the driver preview time and transport delay parameters are fixed at 1.25 and 0.25 seconds respectively. (For programming simplicity in this example run, all tires are assumed to encounter any surface friction change coincidentally with the location of the vehicle mass center, as opposed to a more strictly accurate sequential encounter, one by one, as they cross the frictional boundaries independently.)

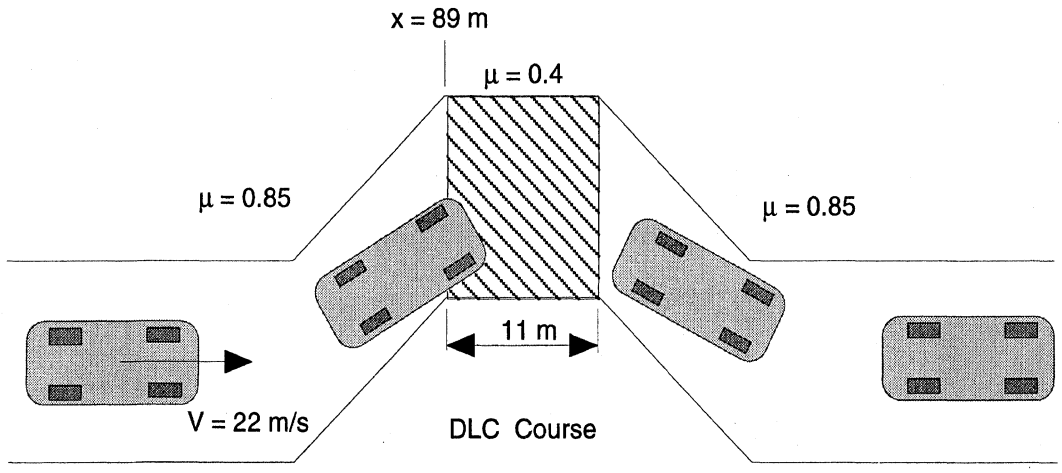

Figure 4.3-1. Double Lane-Change Maneuver with a Low Friction Pavement Section.

The path responses corresponding to the nonlinear driver model and the linear driver model for this case are seen in Figure 4.3-2. The previous baseline reference runs (without the slippery patch) are also shown as lighter dashed lines for comparison purposes. The corresponding driver model steering responses are seen in Figure 4.3-3.

As seen in Figure 4.3-1, insertion of an 11 meter length of low friction pavement into the mid-section of the run acts as a modest path disturbance to the vehicle causing it to slide momentarily more to the outside of the turn, prior to its subsequent recovery. The influence on the nonlinear driver model response is somewhat greater, only because that system is experiencing a higher lateral acceleration deriving from the more aggressive steering input provided by the nonlinear driver model, at the time of the surface friction disturbance.

However, as seen in Figure 4.3-3, the steering angle responses predicted by the two models are significantly different. The linear model responds very similarly as it did previously in the baseline reference run where no surface friction change occurs. Only a small change in steer response occurs after the low friction surface encounter occurs due to the state disturbance to the vehicle.

In contrast, the nonlinear driver model responds not only to the state disturbance to the vehicle, but also directly to the sudden change in tire forces occurring as the vehicle crosses the low friction patch of pavement. This latter behavioral response is directly attributable to the nonlinear internal vehicle model and its associated nonlinear tire model (within the structure of the nonlinear vehicle model) providing superior prediction of future vehicle response, particularly when the vehicle engages the low friction surface. As seen, the nonlinear driver model immediately steers more aggressively when encountering the low friction surface area so as to compensate for the loss of tire side force and still maintain the desired path. Once the vehicle reacquires the high friction ($\mu = 0.85$) surface again, the nonlinear driver model returns to steering behavior appropriate for that surface condition as seen above, for example, in the baseline reference run of Figure 4.2.3. The corresponding lateral acceleration responses appear in Figure 4.3-4.

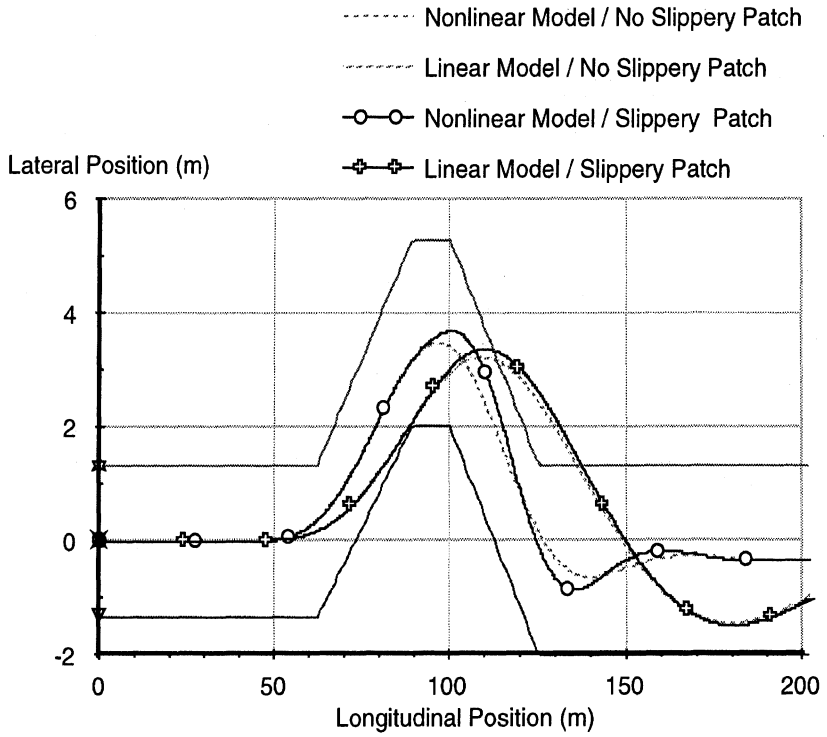

Figure 4.3-2. Path Responses for the Nonlinear and Linear Driver Models for the Slippery Pavement Encounter.

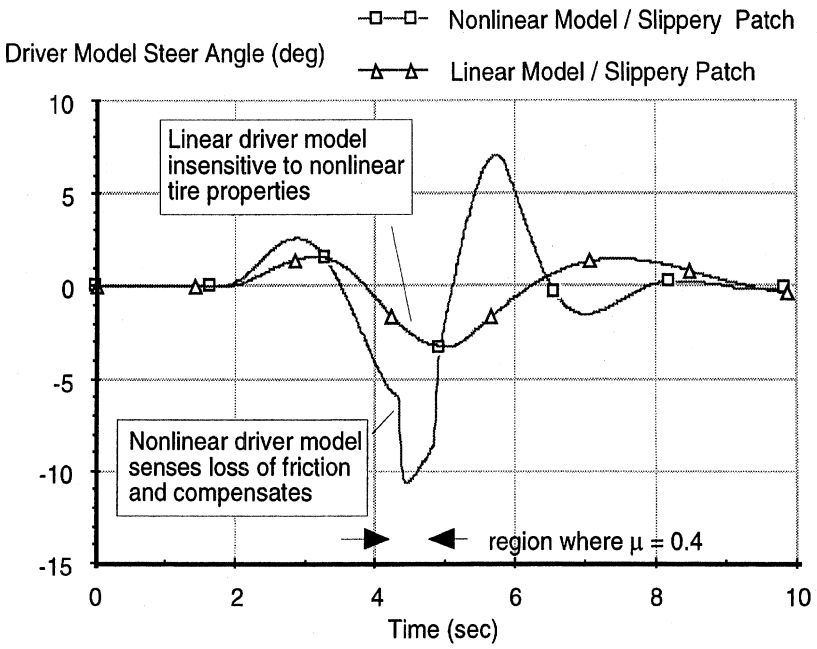

Figure 4.3-3. Driver Model Steer Responses / Slippery Patch.

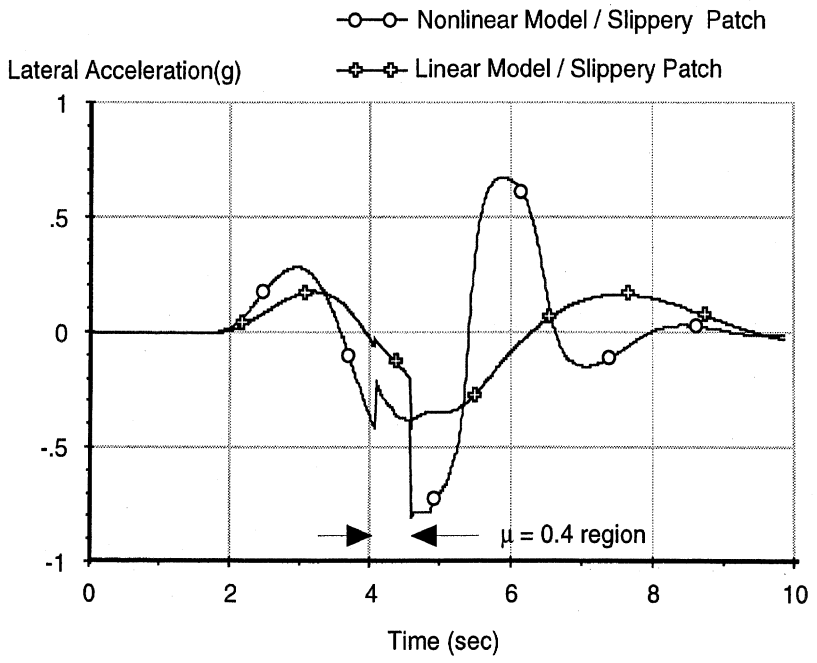

Figure 4.3-4. Lateral Acceleration Responses.

Figures 4.3-5 and 4.3-6 contain the corresponding animation sequences for the linear driver model and nonlinear driver model responses in the slippery patch example. As before, the frame interval is 0.5 seconds. The first frame corresponds to time equal to 2.9 seconds.

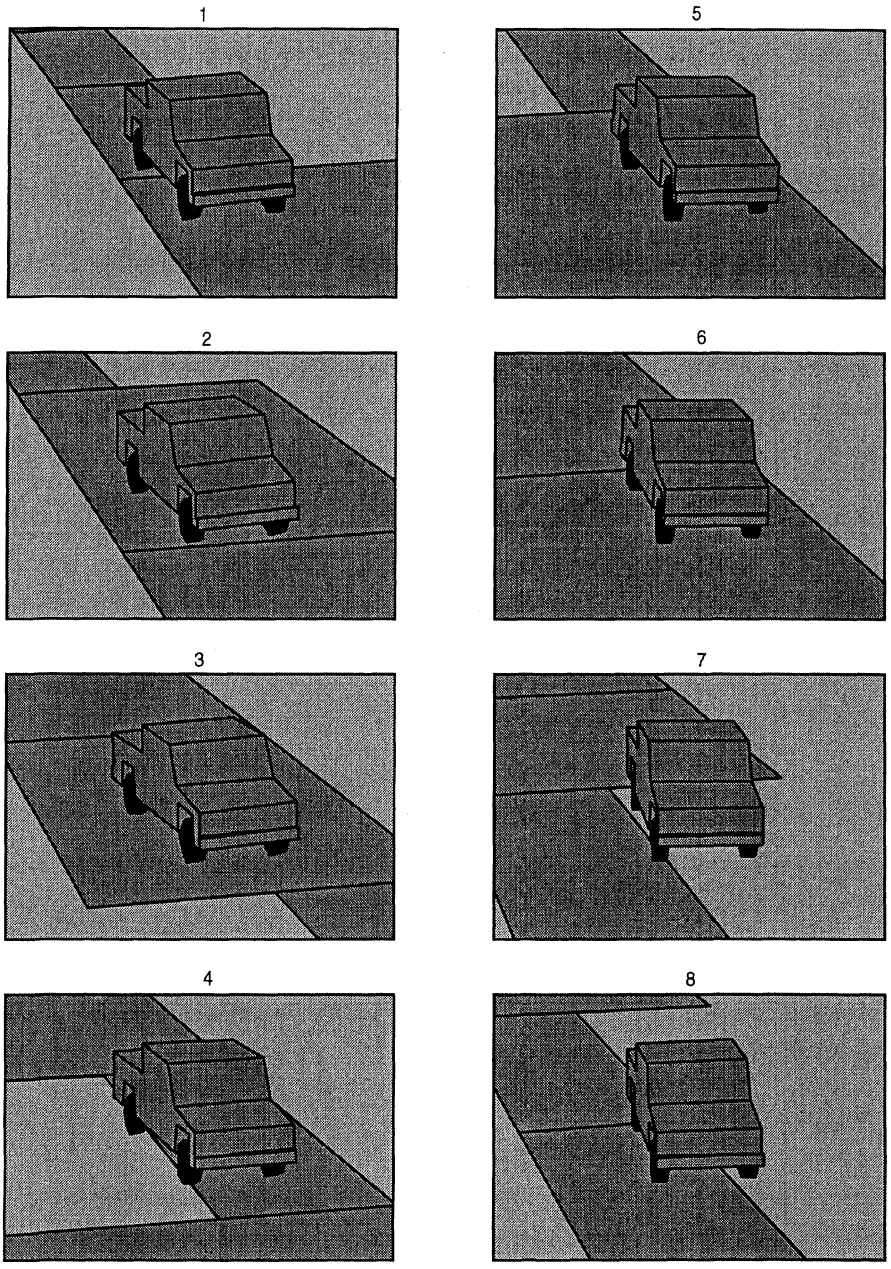

Figure 4.3-5. Animation Sequence for the Linear Driver Model and Slippery Patch Encounter.

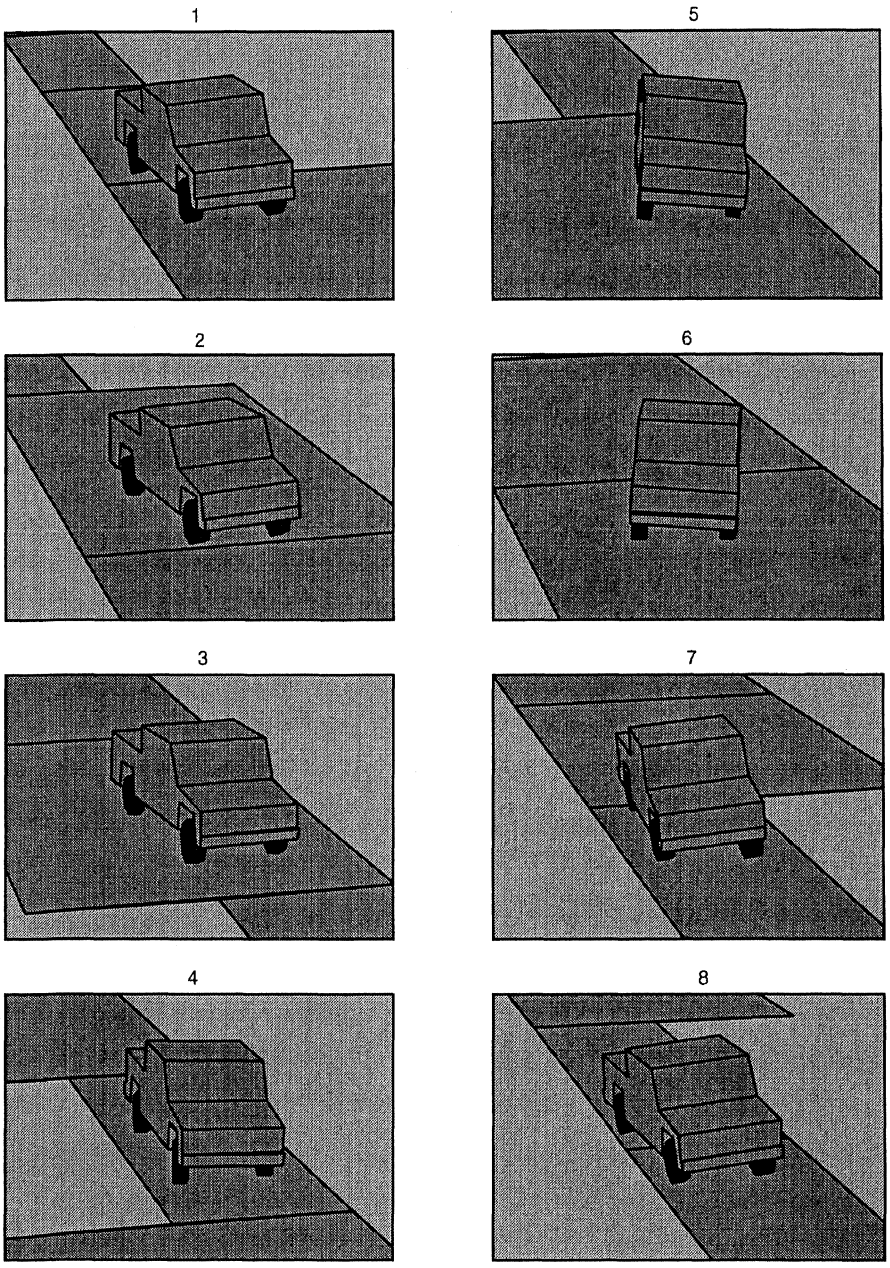

Figure 4.3-6. Animation Sequence for the Nonlinear Driver Model and Slippery Patch Encounter.

4.4 Double Lane-Change Example Run With a Tire Blow-Out

This example is similar to the previous low friction encounter, except that a single tire loses 90% of its force capability and the change in tire effectiveness remains for the duration of the run, not just for a short time, following the blow-out event. As depicted in Figure 4.4-1, the blow-out occurs at x = 89 meters of longitudinal vehicle position, causing the left front tire to drop to 10% of its normal cornering capability for the remainder of the run. Figures 4.4-2 and 4.4-3 show the corresponding path trajectories and driver model steering responses. Also overlaid on these plots are the two prior reference baseline runs (dashed lines) for the nonlinear and linear driver models absent the tire blowout event.

As seen in Figure 4.4-3, the driver model steering responses following the left front tire blowout event are dramatically different in their respective reactions to the blowout. The linear driver model shows a modest continuous departure from its baseline reference case as a result of the altered vehicle trajectory and vehicle directional response to the blowout. It is not directly aware of an immediate loss of tire force since no provision exists within that model to adapt to on-the-fly to sudden changes in operating conditions and it sees a "linear world." On the other hand, the nonlinear driver model does react immediately to the blowout by nearly doubling its steer input to compensate for the sudden loss of tire force at the left front wheel location. It also provides a steer input level (with and without a tire blowout) that is consistent with a "nonlinear world" insofar as realizing a tire/road friction limitation within this nonlinear operating environment. As the run proceeds, the nonlinear model then steers accordingly to return the vehicle to the desired course.

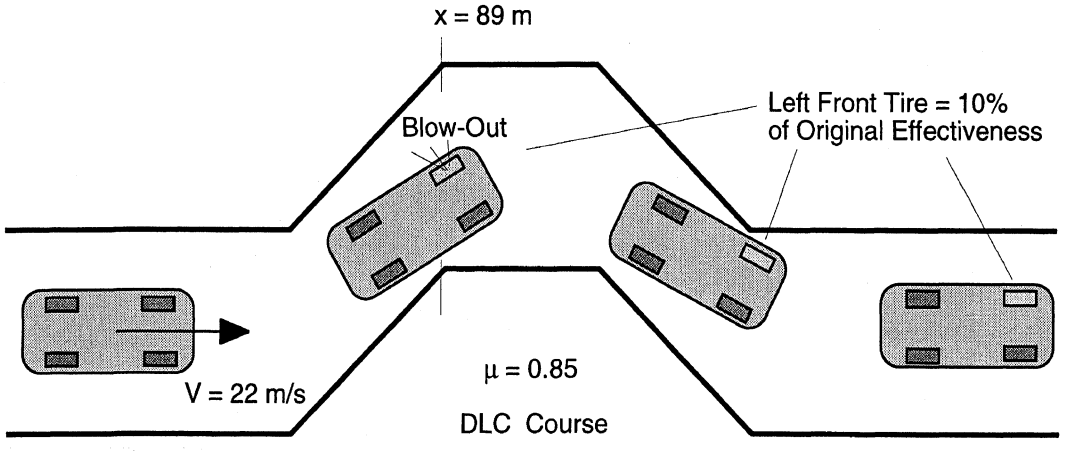

Figure 4.4-1. Double Lane-Change Maneuver with a Left Front Tire Blow-Out.

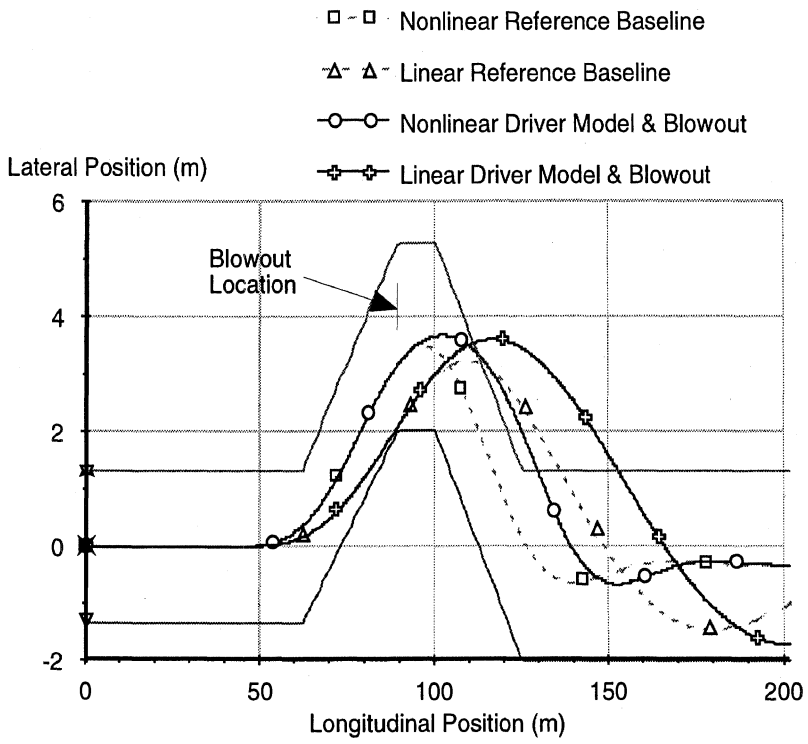

Figure 4.4-2. Path Trajectories With and Without Front Tire Blowout.

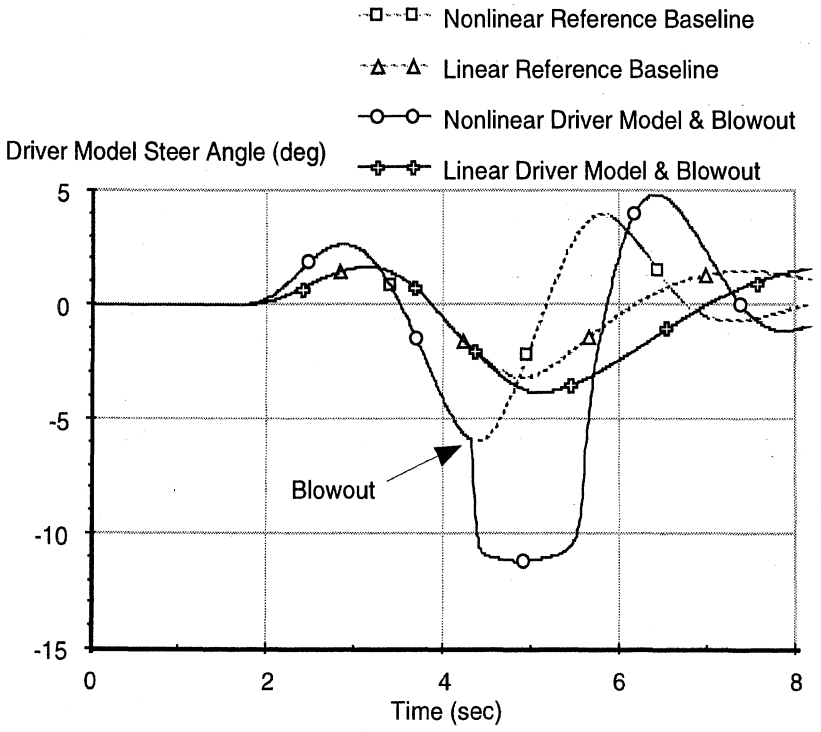

Figure 4.4-3. Driver Model Steering Responses – With & Without Front Tire Blowout.

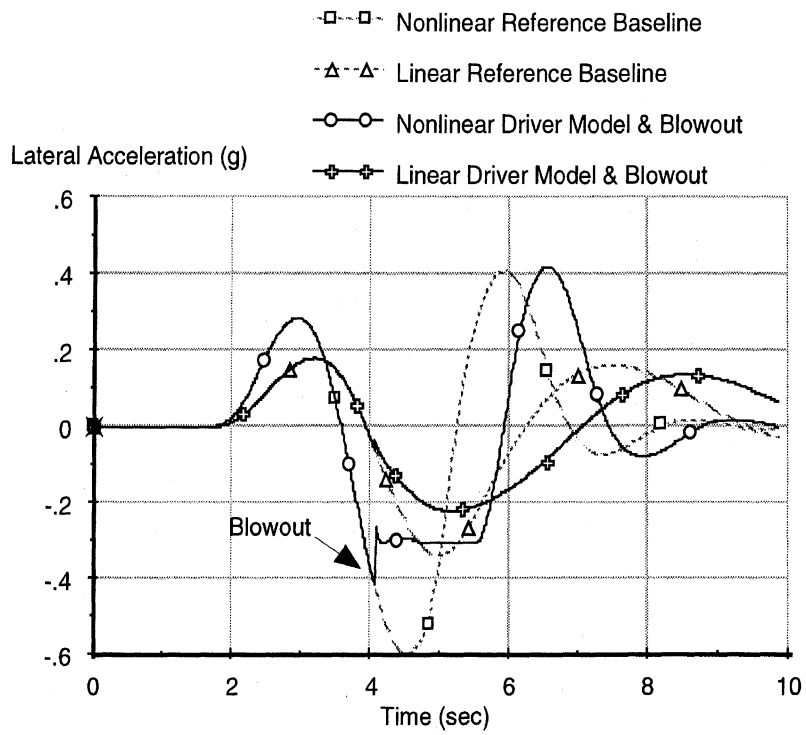

Figure 4.4-4. Lateral Acceleration Responses With & Without Front Tire Blowout.

The tire blowout example and the slippery pavement patch example both illustrate the increased sensitivity of the nonlinear driver model to external vehicle conditions over that exhibited by the linear model, particularly during maneuvers calling for elevated levels of lateral acceleration in which the dynamics of the controlled vehicle are operating for significant periods of time under nonlinear conditions. Under these circumstances, the internal vehicle dynamics present in the nonlinear driver model help to better predict and provide more accurate steering responses to those nonlinear factors present in the external vehicle model.

4.4.1 Nonlinear Driver Model Adaptation

One last topic for the nonlinear model relates to the issue of driver model adaptation to changes in the external vehicle environment. In the case of the fully adaptive driver model (default case), on-the-fly changes in the external vehicle model are communicated continuously to the nonlinear driver model. This includes surface friction changes or even individual tire force status information, as well as the normal state response of the external vehicle.

The non-adaptive version of the same nonlinear model can be implemented by not updating these acceleration-based information channels — such as tire/road surface friction or tire force status — to the driver model, only the vehicle state velocity and position information. In this case, the nonlinear model responds only to the change in positional or velocity state (over time) of the external vehicle model as a result of a particular force

disturbance or change in operating conditions (such as a surface friction change or tire force alteration). This is also the normal case for the linear driver model.

To compare how this continuous updating of acceleration-based information affects the nonlinear model performance, the blowout example is used to illustrate the differences. Figure 4.4-5 shows the steering responses for the fully adaptive model (as above) and the same model but without continuous updating of the tire force status. That is, the fully adaptive nonlinear model utilizes the vehicle state response information (positions and velocities) as well as current tire force information in order to predict future vehicle response and arrive at an appropriate compensatory steer response.

In the case of the non-adaptive nonlinear driver model, only the vehicle state response information is utilized for the prediction of future vehicle responses. The change in tire force status (i.e., a drop of 90% in tire force production by the left front tire at the time of the blowout until the remainder of the maneuver) is not communicated to the non-adaptive driver model. It responds only in reaction to the altered vehicle state response information following the blowout. Consequently, it reacts more gradually to the blowout event than the fully adaptive model, but still provides an effective steer response to the blowout event. The resulting path response is very close to that provided by the fully adaptive model. Furthermore, when compared to the comparable non-adaptive response provided by the linear model (seen above in Figure 4.3-3), the non-adaptive nonlinear driver model still far outperforms its linear counterpart.

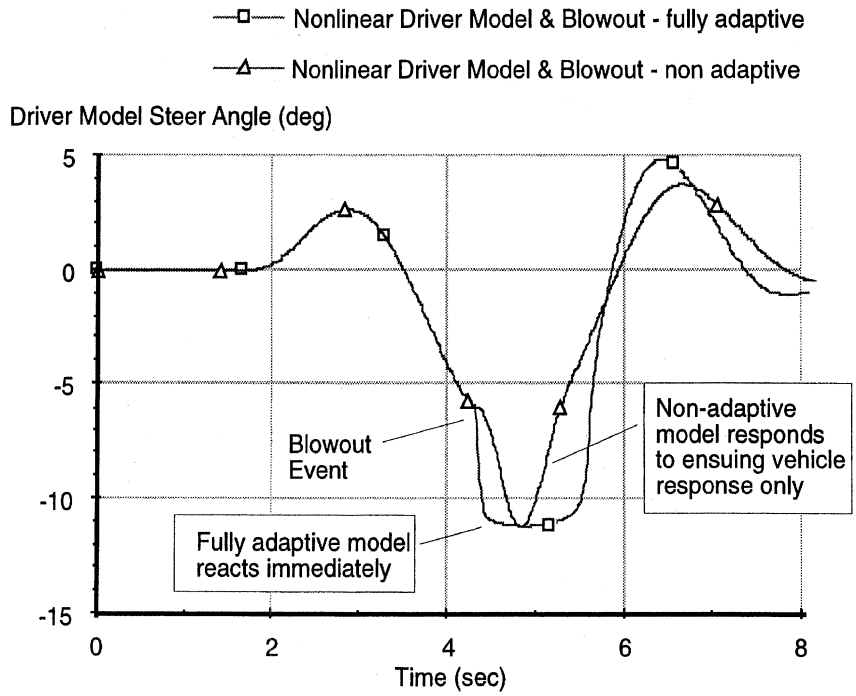

Figure 4.4-5. Influence of On-the-Fly Adaptation in the Nonlinear Driver Model.

Lastly, Figures 4.4-6 and 4.4-7 contain the animation sequences corresponding to the linear driver model and nonlinear (fully adaptive) driver model blowout example.

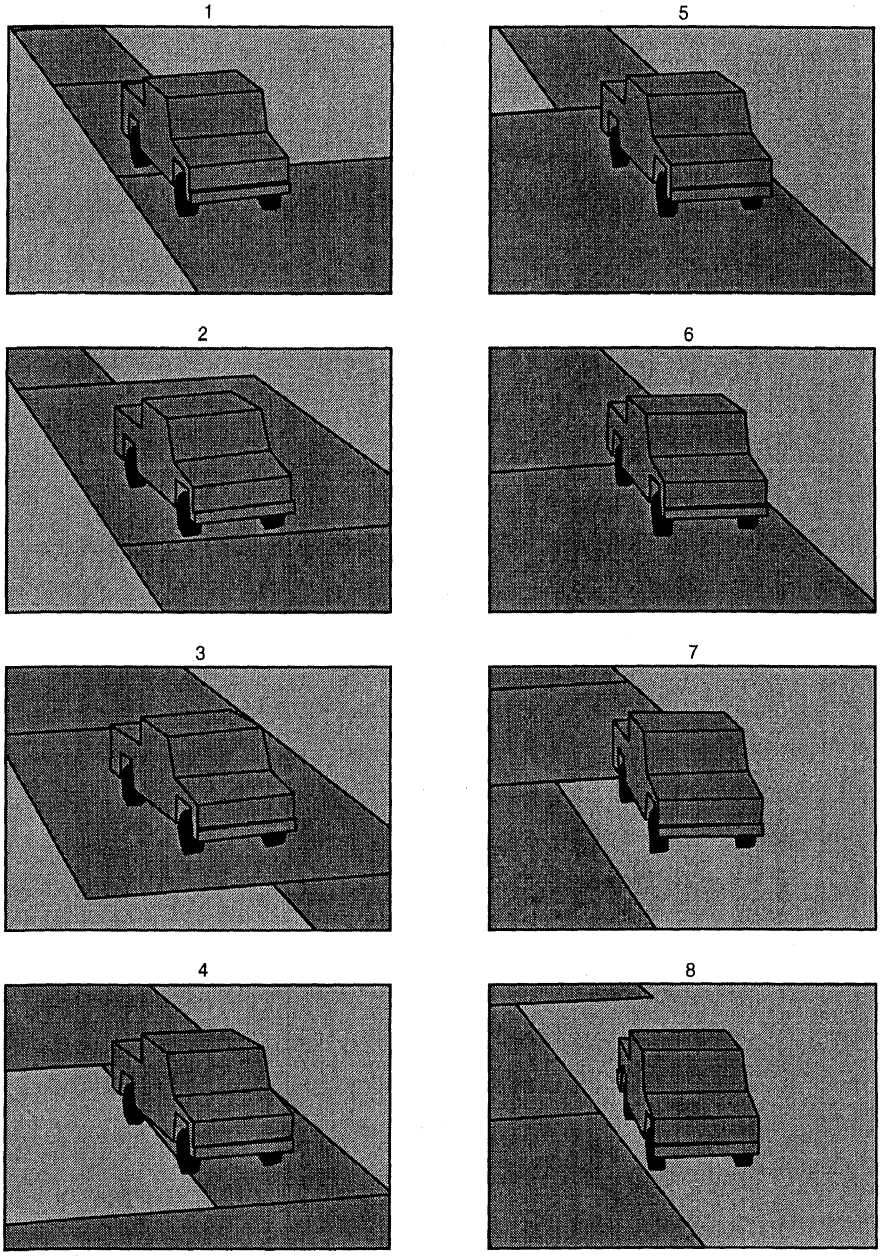

Figure 4.4-6. Animation Sequence for the Linear Driver Model and Tire Blowout Event.

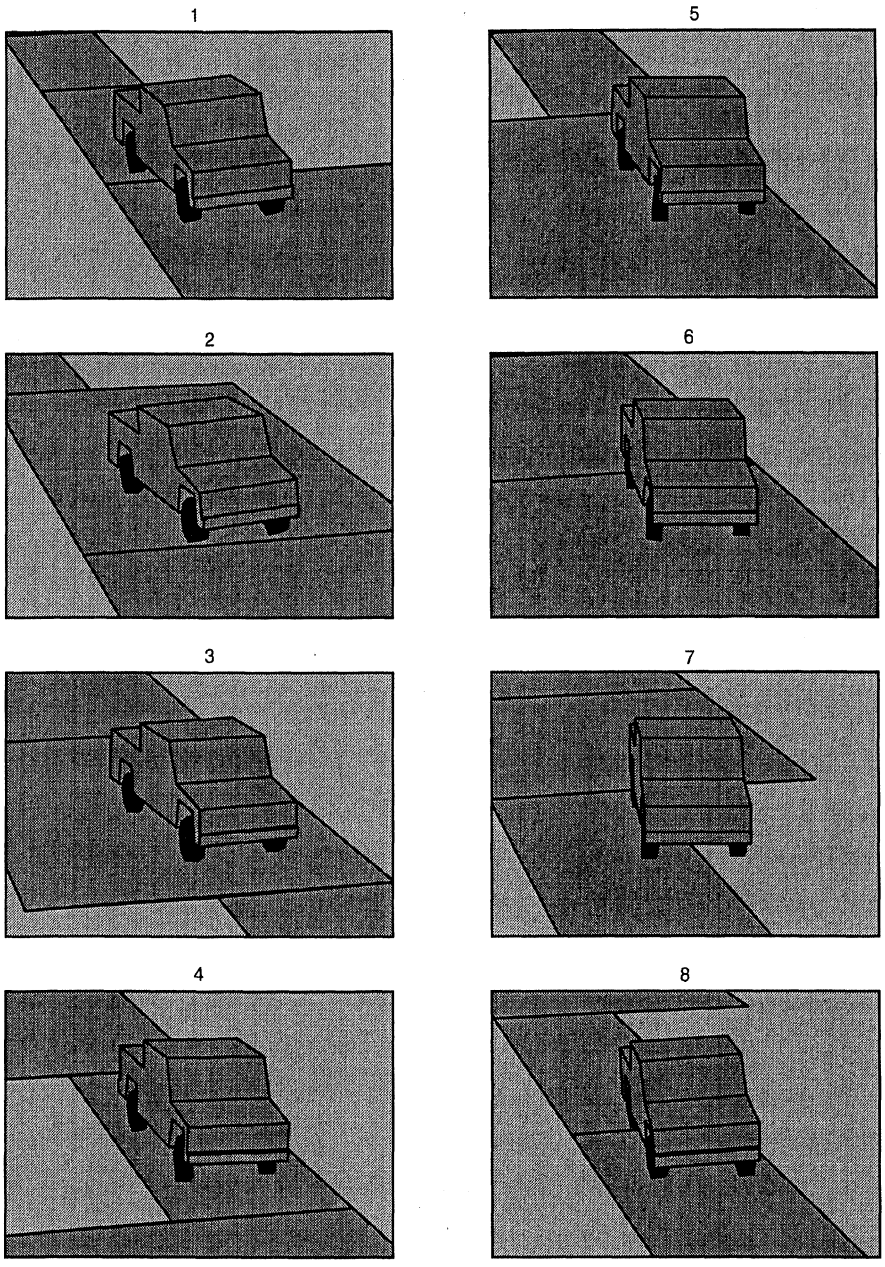

Figure 4.4-7. Animation Sequence for the Nonlinear Driver Model and Tire Blowout Event.

blank page

5.0 Driving Simulator Tests

A series of separate driving simulator tests were conducted for GM by a third party in order to collect a variety of test data intended for validation of the new GM nonlinear driver model. Three basic maneuvers were used in conjunction with twelve drivers. The drivers ranged in age from 15 to 67 and included three basic skill designations (novice, typical, and expert). The simulator test vehicle was a 3/4 ton pickup truck. The test matrix included two loading configurations of the vehicle and two surface friction conditions.

This section of the report describes the test configurations and driver profiles and then presents an initial analysis of the test data performed by UMTRI to help sort out the relative skill level of the twelve drivers.

Four drivers from this group of twelve were subsequently used in the driver model validation effort that is described in the next Section 6. Future work by GM can address similar validation or analysis efforts for the remaining drivers in the simulator test program data set or for other full-scale road test data that may be collected.

5.1 Driving Simulator Test Maneuvers

Three basic simulator maneuvers were primarily used to evaluate subject steering responses in the simulator environment. A fourth surprise obstacle avoidance maneuver was also mixed in intermittently. The three primary maneuvers included a) a double lane-change test procedure (DLC) similar to the ISO 3888 maneuver, but modified to make it more manageable for all drivers at mid-range speeds, b) a slalom course with non-repeatable longitudinal cone spacings, and c) a lane-change along a fixed-radius curve maneuver (LCIC). Each of these is described further below.

The speeds were held fixed in each of the tests and the driving subject was asked to perform the maneuver with steering control only. Each series of tests began at a lower speed for which the maneuver could be easily accomplished by the test subject. Most speeds were typically in the range of 10-20 m/sec. Each subsequent test incremented the speed by 1 m/sec. A test series was considered complete if the subject could not complete the maneuver — as defined by more than four cone-strikes or loss of control of the vehicle (spin-out or driving off the course). The highest five speeds achieved by a driver in any test maneuver and the number of average cone strikes in those five highest speed runs were then used subsequently as a measure of driver performance in that maneuver.

The matrix of test runs included two vehicle loading configurations (LVW / GVW), two tire/road surface conditions (dry / wet), and a numbers of test runs (ten or so) for each configuration at speeds below the maximum successful speed.

Double Lane-Change Maneuver — Figure 5.1-1 shows the course layout for the double lane-change maneuver used in the simulator tests. An example trajectory through the course is also seen in the figure. Distances shown are in meters.

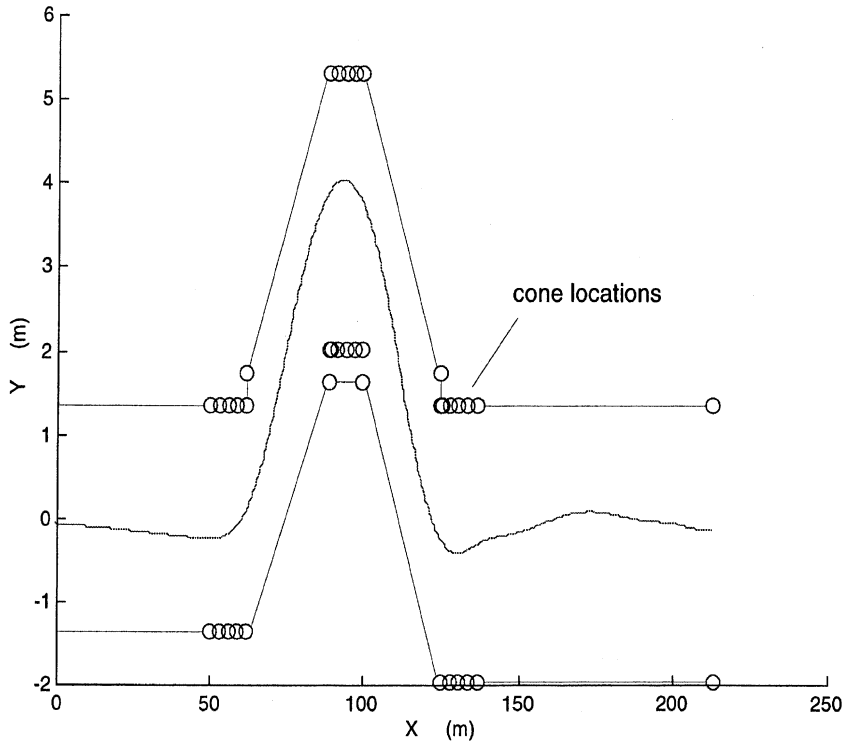

Figure 5.1-1. Double Lane-Change (DLC) Geometry Used in the Driving Simulator Tests.

Slalom Maneuver — Figure 5.1-2 shows the course layout for the slalom maneuver used in the simulator tests. As above, an example trajectory through the course is also seen in the figure. Distances are in meters. The longitudinal distances between cone placements are not equal. Also, no outer cones were used to bound a driver's lateral wandering when rounding a corner. (This was later seen to provide a fair amount of trajectory scatter in some drivers at lower and intermediate speeds since they would utilize a wide margin between the vehicle and the inner cone in order to play it safe at these speeds. Future slalom tests should probably use an outer cone, thereby providing a gate of comfortable width that at least limits excessive lateral wandering by some drivers.)

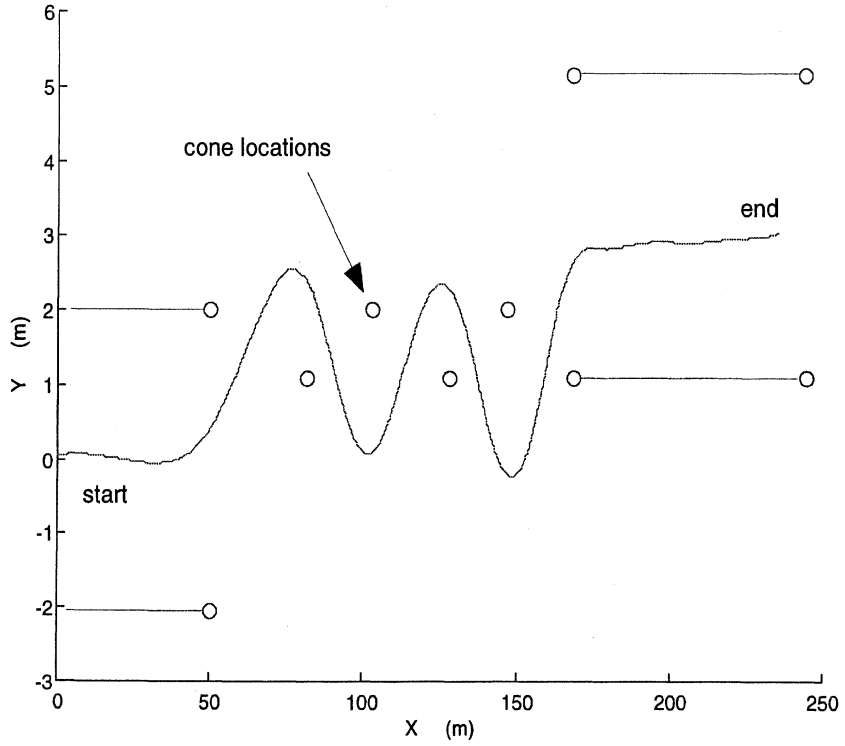

Figure 5.1-2. Slalom Geometry Used in the Driving Simulator Tests.

Lane-Change In a Curve (LCIC) Maneuver — Figure 5.1-3 shows the course layout for the lane-change in a curve maneuver also used in the simulator tests. An example trajectory through the course is seen in the figure. Distances are again in meters. The maneuver starts on a straight, then proceeds along a fixed radius curve. Fifty meters or so along the initial curve, a lane-change to a parallel inside fixed-radius curve is encountered. A straight-section then completes the maneuver 20 meters or so after completion of the lane-change. The lateral displacement of the lane-change is approximately 3.5 meters towards the inside of the curve.

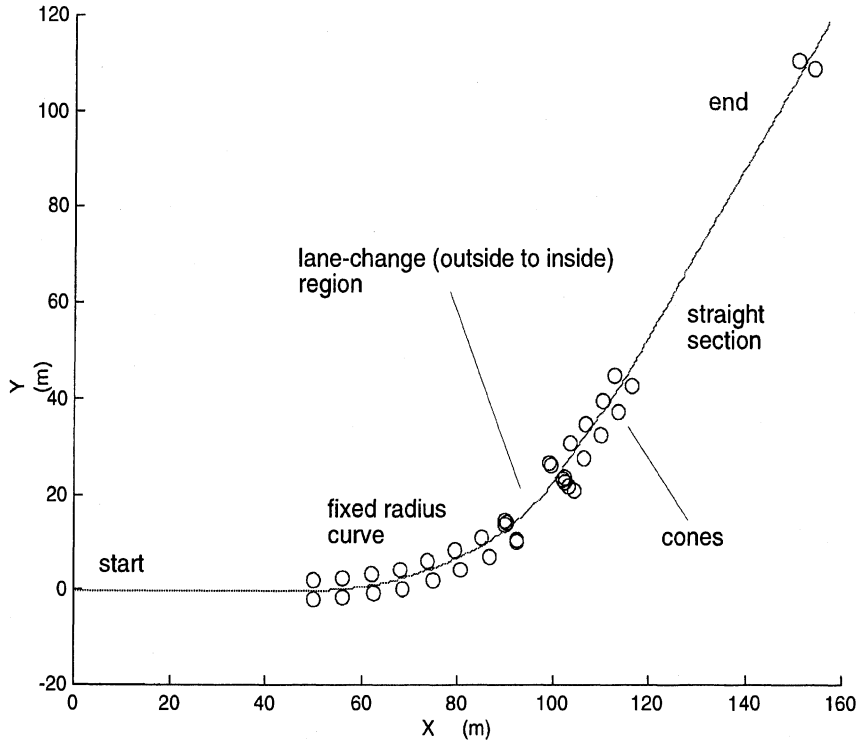

Figure 5.1-3. Lane-Change In a Curve (LCIC) Geometry Used in the Simulator Tests.

5.2 Test Driver Descriptions

Twelve subjects participated in the driving simulator tests. Each subject usually required two several-hour sessions to complete the entire matrix of simulator tests. Each session often took place on different days. In some cases several weeks separated the two sessions. Table 5.2-1 lists the twelve subjects by Subject Number, Name, Skill Category, Age, and Sex.

As seen in the table, driver age ranges from 15 to 67 years. Four subjects were classified as expert, including two GM staff engineers. Six subjects were classified as Typical. The two drivers classified as Novice were female teenagers with less than a year of total driving experience. The 15-year-old female subject had about three months of driving experience. The 16-year-old had been driving for about 6 months.

Table 5.2-1. Test Subjects Used in the Driving Simulator Tests.

Subject Number	Skill Category	Age	Sex
6	Typical	67	M
250	Typical	49	F
257	Typical	65	F
258	Typical	21	M
262	Typical	21	F
353	Novice	16	F
356	Expert	56	M
357	Expert	47	M
358	Typical	50	M
360	Novice	15	F
9964	Expert	31	M
9996	Expert	44	M

5.3 Initial Analysis of the Driving Simulator Test Data

The simulator test data were initially processed by UMTRI to obtain general information on overall average speed of travel and overall average cone strike performance for each driver. Test speeds and cone strikes for each maneuver were cumulatively averaged over each driver to obtain an approximate overall rating of driver steering accuracy (represented by a lower cone strike average) and an overall average test speed covering all test conditions/maneuvers. An initial plot of these results was then made to summarize the range of average travel speed and average cone strike performance (steering accuracy) for each of the twelve test drivers. Figure 5.3-1 shows this plot with each driver designated with a subject identification number (from Table 5.2-1) and symbols denoting their respective skill level.

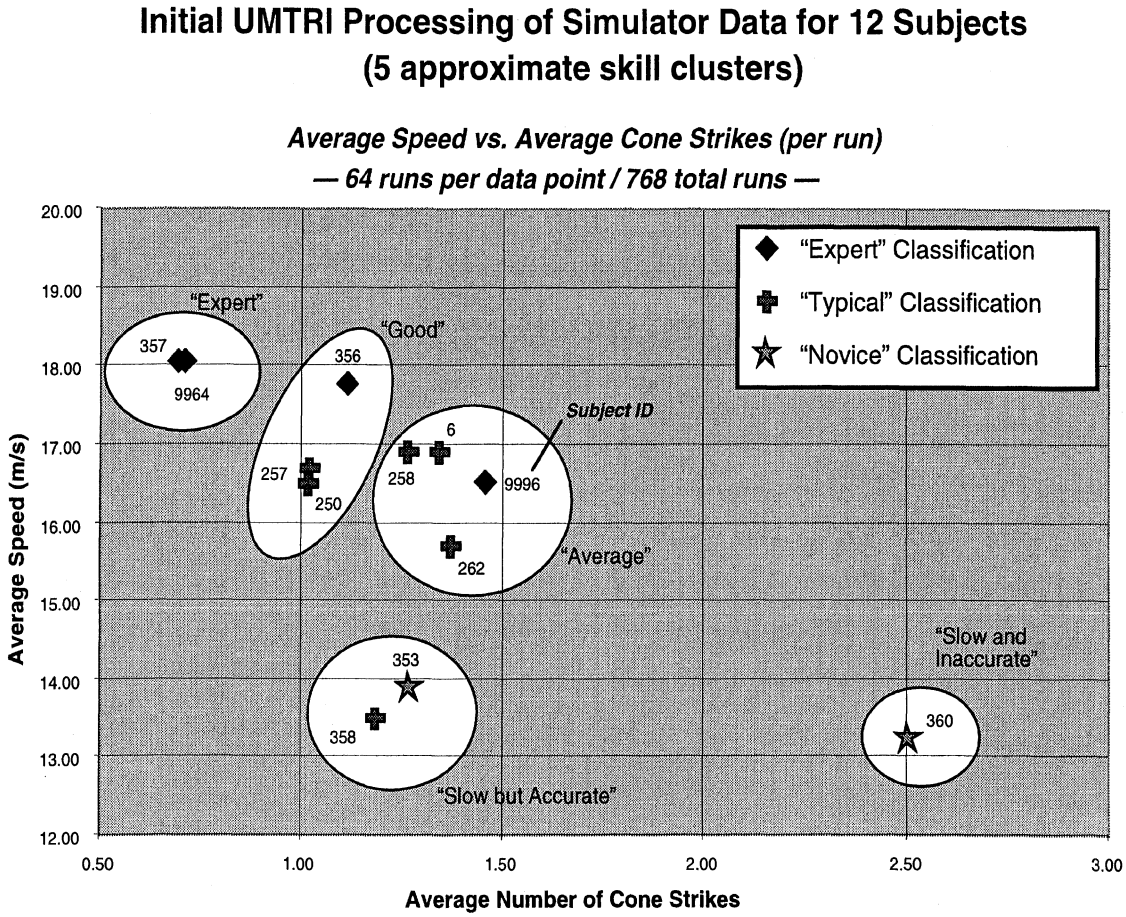

Figure 5.3-1. Speed vs. Cone Strike Plot for All Simulator Test Drivers.

In general, the plot shows a reasonable trend and grouping of expected and actual skill levels versus associated travel speeds. The highest skill level region on this plot is in the upper left corner where higher speeds and lower cone strike activity occurs. Correspondingly, the lowest skill level region is in the lower right corner where lower speeds and greater cone strike activity combine. Five simple clusters of overall skill are designated on the plot indicated by the ellipsoid regions and descriptive tags labeled as "expert," "good,'" "average," "slow but accurate," and "slow and inaccurate." These latter skill labels were assigned by UMTRI based upon the groupings seen in the figure. Clearly, other grouping arrangements could be designated and labeled accordingly. This initial grouping was simply an attempt to categorize the indicated data into five or so different skill levels.

The data show that indeed three of the four 'expert' drivers (356, 9964, and 356) performed as about as expected, lying in the upper left corner of the plot. The remaining 'expert' driver performed more as a 'typical' driver within this sample of drivers. Also, the 15-year-old 'novice' driver is located on the far lower right of the plot where the lowest average speed and highest cone-strike activity occurs. The other novice driver (#353) is seen within the "slow but accurate" category along with a 50-year-old male driver.

It should be noted that the indicated rankings here correspond to overall average performance and do not necessarily reflect individual achievement in every maneuver. That is, a particular test subject may have outperformed another test subject in two of the three test maneuvers by a small margin, but performed significantly poorer in the one remaining maneuver, thereby placing slightly lower in the overall ranking.

The data appearing in Figure 5.3-1 were obtained by processing the five highest speed runs performed successfully by each driver in each maneuver. The average travel speed in each maneuver was calculated along with the average number of cones hit in each maneuver. This comprised 64 runs per subject (3 maneuvers x 2 vehicle loading configurations x 2 surface friction conditions x 5 highest speed runs + 4 surprise obstacle avoidance maneuvers). Hence, a total of 768 runs (64 runs x 12 subjects). Each subject data point appearing in Figure 5.3-1 therefore represents an average result of 64 simulator test runs.

An example of this type of calculation is seen in Table 5.3-1 for subject 357. Each row is a separate run corresponding to one of the 64 tests. The first column is the file name, the second column is the subject ID, the third column shows the maneuver code, and the fourth column contains the number of cone strikes recorded in each run. The remaining column tag abbreviations are:

speed	- average speed for the run (meters/sec)
aymin	- minimum lateral acceleration experienced (g)
aymax	- maximum lateral acceleration experienced (g)
dswmin	- minimum steering wheel angle value (deg)
dswmax	- maximum steering wheel angle value (deg)
betamin	- minimum vehicle sideslip angle (deg)
betamax	- maximum vehicle sideslip angle (deg)
r-min	- minimum vehicle yaw rate (deg/s)
r-max	- maximum vehicle yaw rate (deg/s)
Csi	- average cone strike/run for the maneuver (5 run average)
Vi	- average speed/run for the maneuver (5 run average)

These latter min/max numerics were obtained by scanning each time history test file for their minimum and maximum values.

At the very bottom of the Table 5.3-1, values for the average cone strike per run and for the average travel speed per run are seen. In this example for subject 357, the two numbers are 0.7031 cone strikes per run and 18.092 meters/sec respectively. These two values are then plotted for subject 357 on the graph of Figure 5.3-1. Identical calculations were performed for the remaining 11 subjects appearing in Figure 5.3-1.

Table 5.3-1. Example Processing Result for Driver No. 357.

file-name	subj	maneuv	cones	speed	aymin	aymmax	dswmin	dswmax	betamin	betamax	r-min	r-max	Csi	Vi
/sd0/GMDM2123.DAT	357	1	0	16.2	-0.22	0.57	-50.5	153.4	-0.6	0.9	-8.5	21.9		
/sd0/GMDM2124.DAT	357	1	0	17.1	-0.18	0.57	-40.3	147.5	-0.5	0.6	-6.8	21		
/sd0/GMDM2125.DAT	357	1	0	18.1	-0.36	0.63	-74.7	172	-1.9	0.7	-13.3	23.5		
/sd0/GMDM2126.DAT	357	1	2	19	-0.52	0.64	-113.7	178.7	-6.8	1.1	-27.2	27.4		
/sd0/GMDM2127.DAT	357	1	4	20	-0.01	0.69	-161.8	208.7	-58.8	0.3	-0.3	47.1	1.2	18.08
/sd0/GMDM2082.DAT	357	2	0	15.2	-0.31	0.54	-79	139.6	-1	1.4	-11.8	21.5		
/sd0/GMDM2083.DAT	357	2	0	16.2	-0.17	0.6	-41	152.4	-0.5	1.1	-6.6	22.8		
/sd0/GMDM2084.DAT	357	2	0	17.1	-0.4	0.63	-99.8	156.7	-1	1	-15.3	22.6		
/sd0/GMDM2085.DAT	357	2	2	18.1	-0.16	0.62	-36.3	150.4	-0.5	0.5	-6.3	21.8		
/sd0/GMDM2086.DAT	357	2	2	19	-0.37	0.69	-80.2	182.1	-3.4	0.7	-17	25.5	0.8	17.12
/sd0/GMDM2075.DAT	357	3	0	21.5	-0.63	0.54	-157.4	123	-1	1.9	-21.1	18.3		
/sd0/GMDM2128.DAT	357	4	0	21.4	-0.65	0.58	-147.8	130.8	-1	1.3	-21.2	19.7		
/sd0/GMDM2150.DAT	357	5	3	18.1	-0.44	0.45	-91.8	94.3	-0.5	0.6	-14.8	15.3		
/sd0/GMDM2151.DAT	357	5	0	19	-0.48	0.48	-100.5	111.7	-0.4	0.5	-15.7	17.1		
/sd0/GMDM2152.DAT	357	5	0	20	-0.53	0.49	-114.8	111.1	-0.6	0.7	-16.8	17.3		
/sd0/GMDM2153.DAT	357	5	4	20.9	-0.45	0.6	-85.8	147.9	-1.5	0.6	-13.5	20.7		
/sd0/GMDM2154.DAT	357	5	0	21.9	-0.56	0.53	-116.6	125.6	-1.1	0.9	-16.5	18.8	1.4	19.98
/sd0/GMDM2096.DAT	357	6	0	17.1	-0.36	0.49	-74.5	110.9	-0.6	0.9	-12.7	17.9		
/sd0/GMDM2097.DAT	357	6	0	18.1	-0.48	0.39	-101	84.8	-0.6	0.7	-16.4	14		
/sd0/GMDM2098.DAT	357	6	0	19	-0.5	0.54	-100.6	120.6	-0.4	0.6	-16.1	18.8		
/sd0/GMDM2099.DAT	357	6	0	20	-0.39	0.63	-75.1	142.8	-0.9	0.6	-12.6	21.3		
/sd0/GMDM2100.DAT	357	6	2	20.9	-0.56	0.47	-112.3	100.8	-0.4	0.6	-17.2	16.2	0.4	19.02
/sd0/GMDM2108.DAT	357	7	0	13.4	-0.37	0.49	-107.9	153.3	-1.8	2.2	-17	22.6		
/sd0/GMDM2109.DAT	357	7	0	14.3	-0.44	0.55	-121.5	165	-1.6	1.9	-18.8	23.9		
/sd0/GMDM2110.DAT	357	7	0	15.2	-0.6	0.64	-271.8	283.4	-2.3	1.8	-29.6	31		
/sd0/GMDM2111.DAT	357	7	0	16.2	-0.61	0.64	-219.7	253.2	-2.9	1.5	-27	29.9		
/sd0/GMDM2112.DAT	357	7	1	17.1	-0.35	0.53	-80.8	129.8	-0.7	1	-12.9	19.7	0.2	15.24
/sd0/GMDM2134.DAT	357	8	0	14.3	-0.5	0.54	-135.6	157	-1.7	2	-21.1	23.6		
/sd0/GMDM2135.DAT	357	8	0	15.2	-0.44	0.52	-108.1	137.4	-1.2	1.6	-17.5	20.8		
/sd0/GMDM2136.DAT	357	8	0	16.2	-0.55	0.6	-137	163	-1.1	1.4	-21	23.9		
/sd0/GMDM2137.DAT	357	8	0	17.1	-0.55	0.58	-131.3	137.9	-1.2	1.1	-20.3	21		
/sd0/GMDM2138.DAT	357	8	2	18.1	-0.55	0.64	-131.8	159.8	-1	1	-20.3	23.1	0.4	16.18
/sd0/GMDM1966.DAT	357	9	0	15.8	-0.24	0.52	-63.8	135	-0.6	0.5	-10.6	21.1		
/sd0/GMDM1967.DAT	357	9	0	16.7	-0.36	0.58	-96.5	148.2	-0.9	0.6	-15.3	22.1		
/sd0/GMDM1968.DAT	357	9	0	17.6	-0.33	0.6	-74.6	151	-1.4	0.6	-13.1	22		
/sd0/GMDM1969.DAT	357	9	0	18.5	-0.33	0.64	-76.1	179.2	-3	0.6	-14.1	23.9		
/sd0/GMDM1970.DAT	357	9	2	19.4	-0.32	0.65	-63.7	197.9	-4.9	0.5	-15.5	24.2	0.4	17.6
/sd0/GMDM1925.DAT	357	10	0	17.2	-0.17	0.61	-46.7	143.6	-0.8	0.4	-7.6	22.5		
/sd0/GMDM1926.DAT	357	10	0	18.1	-0.32	0.63	-72.4	143.2	-1.2	0.5	-12.7	22		
/sd0/GMDM1927.DAT	357	10	2	18.9	-0.24	0.67	-60.6	161.1	-2.4	0.3	-11.6	23.8		
/sd0/GMDM1928.DAT	357	10	3	19.9	-0.41	0.72	-73.2	185.9	-4.8	0.7	-16.6	25.7		
/sd0/GMDM1929.DAT	357	10	2	20.9	-0.2	0.71	-31.7	177.1	-4.1	0.3	-9	23.6	1.4	19
/sd0/GMDM1956.DAT	357	11	0	21.4	-0.65	0.55	-155.4	124.8	-1.9	3.8	-23.3	19.6		
/sd0/GMDM1955.DAT	357	12	0	21.4	-0.72	0.67	-169	147.9	-4.2	4.4	-25.2	26.9		
/sd0/GMDM1991.DAT	357	13	0	16.1	-0.35	0.41	-75.7	94.8	-0.3	0.5	-13	15.4		
/sd0/GMDM1992.DAT	357	13	1	17.2	-0.42	0.4	-89.7	92.9	-0.4	0.3	-15.2	15.3		
/sd0/GMDM1993.DAT	357	13	0	18.1	-0.43	0.47	-88	109.8	-0.7	0.3	-14.8	17.5		
/sd0/GMDM1994.DAT	357	13	4	18.9	-0.39	0.6	-72.5	158.2	-2.2	0.7	-12.5	23.4		
/sd0/GMDM1995.DAT	357	13	3	19.9	-0.44	0.62	-83.7	169.6	-3.1	0.8	-13.9	24.5	1.6	18.04
/sd0/GMDM2006.DAT	357	14	1	18.1	-0.44	0.59	-88.5	136	-1.1	0.5	-15.1	21.6		
/sd0/GMDM2007.DAT	357	14	0	18.9	-0.51	0.47	-110.5	99.5	-0.7	0.8	-17.2	16.7		
/sd0/GMDM2008.DAT	357	14	0	19.9	-0.55	0.67	-114.5	164.8	-2.8	1.1	-18.3	25.4		
/sd0/GMDM2009.DAT	357	14	4	20.9	-0.53	0.68	-102.2	165.3	-3.4	1.2	-17.1	25.5		
/sd0/GMDM2010.DAT	357	14	0	21.9	-0.6	0.61	-118.7	124.2	-2.1	1.7	-18.1	20.6	1	19.94
/sd0/GMDM2062.DAT	357	15	0	15.3	-0.41	0.51	-103.9	144.7	-0.6	0.8	-16.8	22		
/sd0/GMDM2063.DAT	357	15	0	16.1	-0.48	0.58	-119.2	167.1	-1	0.8	-19.3	24.8		
/sd0/GMDM2064.DAT	357	15	0	17.2	-0.63	0.65	-191.8	183.5	-3	3.4	-28.7	26.5		
/sd0/GMDM2065.DAT	357	15	0	18.1	-0.62	0.63	-171.4	180.7	-3.1	2.1	-24.2	26.6		
/sd0/GMDM2066.DAT	357	15	0	18.9	-0.61	0.65	-164.1	191.4	-4.5	3.5	-26.6	27.3	0	17.12
/sd0/GMDM2048.DAT	357	16	0	15.3	-0.5	0.58	-134.3	155.1	-0.9	0.9	-20.9	24.2		
/sd0/GMDM2049.DAT	357	16	0	16.1	-0.65	0.73	-216.1	301.8	-3.9	2	-29.8	32.7		
/sd0/GMDM2050.DAT	357	16	0	17.2	-0.51	0.65	-125.4	172.2	-1.5	0.7	-20.6	26		
/sd0/GMDM2051.DAT	357	16	0	18.1	-0.66	0.69	-160.5	190.8	-2.9	1.8	-24.4	28.1		
/sd0/GMDM2052.DAT	357	16	1	18.9	-0.71	0.71	-200.4	186.8	-4.5	3.2	-27.1	30.4	0.2	17.12

			CS-ave	V-ave									CS-ave	V-ave
			0.7031	18.092									0.75	17.87
													CS/V-ave	

An important observation regarding the data appearing in the skill diagram of Figure 5.3-1 is worth noting. The level of discrimination between the different skill levels is not terribly large (other than for the 15-year-old driver # 360). In fact, nine of the twelve drivers are grouped within about 2 m/sec of each other in terms of average speed. In addition, less than one cone strike per run separates eleven of the twelve drivers from one another in terms of steering accuracy. Consequently, subsequent efforts to associate skill level with relatively subtle differences in the closed-loop performance of the different drivers may prove challenging with these data.

5.4 Sample Data from the Simulator Tests

To illustrate the range of time history behavioral differences existing within the subject pool, the next two figures are helpful. Figures 5.4-1 and 5.4-2 show example path trajectories and corresponding steering responses for one expert and one novice driver (#357 and 353 respectively). The simulator responses seen in the two figures correspond to the four highest speed runs performed successfully for each respective driver in this maneuver. The test configuration is the GVW vehicle on the high friction surface. These data help to illustrate the type of trajectory scatter that can occur with different driver skill levels and the differences in speed between such drivers at their respective near-limit condition. As noted later, the lower speeds utilized by the novice driver are self-imposed and not related to vehicle or surface friction limitations. The lower travel speed selected by the novice driver also produces the marked time-shift in the steering responses seen in Figure 5.4-2. If these were normalized by time, the basic closed-loop damping characteristics would be fairly similar for the two drivers.

The model validation effort that followed this preliminary analysis of all twelve subjects focused on a subset of four drivers. This paring of data was necessary within the scope of this project effort in order to accomplish a basic validation analysis within the allotted time schedule initially proposed. The four drivers selected for the validation analysis were subjects 356, 357 (experts, GM staff), subject 6 (typical, 67-year-old male), and subject 353 (novice, 16-year-old female). These validation analyses are described in the next Section 6.

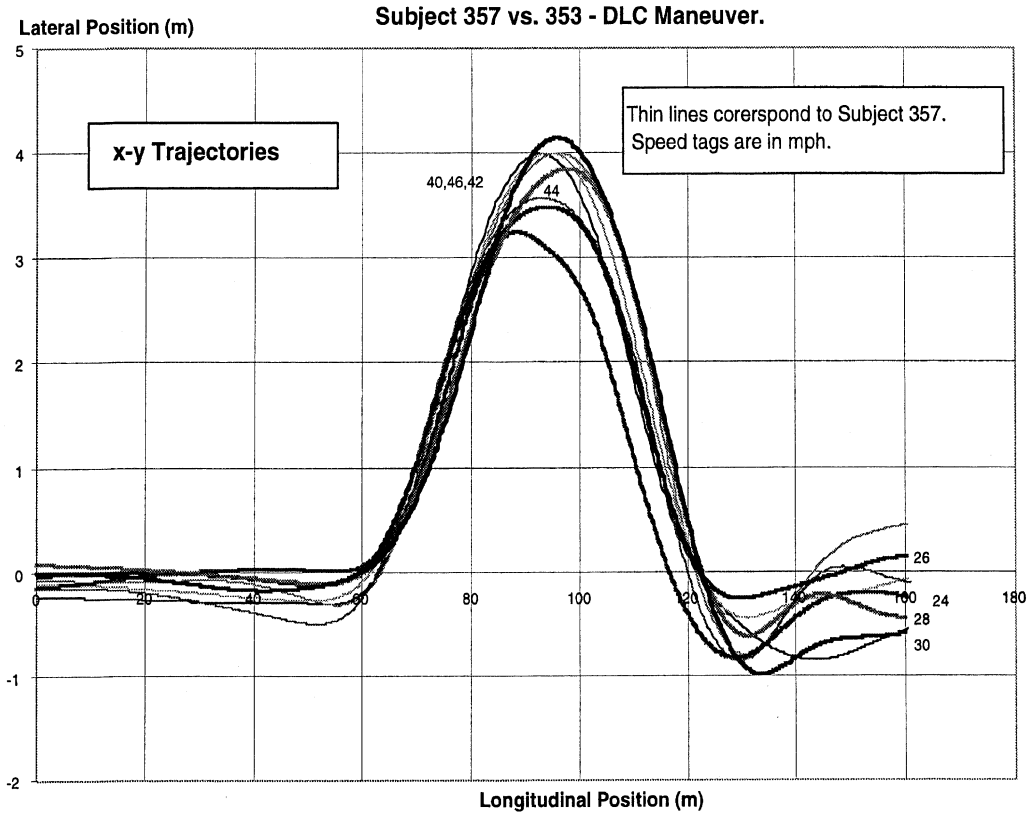

Figure 5.4-1. Example Trajectories for Subjects 357 and 353 in the DLC Test.

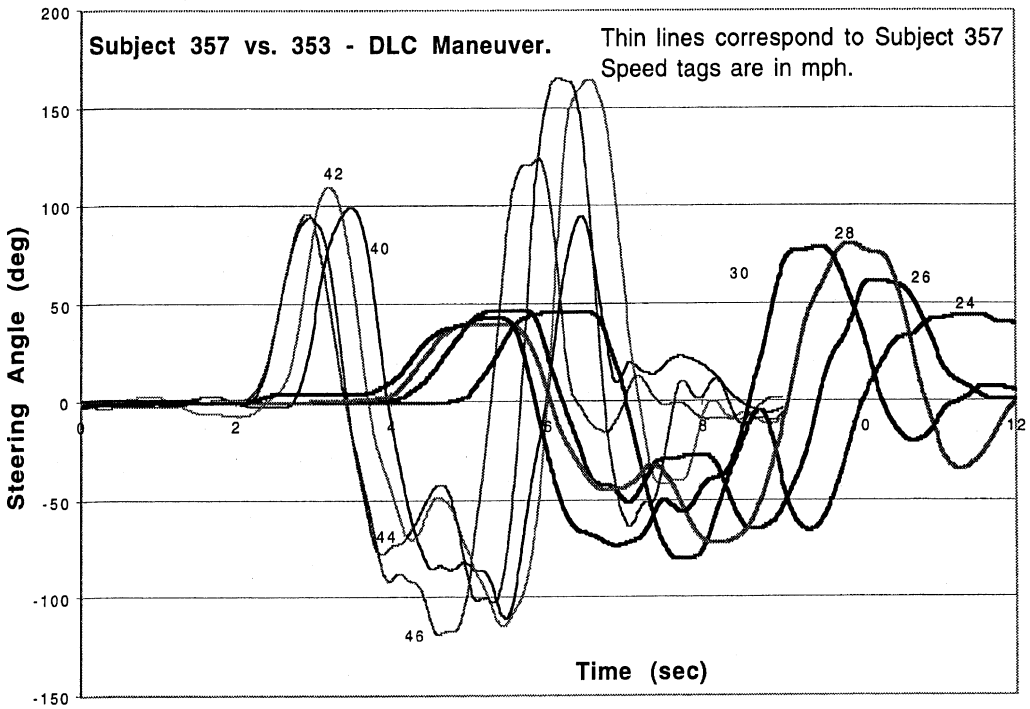

Figure 5.4-2. Corresponding Steering Responses for Subjects 357 and 353.

6.0 Driver Model Validation

It should be noted that the initial proposal to GM recommended that the validation tests conducted under this modeling effort be full-scale test track experiments so as to gather reliable experimental driver/vehicle test data that represent fully realistic interactions between the vehicle and the driver. The substitution of driving simulator data for test track data during the course of the project introduced an increased sense of uncertainty as to the meaning of the validation plans for the new driver model. Since most simulators have a limited response capacity in terms of their motion platforms, and also within their visual realms in terms of acuity and depth perception, questions can arise as to what is being validated in such experiments. On the one hand, the driver model developed under this work is intended to represent a driver within an actual driving environment reacting to the sensed motions and forces actually provided by that driving experience and the controlled vehicle. On the other hand, a subject within a simulator is reacting to an artificial environment that only approximates a desired reality and the subject responds to motions, forces, and visual stimuli that can vary considerably in fidelity and thereby provide, in many cases, only gross approximations to the real driving experience. Consequently, the term "validation" needs to be qualified in its usage under this work. The validation that is being presented here is really a validation of the driver model for representing a specific set of driving simulator data. It should not be argued that agreement, or lack of agreement, within the comparisons that follow, provide a sound basis, as yet, for recommending or rejecting the developed model for predicting real world driver-vehicle interactions. Only full scale driver-vehicle measurements provided by test track experiments can unambiguously yield that level of certainty.

Nevertheless, the driving simulator data still offer an opportunity to qualitatively compare responses provided by actual human subjects, in an albeit artificial driving environment, with predicted responses from a model that also offers an artificial reproduction of the real thing. So, bearing this mind, the following "validation" comparisons are provided as a next best substitute for a true validation exercise.

It may also very well turn out that subsequent (future) validations by GM involving full-scale test track data and the new driver model do largely substantiate the observations reported here with respect to these simulator data. If so, the data bank of driver-vehicle simulator data collected under this project will become in a sense validated indirectly and gain greater value as a result.

6.1 Validation Comparisons Between Simulator Tests and the GM Driver Model

Test data from four simulator subjects were selected from the pool of available simulator data in order to compare against predicted responses from the GM driver model in identical maneuvers. The next-to-highest speed run successfully completed by each driver in each maneuver was selected as the target comparison condition. The test configuration selected was the loaded GVW vehicle on the high friction surface. (It turned out that only small differences existed between the selected tire data on wet and dry

surfaces. In addition, no dramatic dynamic differences existed between the loaded and unloaded vehicle configurations. Consequently, any one of the four vehicle/surface configurations would likely yield the same basic information in terms of test versus model in these particular comparisons.)

The four drivers selected for the comparisons were the two GM staff members (driver ID's #356 and #357), the 67-year-old male (driver ID #6), and the 16-year-old female (driver ID #353). Model-simulator comparisons were conducted for each of the three basic maneuvers (DLC, Slalom, and LCIC) at the next-to-highest speed successfully completed in each respective maneuver. Accordingly, twelve simulator versus model comparisons are presented that involve four drivers and three maneuvers.

As indicated, model-simulator comparisons were conducted for each maneuver/driver combination at the next-to-highest speed successfully completed. This criterion guaranteed that most drivers were operating at a near-limit condition determined by the tire-road friction limit. In some cases, particularly with the novice drivers, the near-limit condition was not determined by the vehicle and the tire-road friction level, but rather, by a self-imposed speed restraint or comfort preference set by the driver. Consequently, most simulator tests conducted here with either of the novice drivers will indicate peak levels of lateral acceleration that are commonly 25% to 50% below the actual limit of the vehicle. Most other drivers operated the vehicle at or near its friction limit capability.

The tire-road friction limit for all of the validation runs shown here is approximately 0.75 g's. The actual tire data peak friction is about 0.85 but the mechanical properties of the tire under load and the understeer properties of the vehicle limit the actual lateral acceleration capability to a somewhat lower level.

The first set of comparisons correspond to Driver 357 ("expert" category) and are seen in Figures 6.1-1 through 6.1-3. Figure 6.1-1 shows the double lane-change result for this driver in test number 2010. Also overlaid on each set of graphs is the corresponding response prediction of the GM driver model in the same maneuver.

Before discussing these results, the protocol for the driver model runs should be noted. In each case, the same course geometry as used in the simulator was employed for these runs. Also, 70 ms of sensory input delay was applied to each incoming vehicle signal to the driver model to approximate the known 70 ms transport delay present in the simulator motion/visual system. (Normally this would be zero or near-zero for full-scale road tests.) Two driver model parameters, the driver preview (look-ahead time) and the transport delay (steering output block) were then varied by trial and error to obtain a suitable matching between the simulator tests and the model predictions. In most cases, some modest adjustment of the path boundaries was also performed to improve basic vehicle path trajectory matchings. The output of each test-model matching is then a set of parameters — 1) driver model preview time, and 2) driver model transport delay — that provided the best fit seen in each of the following comparison figures. A summary of these two driver model control parameters for each of the validation comparisons is discussed following the test versus model comparisons in Section 6.2.

As seen in Figure 6.1-1, the level of agreement for the double lane-change maneuver and Driver 357 is quite good. In most of these validation runs, the greatest level of discrepancy will typically show up in the vehicle sideslip response and in occasional wobbles or peculiarities in the driver steering response. The former is due to imperfect matchings between the simulator dynamics/tire data and their counterparts employed in the external vehicle model. Steering differences that do appear can be related to the above, but most likely to normal human variations and steering system properties present in the simulator and not implemented directly in the external vehicle model (other than through the lumped front tire cornering compliance parameter).

Figure 6.1-2 shows results for the same driver in test 2051 corresponding to the Slalom maneuver. Again, as in the DLC maneuver with this same driver, the matchings are quite good.

The results seen in Figure 6.1-3 for the lane-change in a curve (LCIC) maneuver for Driver 357 and test run 1928 now show distinct differences, particularly in regard to timing of the lane-change maneuver along the curve. The principal differences that appear here are all related to when the test subject starts the steering maneuver back into the inner travel lane versus when the driver model starts the same steering maneuver. As indicated in these figures, both the simulated and the actual drivers enter the curve and begin the transition into the inner lane in a similar manner. However, the driver model then elects to transition into the inner lane position by counter-steering approximately 0.5 seconds or so prior to the simulator driver. This produces the indicated timing shift seen in most of the responses during the latter half of this run. Also seen in this figure is a more lightly damped response on behalf of the simulator Driver 357 during the latter stages of the maneuver following return to the inner travel lane. This appears to be related to the delayed response by the test subject (relative to the driver model) in returning to the travel lane, thereby producing a larger (negative) lateral acceleration response but smaller sideslip excursion during the final lane transition.

Differences that are seen here and in the other lane-change-in-a-curve (LCIC) comparisons that follow, are likely related to more complex path selection strategies elected by the individual test subjects and not incorporated into the simpler path selection strategy of the driver model. One example is that the test subjects knew that four or less cone strikes was defined as a successful run. Consequently, path strategies that purposely included corner cone strikes in order to lessen path curvature requirements, particularly under near-limit conditions, provided certain drivers with an additional advantage over simpler strategies that utilized more of the available friction near the limit in order to avoid these same expendable cones.

This latter issue raises an important question of future driver model enhancements related to driver vision and path selection strategies under near-limit conditions, both practiced and surprise scenarios.

The next set of results, seen in Figure 6.1-4 to Figures 6.1-6 apply to Driver 356 ("expert" category) and the same set of three maneuvers. As seen, a similar set of test

versus model results are observed for this driver when compared with Driver 357. Driver 356 is a bit more aggressive in the DLC maneuver, driving with greater speed, but somewhat slower in the LCIC maneuver. The model matchings again are quite good for the DLC and the Slalom maneuvers. In the LCIC maneuver, seen in Figure 6.1-6, Driver 356 and the model show better synchronization in the latter half of the run than that seen for Driver 357. This apparently relates to slightly different path selection strategies employed by these two drivers, wherein Driver 356 elects to start the steering return to the inner lane somewhat sooner and more like that exhibited by the driver model. Interestingly, Driver 357 was able to achieve a nearly 2 m/s higher speed in this maneuver, apparently as a result of his particular path selection strategy.

The next set of three runs apply to Driver 6 ("typical" category) and appear in Figure 6.1-7 through Figure 6.1-9. This driver (67-year-old male), although classified as "typical," performs quite well when compared to the two expert drivers. Similar speeds are achieved by Driver 6 and he comes close to matching their performance in many maneuvers. In the DLC and Slalom maneuvers very similar peak lateral acceleration levels are reached and overall performance is good. The model matchings for this driver are similar in nature. In the LCIC maneuver, Driver 6 is more like Driver 356 in terms of electing to return to the inner travel lane (latter half of maneuver) slightly sooner than Driver 357. Again, and as noted above for the two "expert" drivers, fairly light closed-loop directional damping is observed in the test results versus that seen in the driver model during the latter portions of the LCIC maneuver. This may be a result of the actual drivers adjusting their preview behavior differently along different portions of the LCIC course versus the fixed preview strategy imposed here on the driver model for these runs. Also likely are differences in vehicle directional properties between the simulator model and the driver model's external vehicle characterization at or near the limit where small differences can be magnified due to strong system sensitivities under these conditions. If directional stability limits are being reached, as suggested by the sideslip responses just prior to these light oscillations in the latter portion of the LCIC maneuver, the test drivers may instinctively employ a suddenly altered preview strategy (versus the driver model fixed preview strategy) to re-establish control of the vehicle. In either case, this maneuver seems to highlight questions about transient driver control behavior (during near loss of control events) that probably should be pursued in future work.

The last set of three validation figures pertain to the novice teenage Driver 353. These results are seen in Figure 6.1-10 through Figure 6.1-12. The most noteworthy item related to this driver is the self-imposed speed restraint elected by the driver. Speeds and associated peak lateral acceleration levels for this driver are significantly below those seen for most other drivers, and especially the three other drivers seen in the test versus model comparisons of this validation section. Consequently, the "limit" for this driver is defined more by comfort or an unwillingness to experience elevated vehicle motions associated with higher speed maneuvers, than by the vehicle and tire/road friction limit capabilities. The driver model comparisons in this set of reduced acceleration runs is consistent with the types of matchings seen in the previous nine validation comparisons runs.

Overall, the driver model predictions seen in the 12 validation runs are generally sound. It is not clear how these results might become altered if the same tests were conducted under full scale test track conditions. For example, would drivers under test track conditions utilize the same levels of preview time? How would their respective transport delays compare to those identified here? And, importantly, how willingly would "typical" drivers elect to take the vehicle up to its limit of cornering performance on a test track? It might very well be that such comfort factors, even for "typical" drivers, might be more of an inhibitor of aggressive behavior and that a far greater range of discriminatory performance is then observed under those conditions.

The next sub-section of the report summarizes and discusses the twelve sets of control parameters identified from this validation exercise.

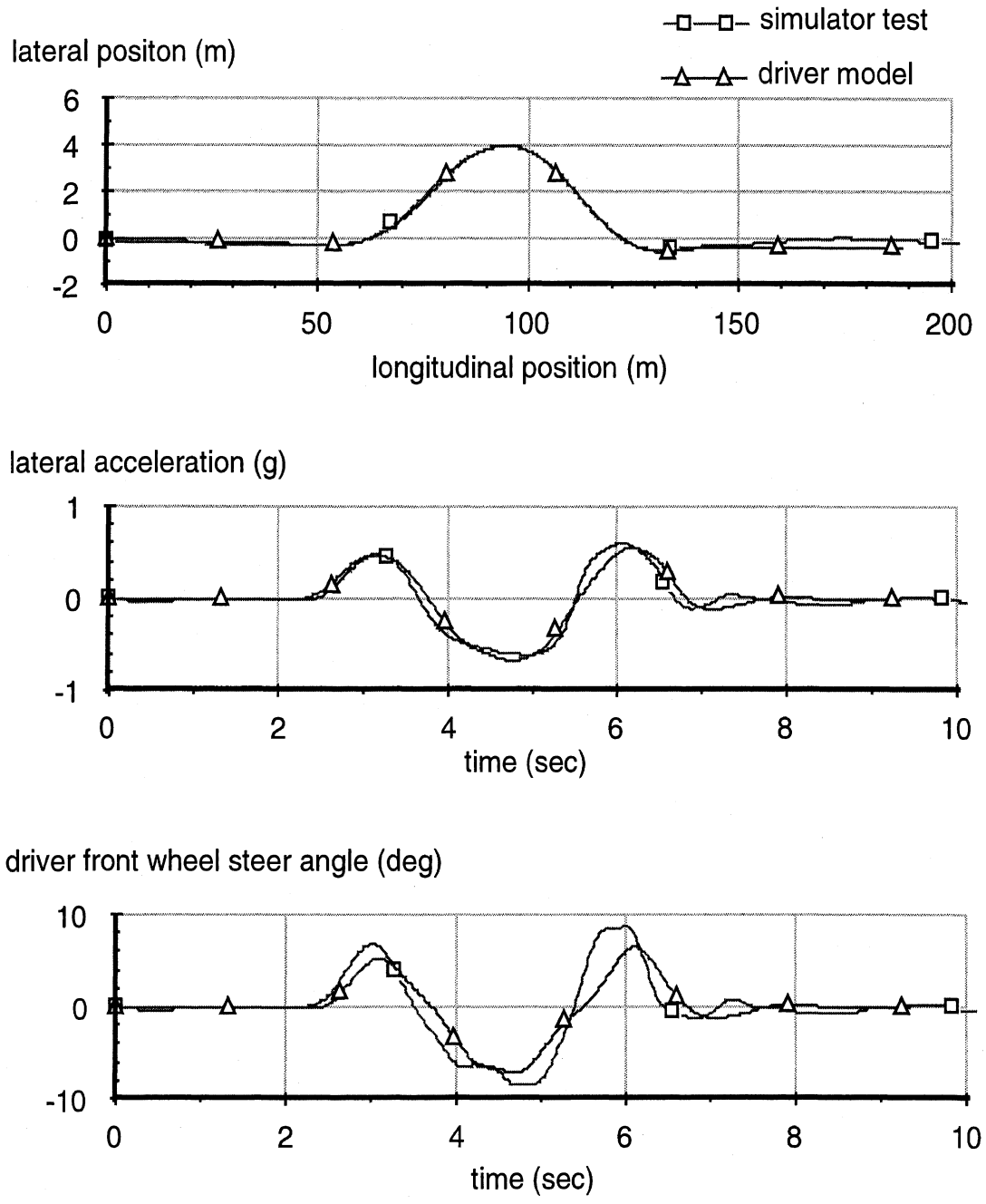

Figure 6.1-1-a. Double Lane-Change, Test Run 2010, Driver 357, 20.6 m/s.

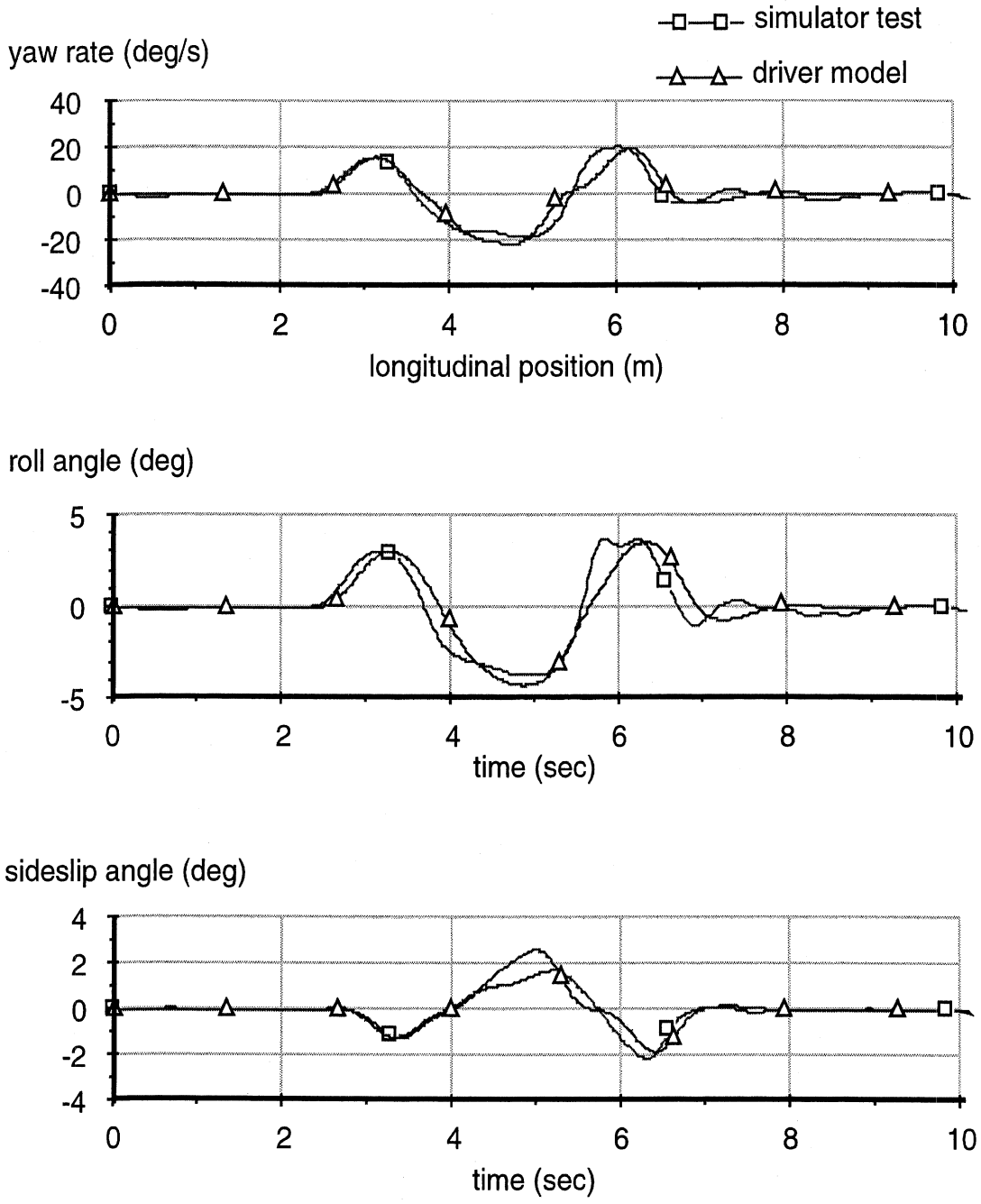

Figure 6.1-1-b. Double Lane-Change, Test Run 2010, Driver 357, 20.6 m/s.

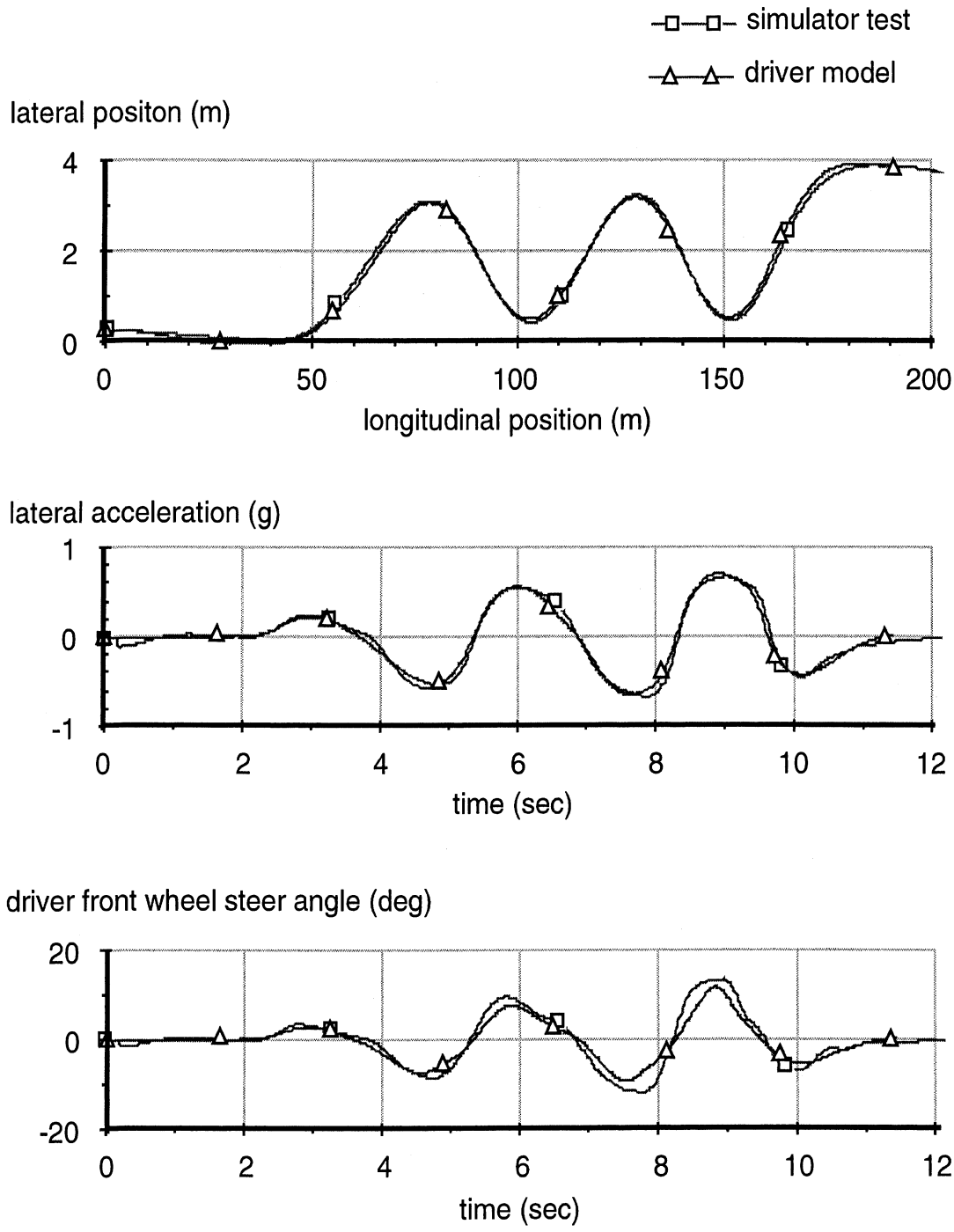

Figure 6.1-2-a. Slalom, Test Run 2051, Driver 357, 17 m/s.

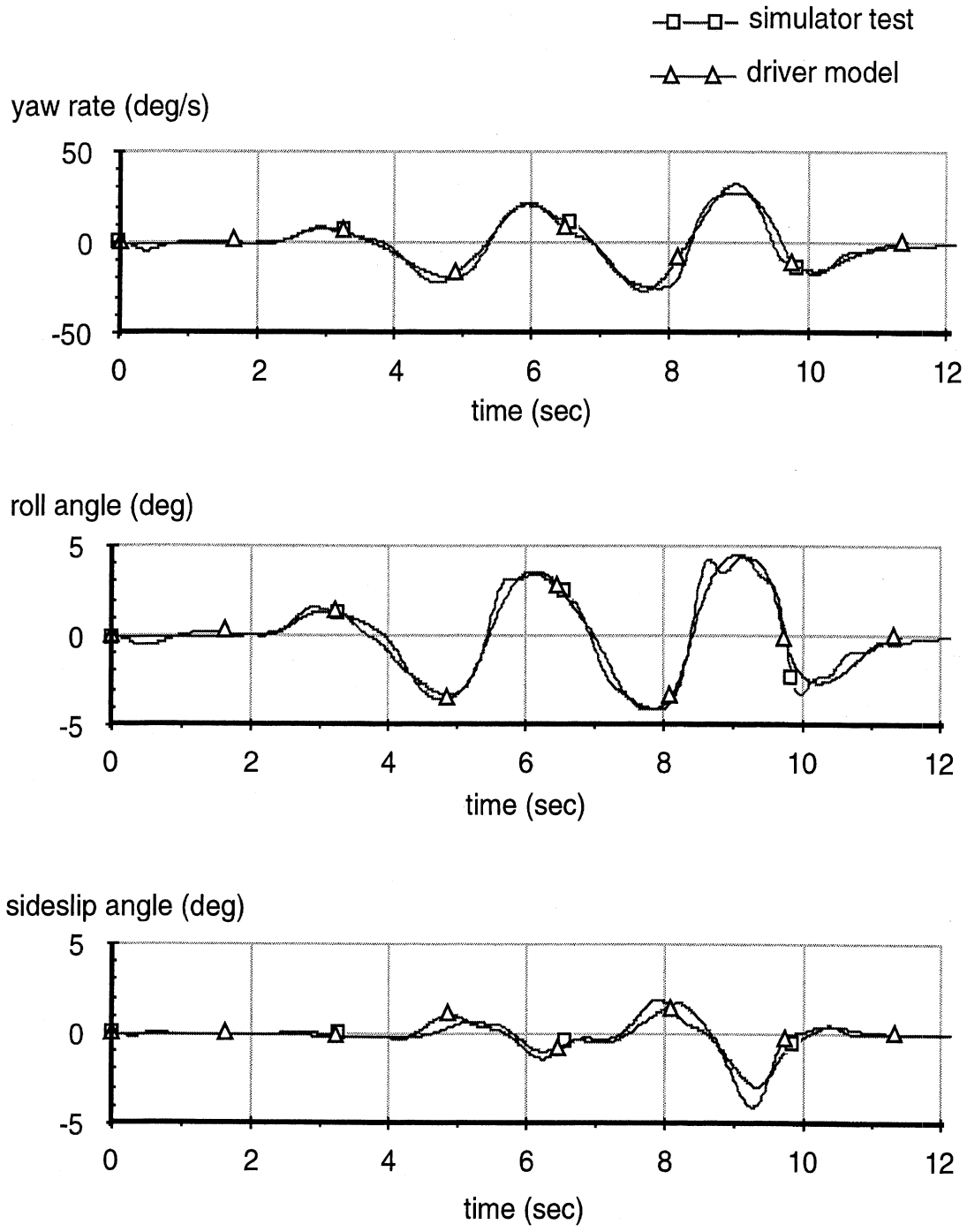

Figure 6.1-2-b. Slalom, Test Run 2051, Driver 357, 17 m/s.

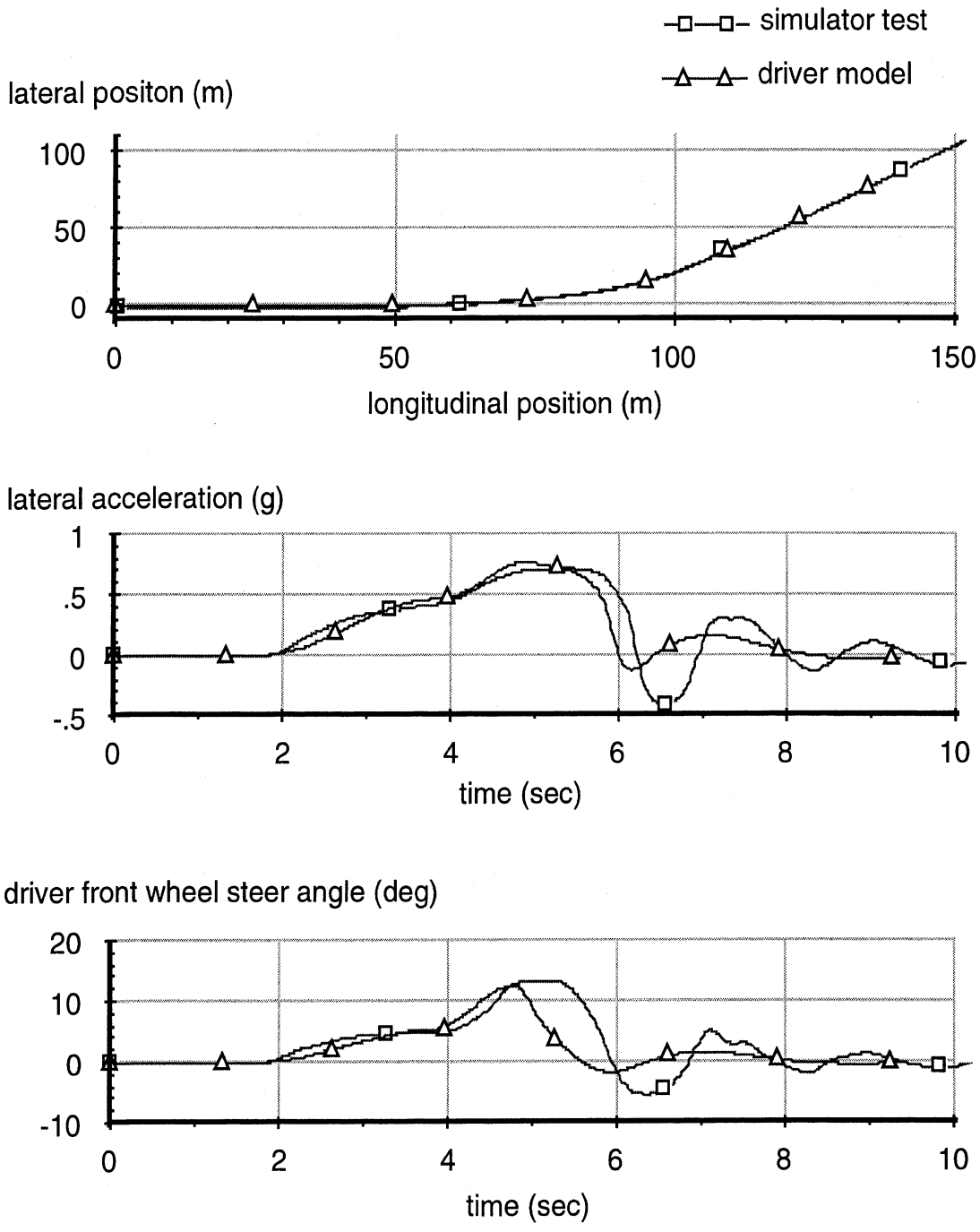

Figure 6.1-3-a. Lane-Change in a Curve, Test Run 1928, Driver 357, 18.8 m/s.

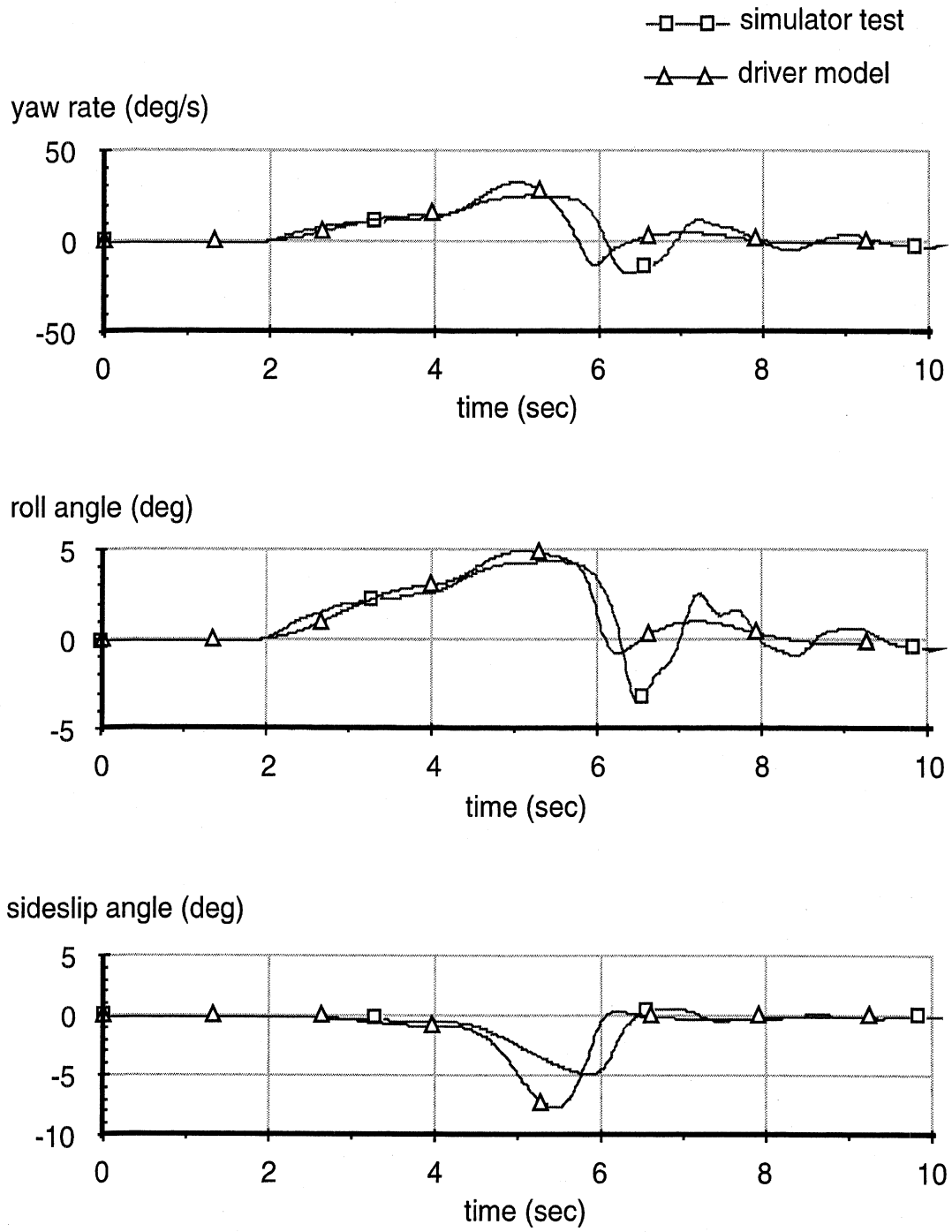

Figure 6.1-3-b. Lane-Change in a Curve, Test Run 1928, Driver 357, 18.8 m/s.

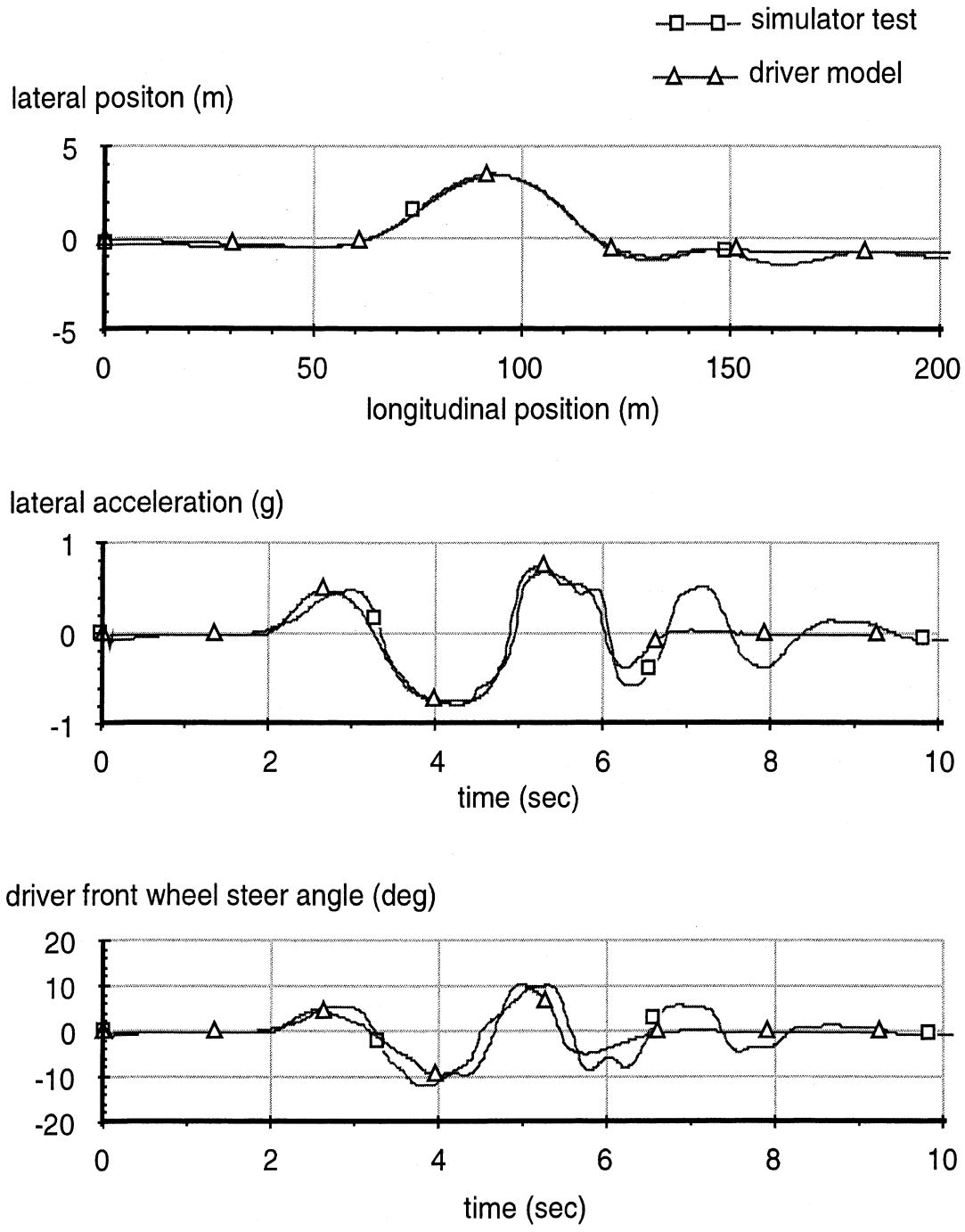

Figure 6.1-4-a. Double Lane-Change, Test Run 1861, Driver 356, 23.3 m/s.

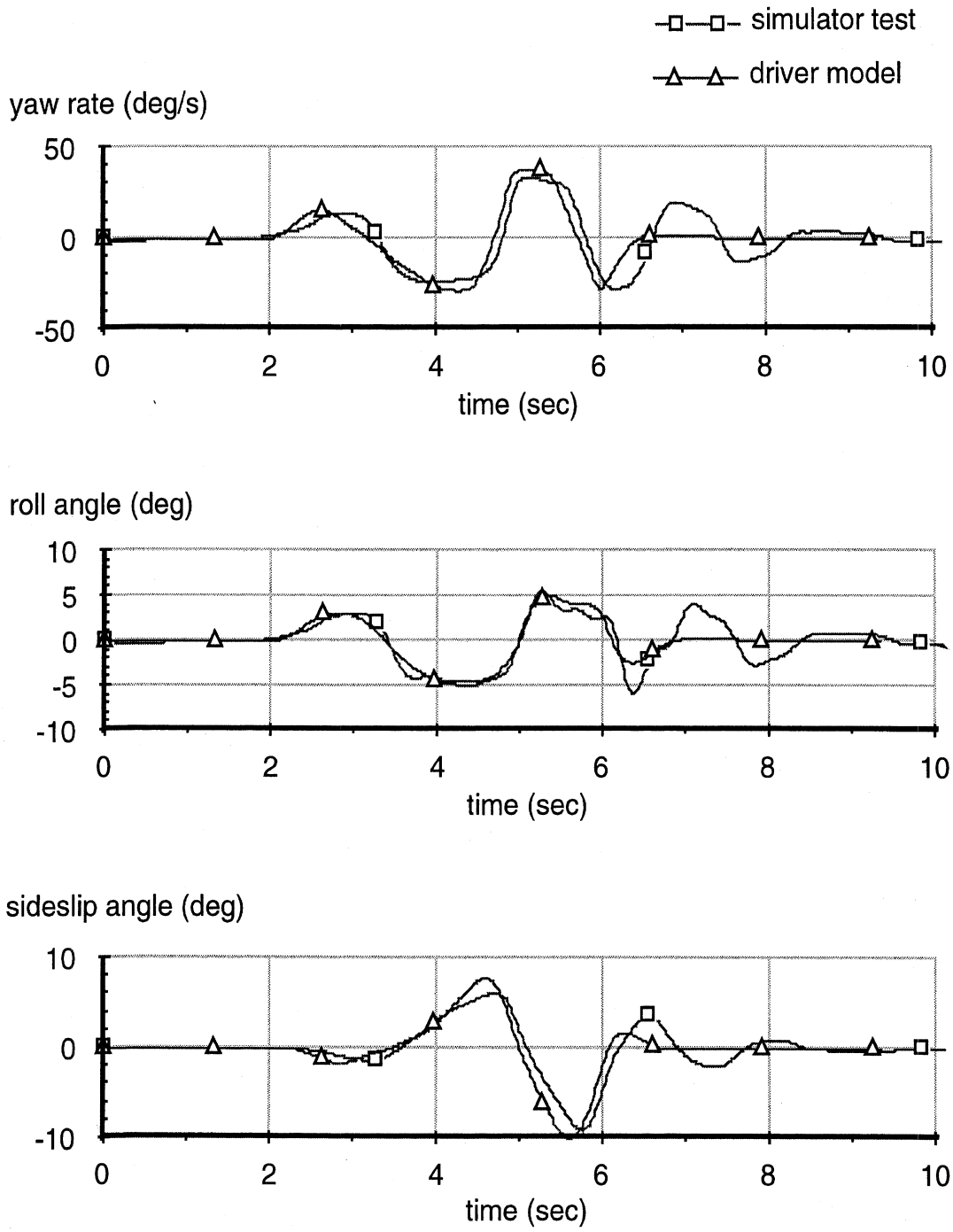

Figure 6.1-4-b. Double Lane-Change, Test Run 1861, Driver 356, 23.3 m/s.

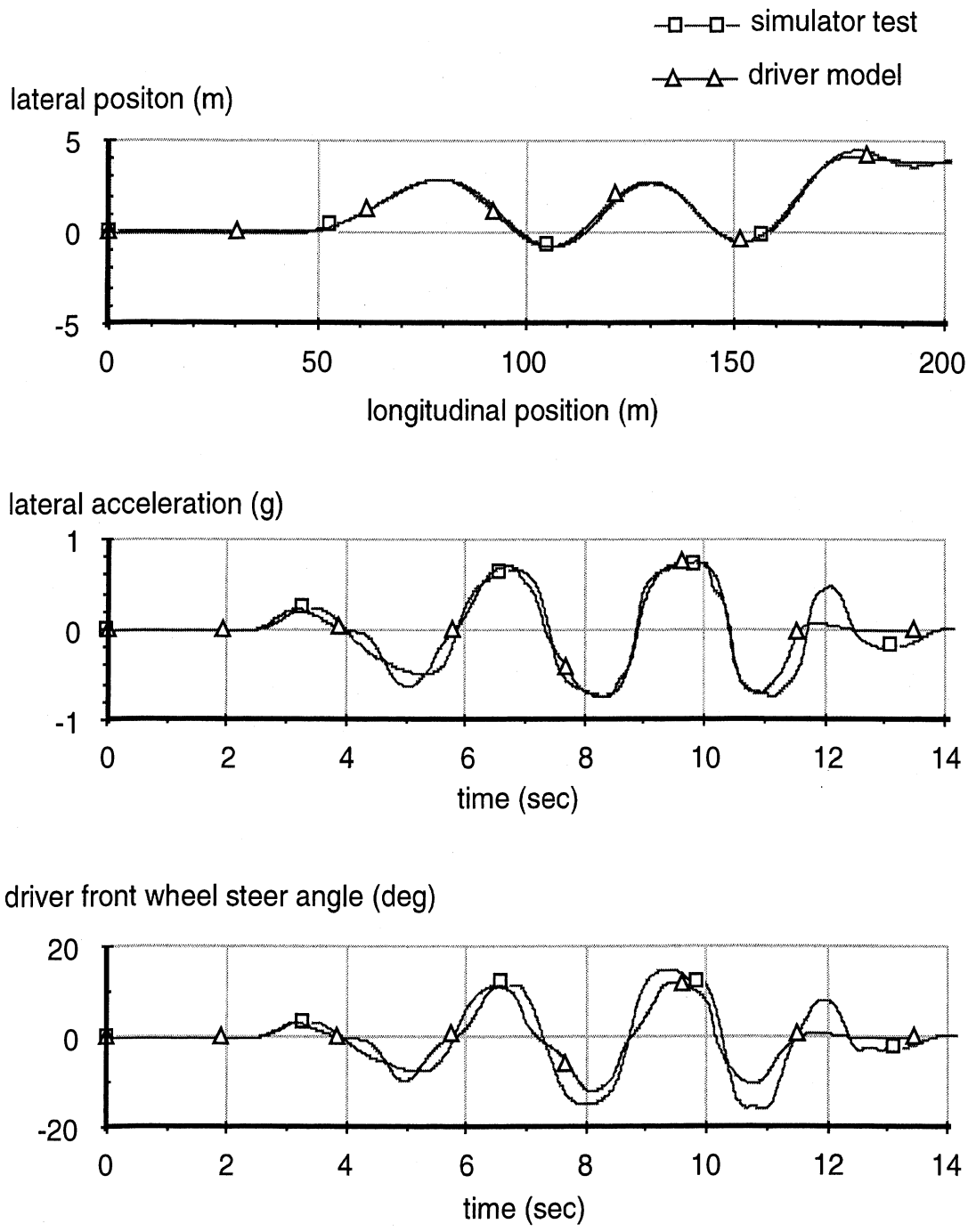

Figure 6.1-5-a. Slalom, Test Run 1885, Driver 356, 16.1 m/s.

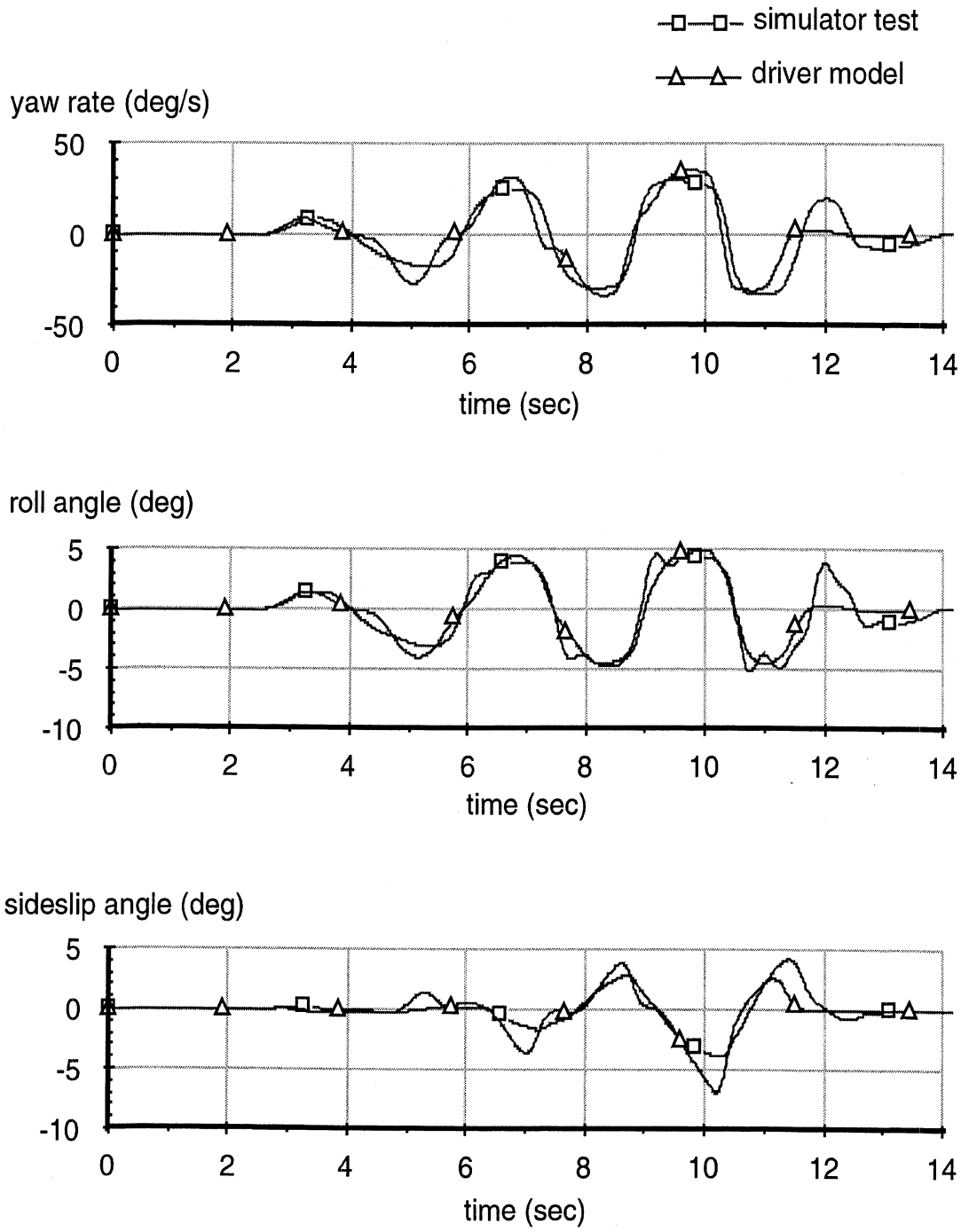

Figure 6.1-5-b. Slalom, Test Run 1885, Driver 356, 16.1 m/s.

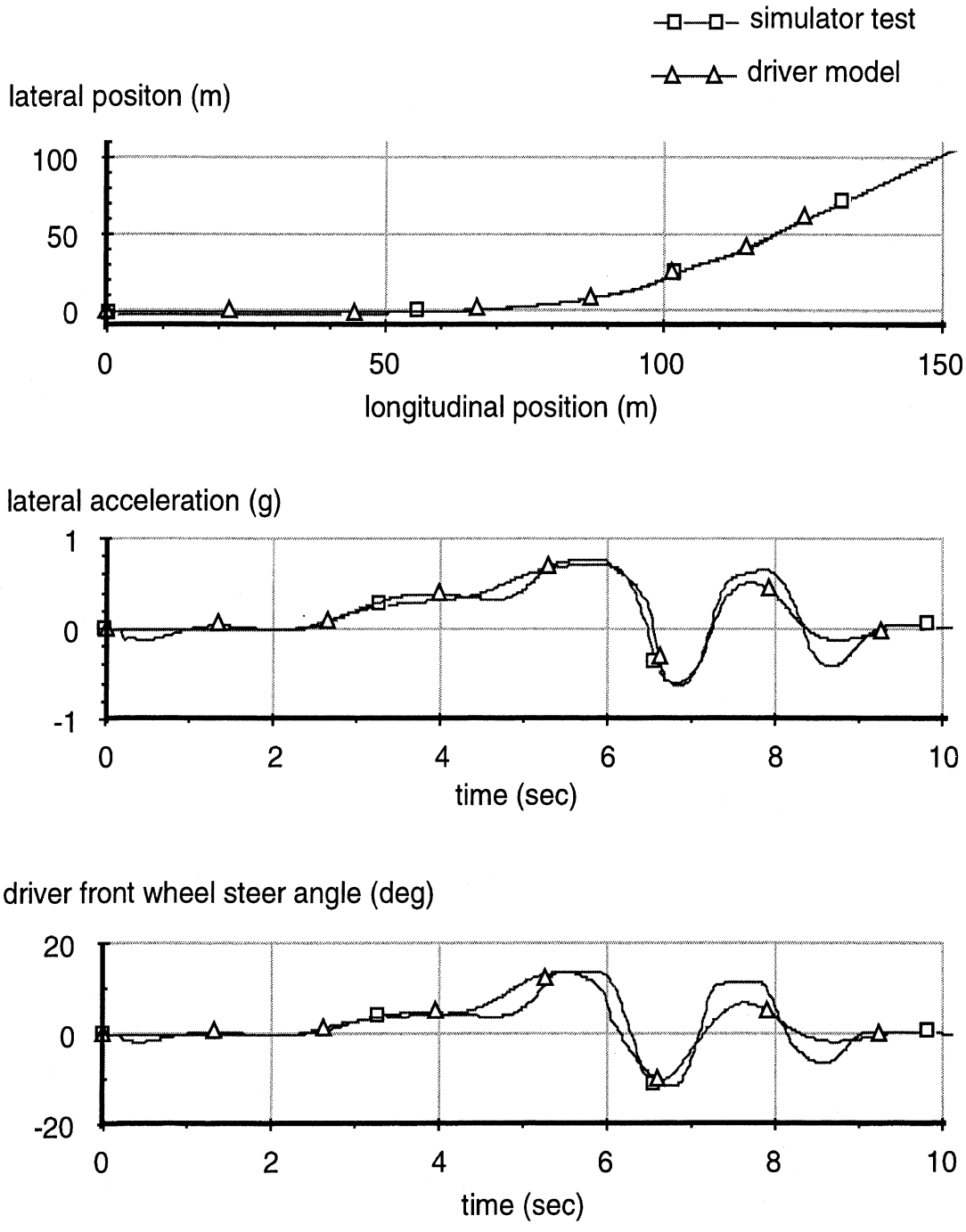

Figure 6.1-6-a. Lane-Change in a Curve, Test Run 1873, Driver 356, 17 m/s.

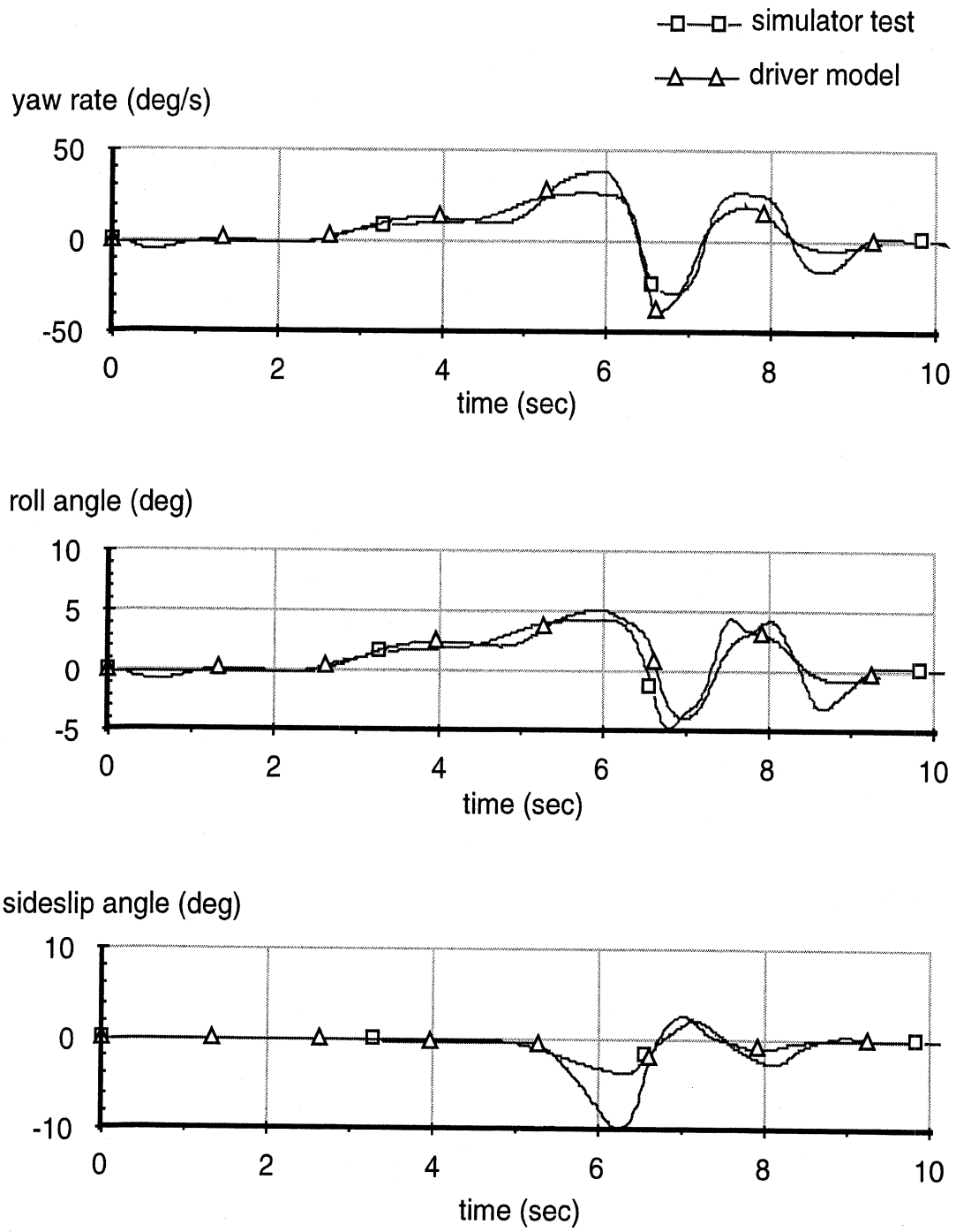

Figure 6.1-6-b. Lane-Change in a Curve, Test Run 1873, Driver 356, 17 m/s.

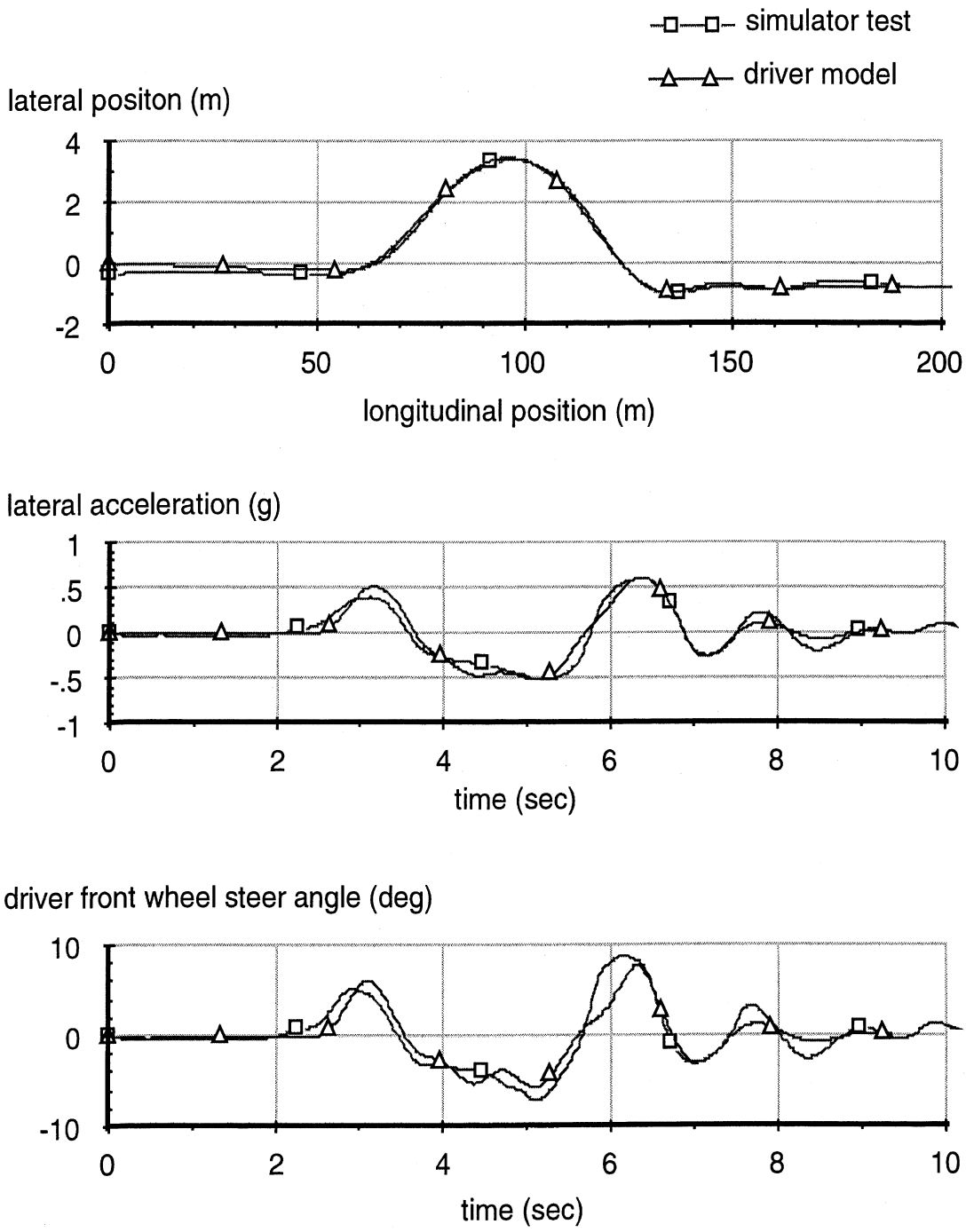

Figure 6.1-7-a. Double Lane-Change, Test Run 1143, Driver 6, 20.6 m/s.

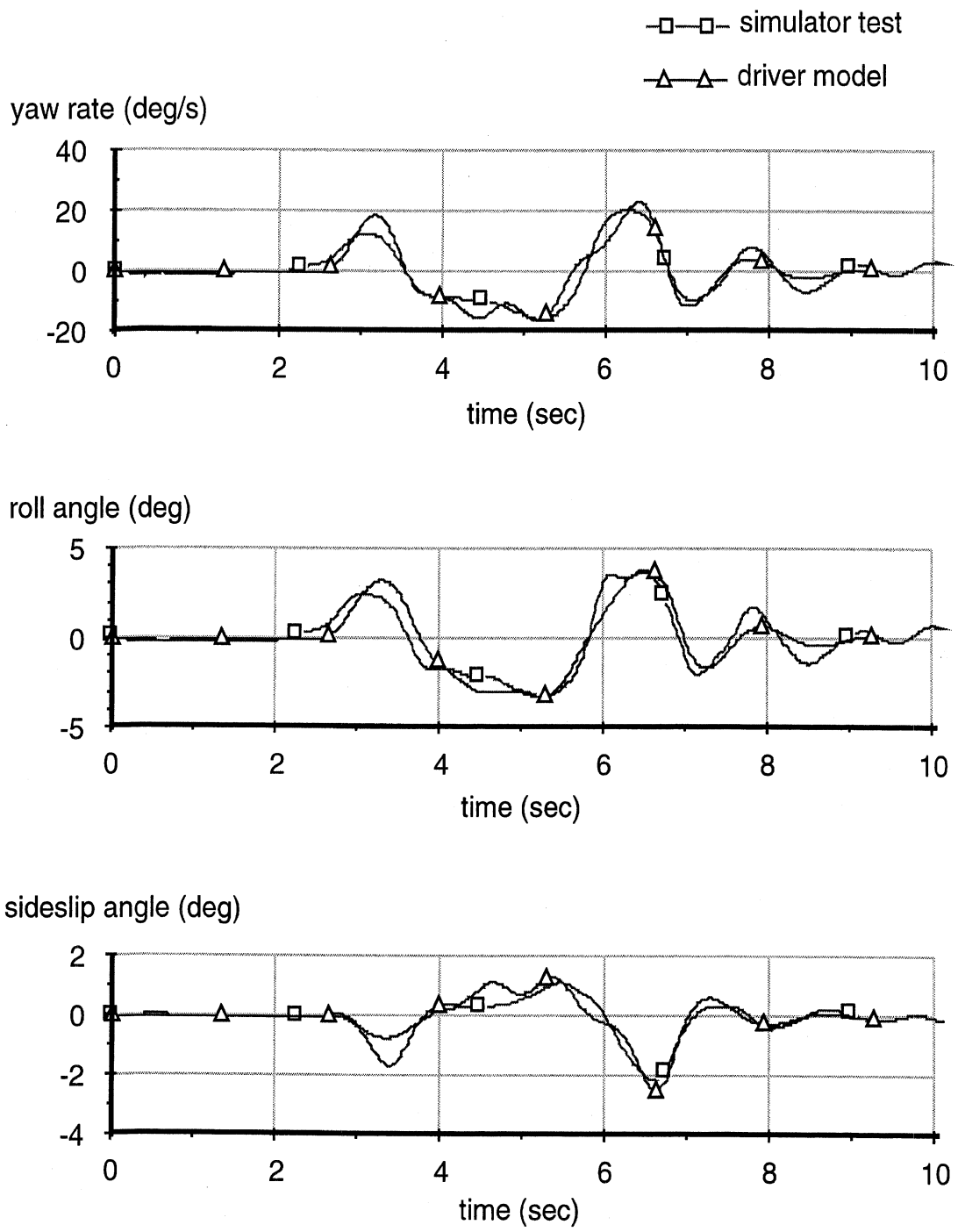

Figure 6.1-7-b. Double Lane-Change, Test Run 1143, Driver 6, 20.6 m/s.

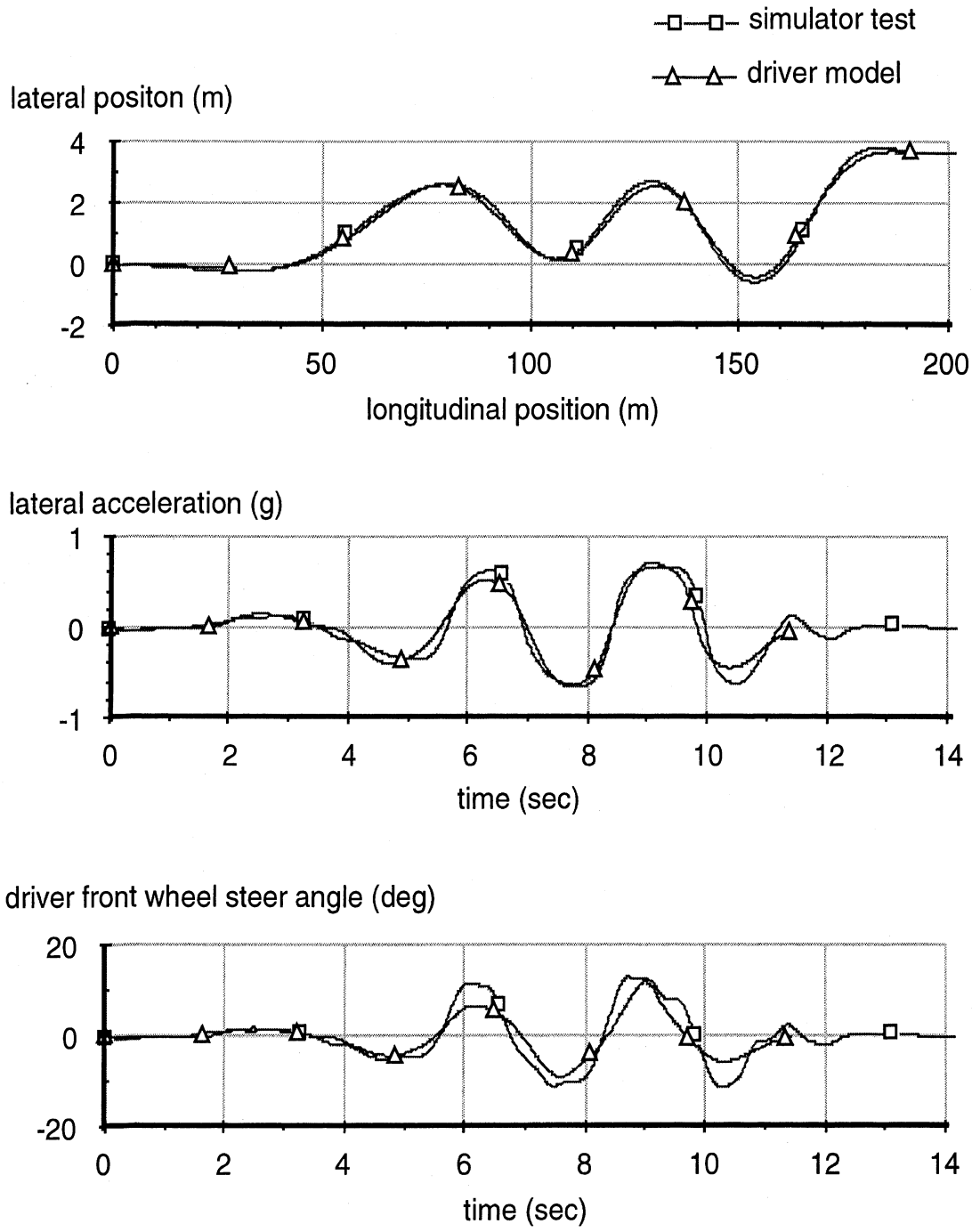

Figure 6.1-8-a. Slalom, Test Run 1016, Driver 6, 17 m/s.

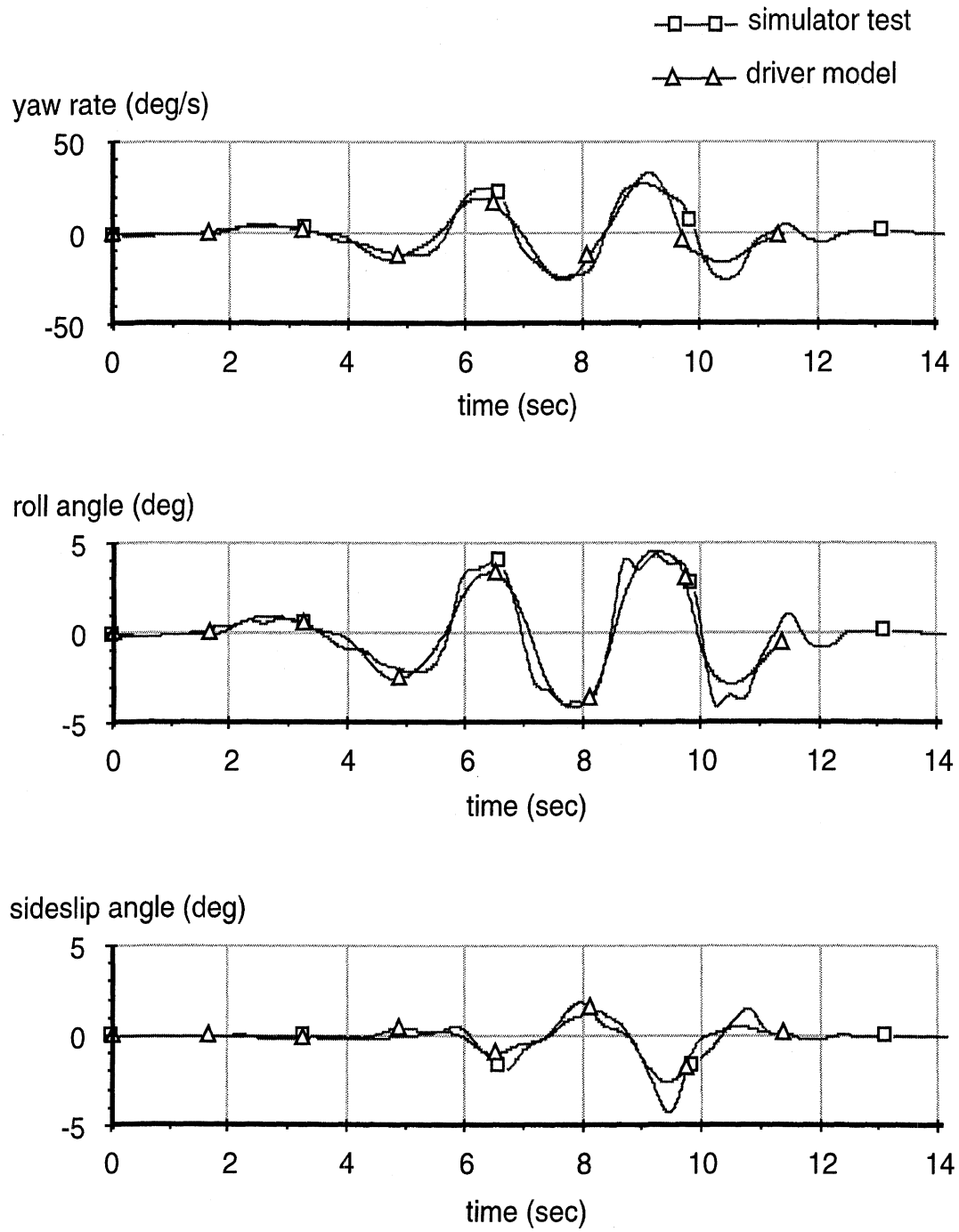

Figure 6.1-8-b. Slalom, Test Run 1016, Driver 6, 17 m/s.

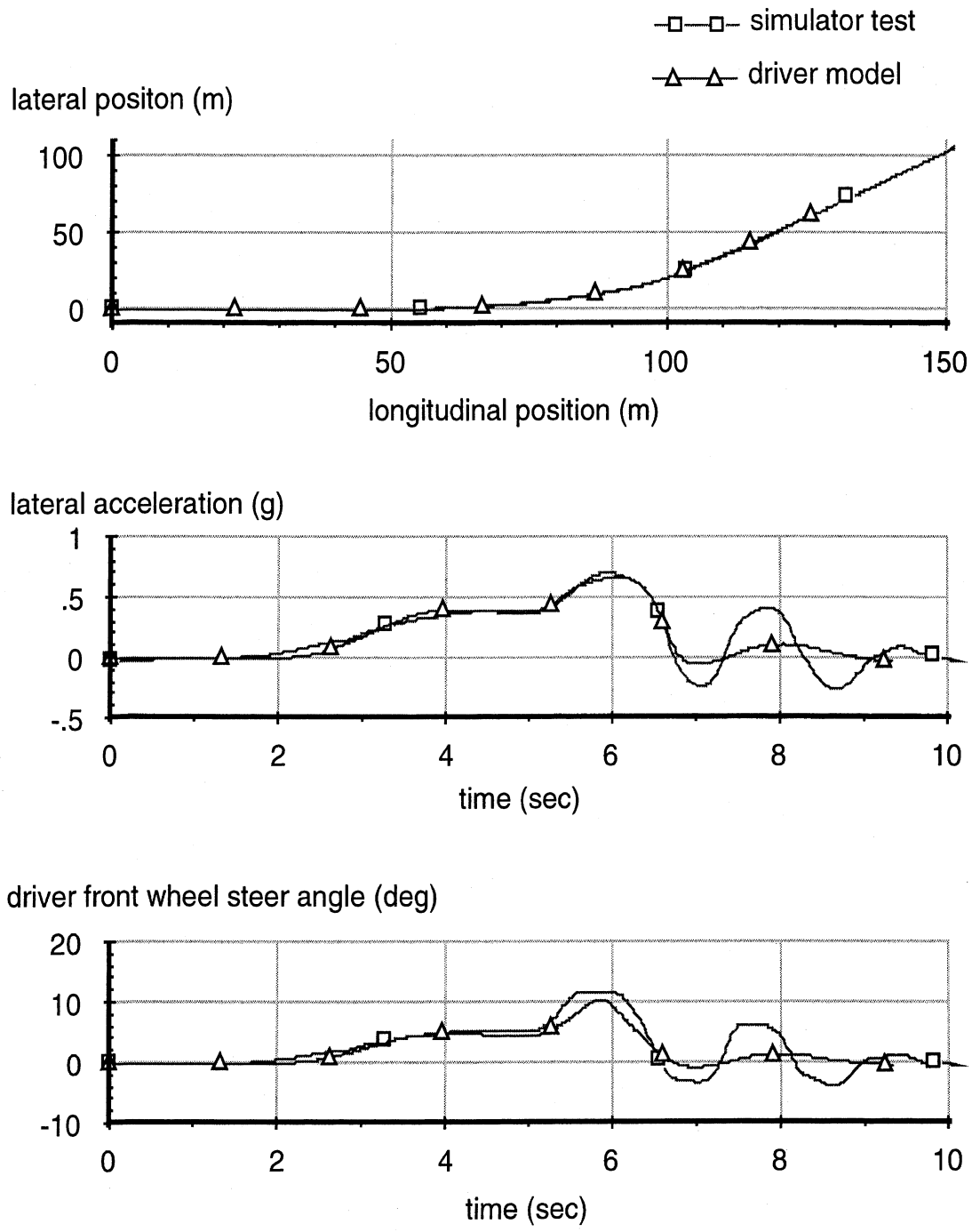

Figure 6.1-9-a. Lane-Change in a Curve, Test Run 1054, Driver 6, 17 m/s.

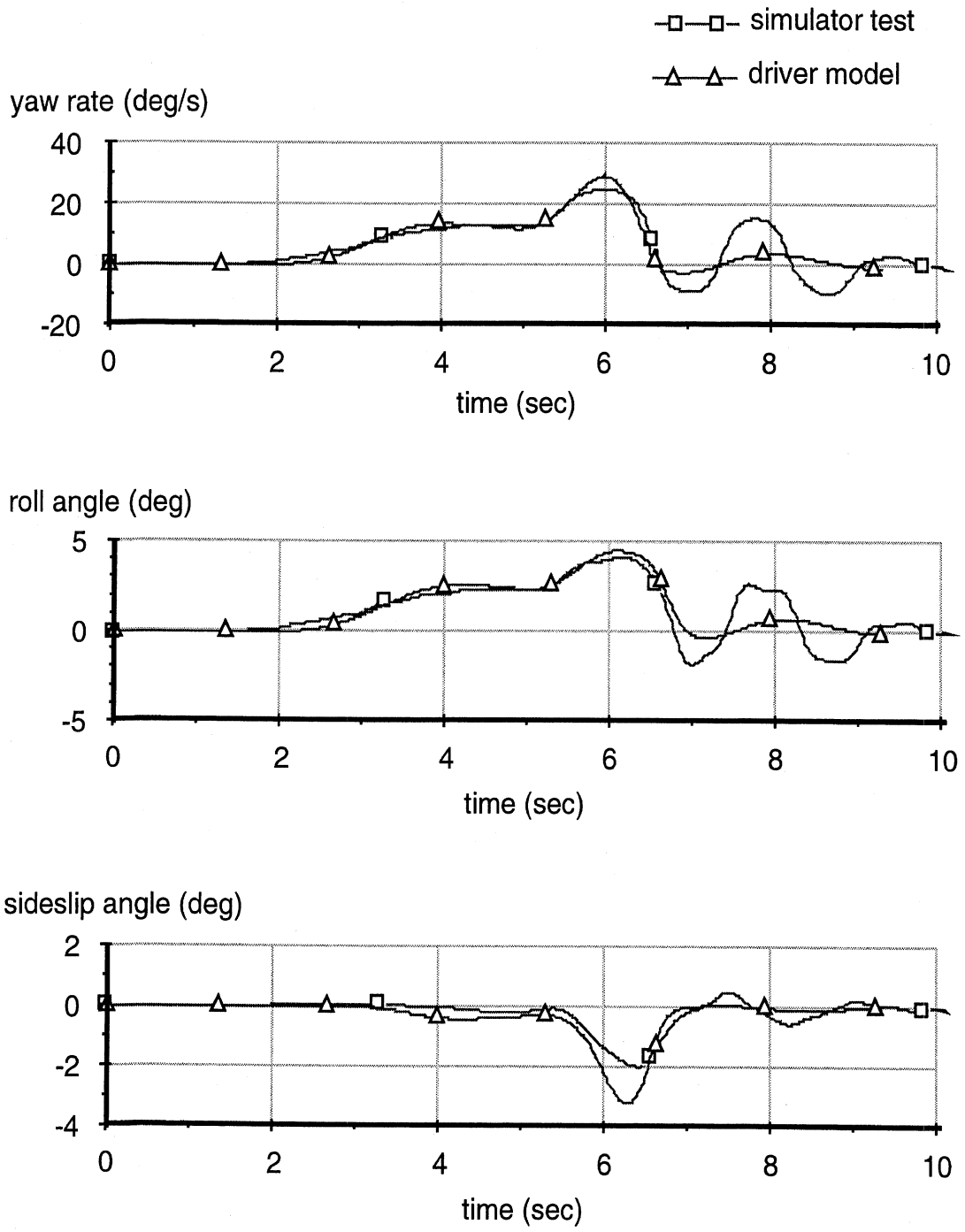

Figure 6.1-9-b. Lane-Change in a Curve, Test Run 1054, Driver 6, 17 m/s.

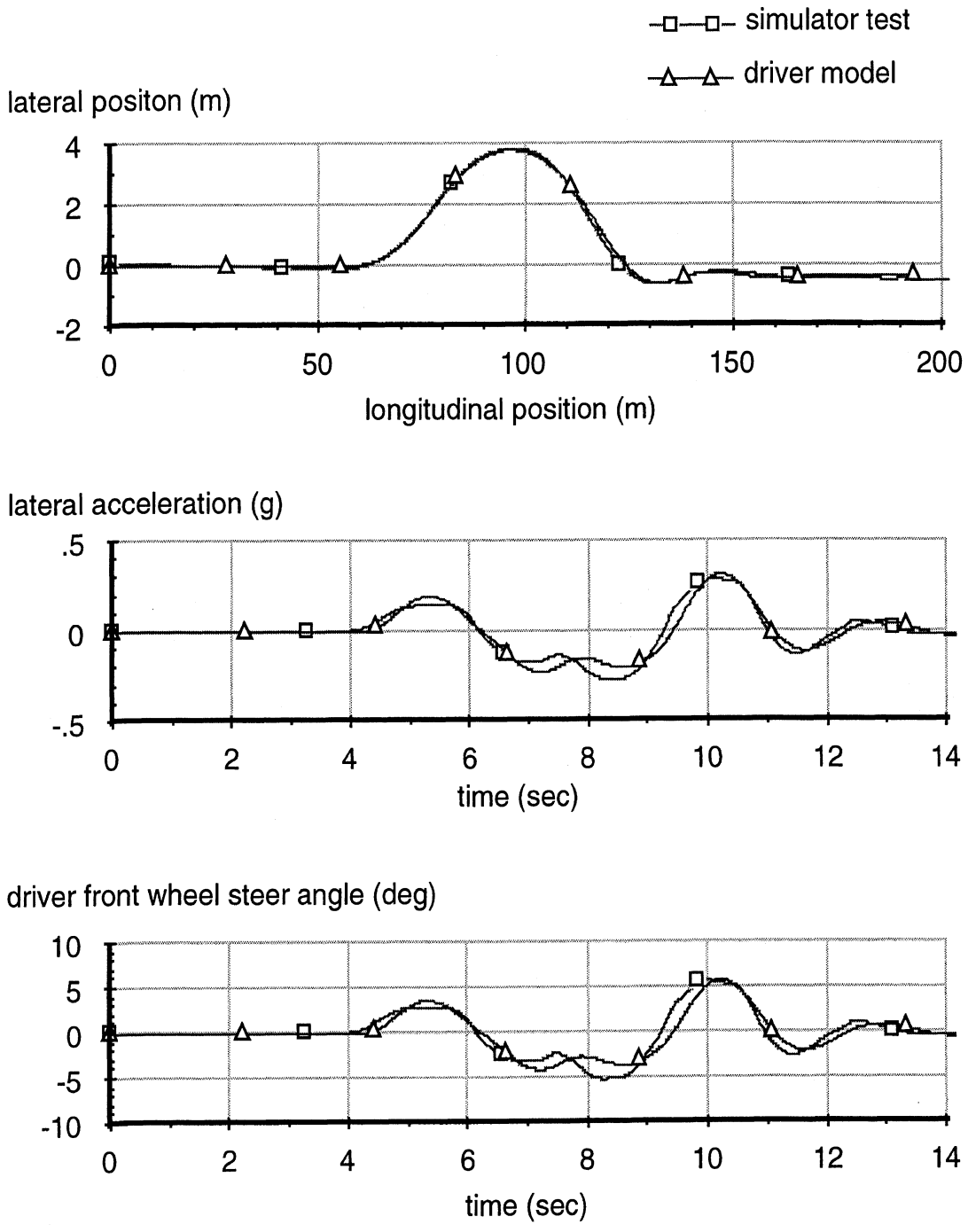

Figure 6.1-10-a. Double Lane-Change, Test Run 1639, Driver 353, 12.5 m/s.

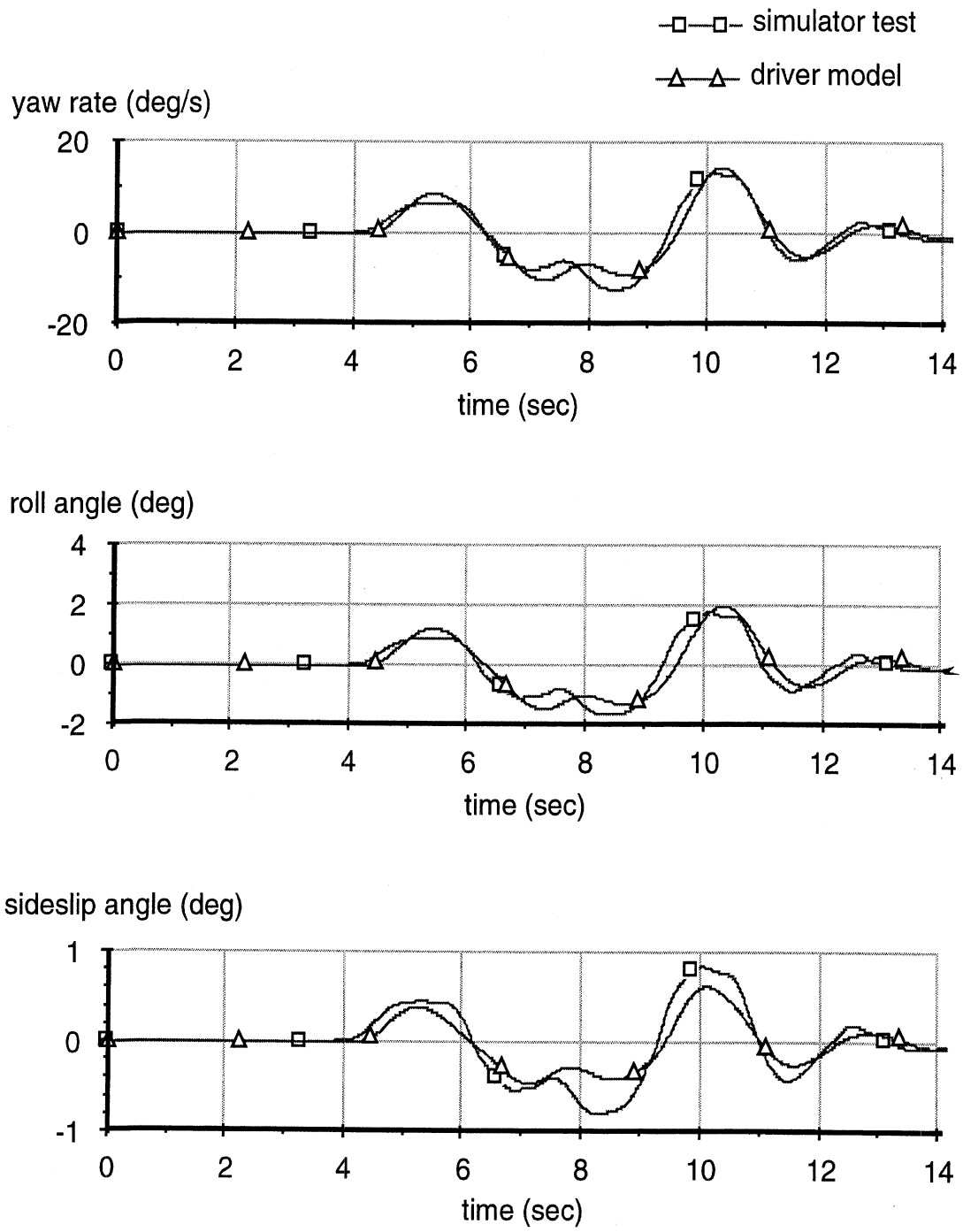

Figure 6.1-10-b. Double Lane-Change, Test Run 1639, Driver 353, 12.5 m/s.

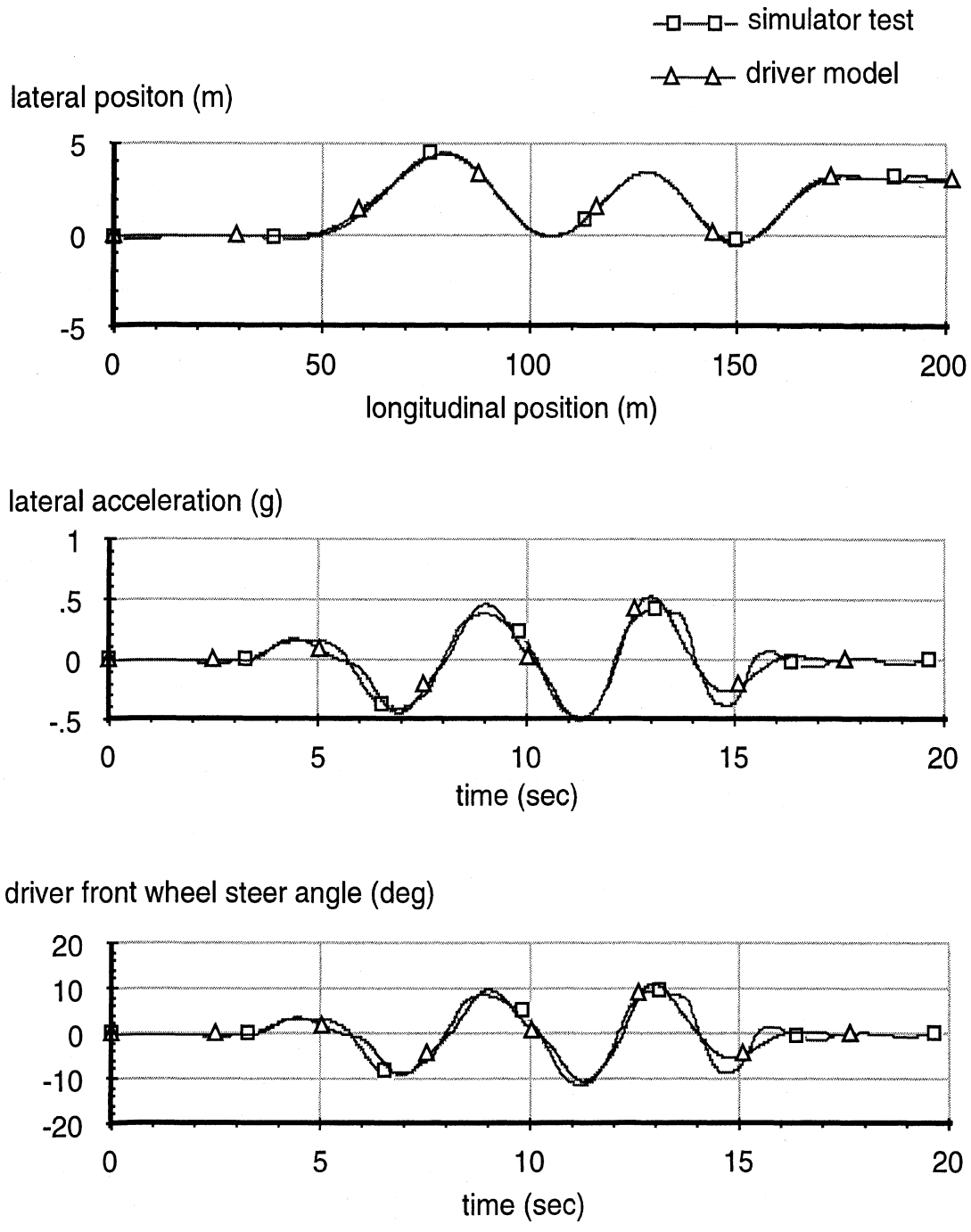

Figure 6.1-11-a. Slalom, Test Run 1631, Driver 353, 11.6 m/s.

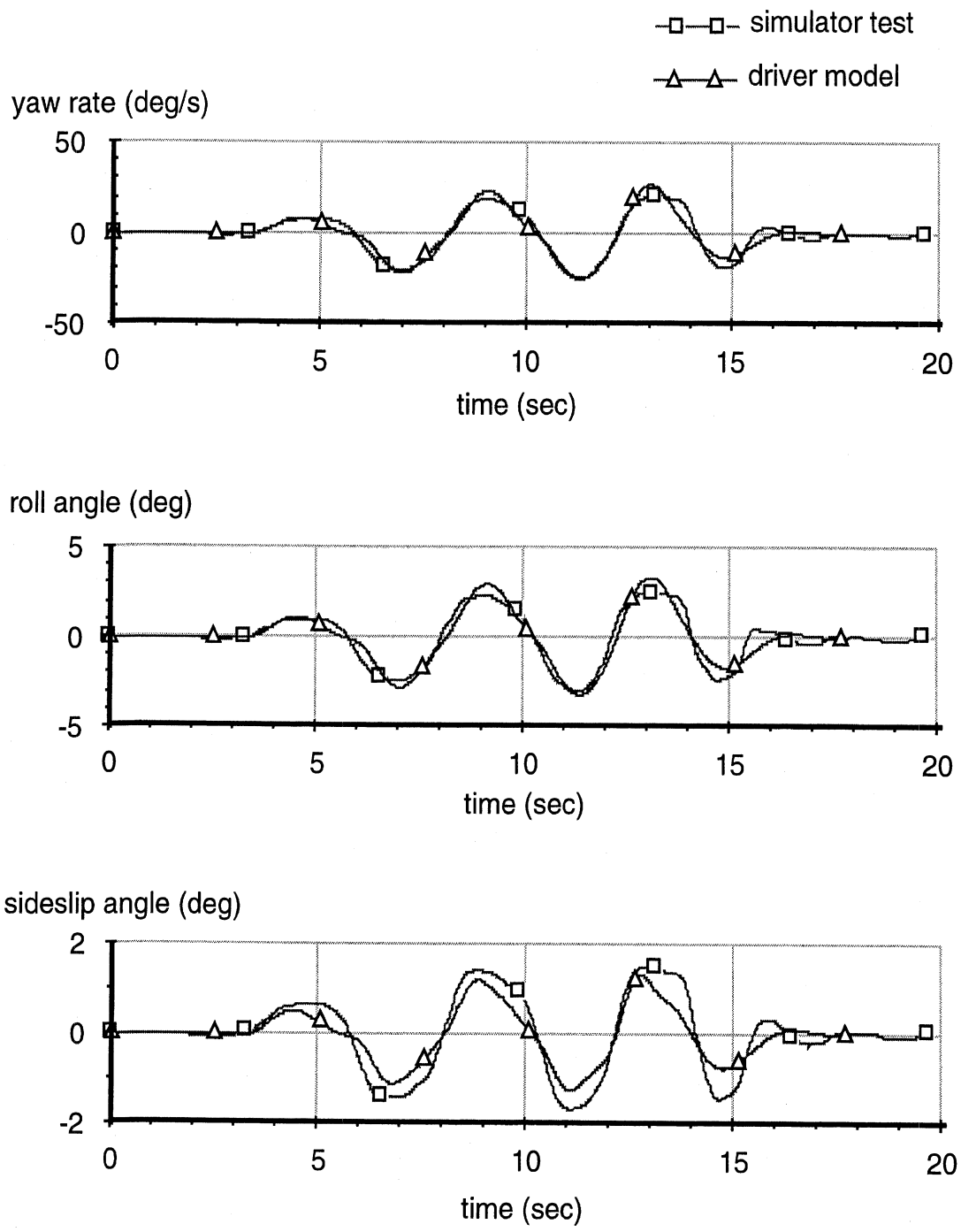

Figure 6.1-11-b. Slalom, Test Run 1631, Driver 353, 11.6 m/s.

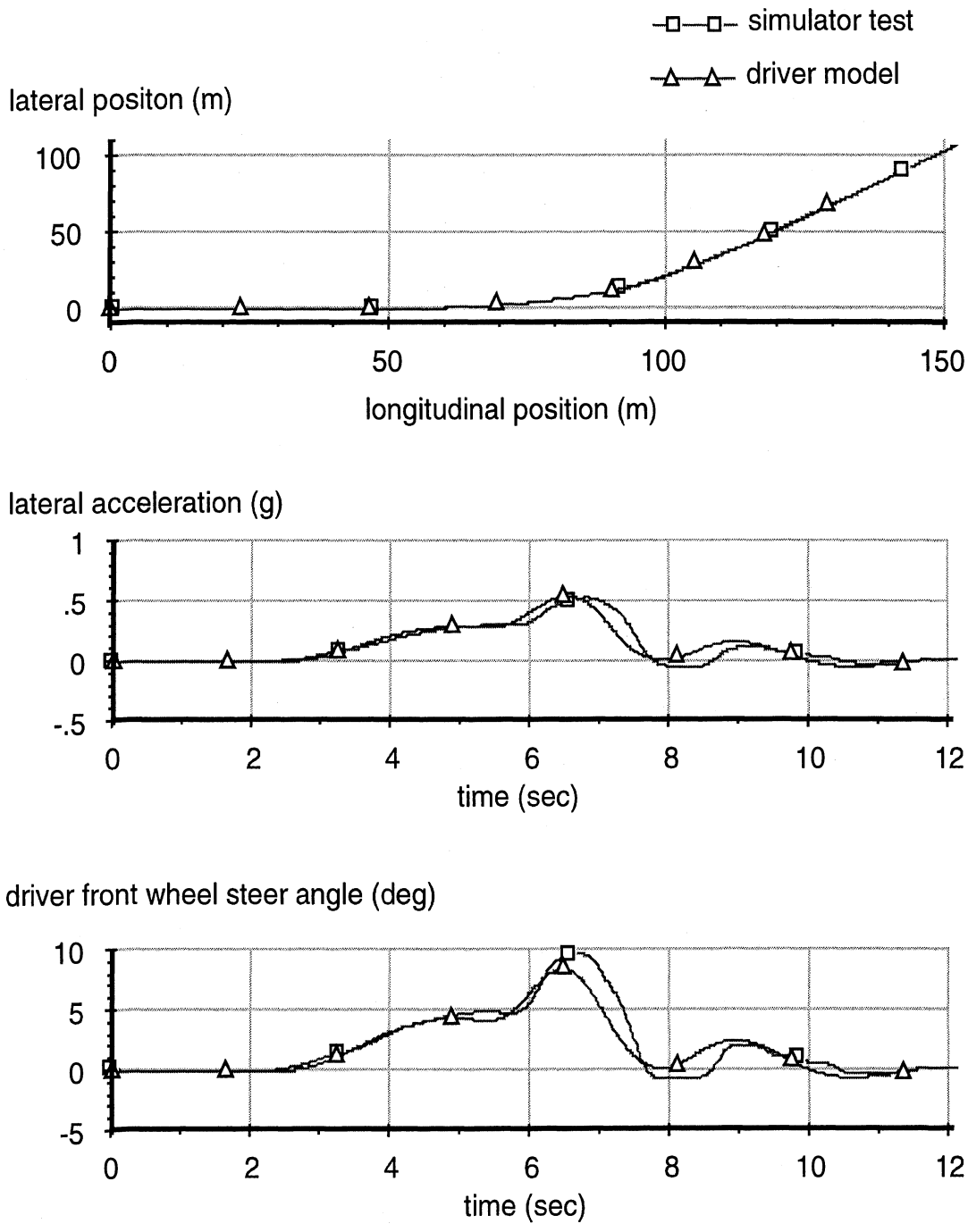

Figure 6.1-12-a. Lane-Change in a Curve, Test Run 1670, Driver 353, 14.3 m/s.

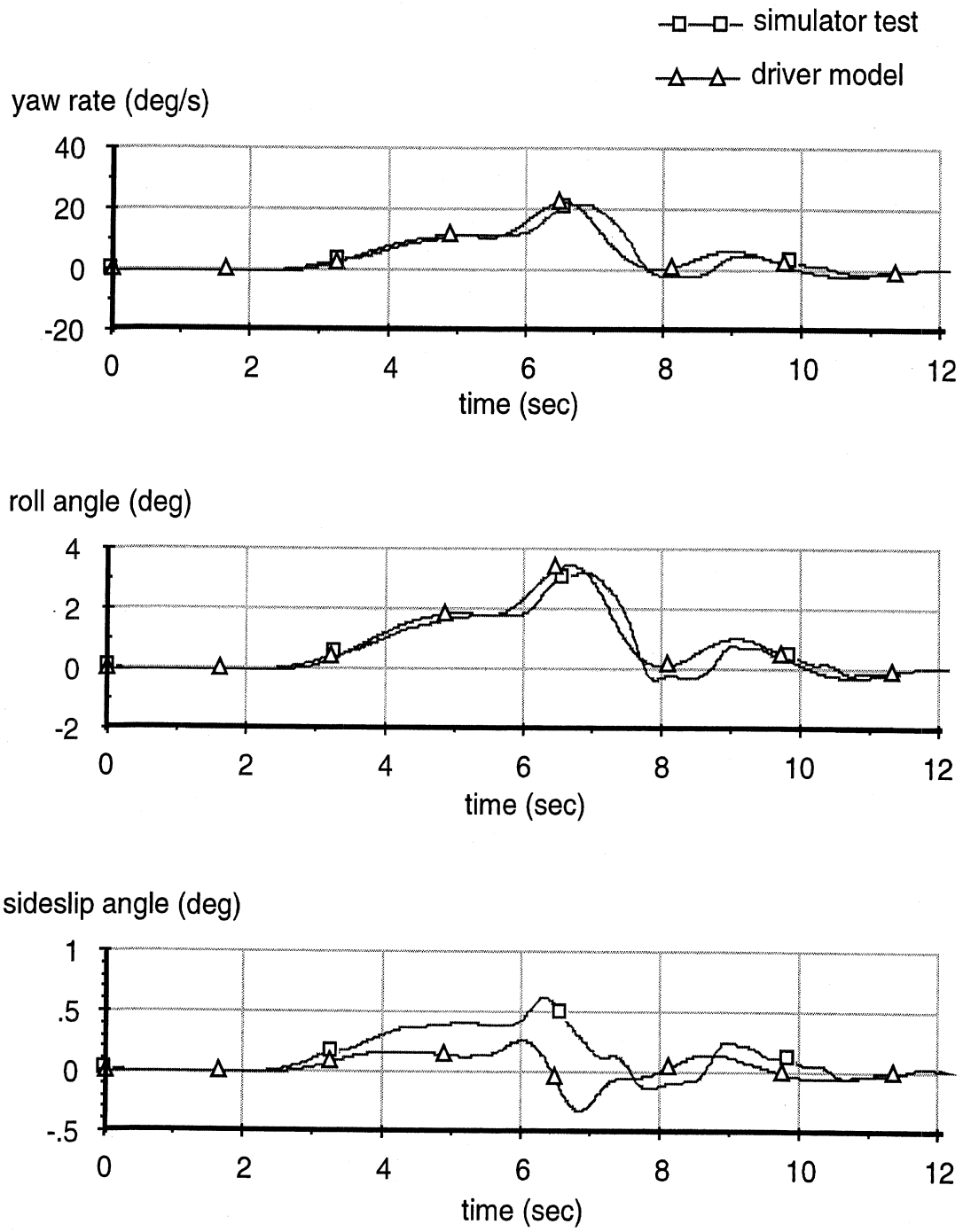

Figure 6.1-12-b. Lane-Change in a Curve, Test Run 1670, Driver 353, 14.3 m/s.

6.2 Driver Model Control Parameters Identified Within the Validation Effort

As noted above, two primary driver model parameters were systematically varied in order to obtain reasonable matchings between the simulator test results and the driver model predictions seen in the previous section. The two driver model parameters were 1) the preview ("look-ahead") time, and 2) the steering transport delay. These two parameters largely control the overall bandwidth capabilities of the driver model (subject to the directional dynamics constraint of the vehicle itself) and the overall degree of closed-loop directional damping. The preview time primarily affects the bandwidth. The transport delay, in combination with the preview time, largely controls the damping.

For each validation run seen in the previous section, a pair of such parameters was identified (T, τ) that can then be plotted simultaneously for all twelve test runs. This plot is seen in Figure 6.2-1. The driver model preview time, T, appears on the ordinate axis. The abscissa axis contains the total transport delay consisting of the sum of the front-end 70 ms sensory delay imposed by the simulator platform/visual system and the driver's ergonomic steering delay, τ. (Within the driver model structure, the total pass-through driver delay consists of any front-end sensory delays plus the driver steering output transport delay — located in Blocks 2 and 6 of Figure 3-1.)

The parameter data seen in Figure 6.2-1 are grouped by driver as noted in the figure legend. The same symbol (square, triangle, diamond, or circle) represents one of the four validation test drivers. The location of any symbol on this plot then identifies the two control parameters (T and τ+0.07) that were identified within the driver model validation effort for that particular test run.

Figure 6.2-2 is a similar plot but groups the same data by maneuver (DLC, Slalom, or LCIC) as indicated in its legend. This plot also contains driver ID numbers next to each symbol as well in order to help keep track of driver and maneuver for each control parameter location. Arrows located on this plot also show the general influence that increasing or decreasing either control parameter will have on the overall behavior of the closed-loop driver/vehicle directional response.

Also seen on the plot of Figure 6.2-1 is an overlay of two ovals that show general regions where the same two parameters were located in previous experimental studies using the linear UMTRI model and test track experiments with passenger cars and a HMMWV military vehicle. Those studies however did not include limit or near-limit cornering maneuvers. Nevertheless, they do provide a point of reference for the same type of information being displayed here for the simulator validation tests.

With respect to the model parameters obtained from the simulator validation effort, Driver 356 (square symbol in Figure 6.2-1) displays a fairly similar set of parameter values for the DLC and the Slalom maneuver located in the lower left portion of the plot. Very small transport delay values (0.02 to 0.05) are identified along with fairly short preview time values (0.55 to 0.70). The minimal levels of delay and look-ahead time (preview) suggest a near open-loop or highly practiced steering behavior for these two maneuvers. This may be a result of high anticipation skills or similar skills developed during repeated

attempts at the same maneuver. Certain drivers can effectively "tune in" to the steering requirements needed for repeated or very familiar scenarios.

At the other end of the control space is the novice Driver 353 (circle symbol). This driver employs consistently longer transport delays (0.25 to 0.31) and preview times (1.2 to 1.4), also well clustered in a fairly small region of the control space. The longer transport delays and associated preview times for this driver suggest a less aggressive and more slowly responding steering behavior, although still exhibiting an effective level of directional damping. In effect, this control parameter combination within the driver model provides less lateral maneuverability in scenarios requiring very fast lateral movements (e.g., DLC and Slalom) due to increased directional damping associated with longer preview times and delayed steering reactions associated with increased transport delays.

In this same general area of the plot of Figures 6.2-1 and 6.2-2 (upper right corner), symbols for the two remaining drivers (357 and 6) appear for the LCIC maneuver. In fact, three of the four drivers have LCIC parameters in this general region. This could be coincidence or it may indicate a tendency for most drivers to employ longer preview times when negotiating road geometries that require less rapid lateral maneuvering over short travel distances. The LCIC geometry is certainly more spaced out longitudinally than either of the DLC or Slalom courses. This may explain some of this observation. Even Driver 356, who displays very short time lag and preview parameters for the DLC and Slalom maneuvers, also exhibits larger values of driver preview (0.90) and transport delay (0.10) for this maneuver, though not as large as that seen for the remaining drivers.

In the center of the control space seen in Figure 6.2-1, the four remaining runs for Drivers 357 and 6 appear. These are all either DLC or Slalom test maneuvers. The preview parameter values for Driver 357 range from 0.85 to 1.0 and the associated transport delays range from 0.08 to 0.11. For Driver 6, the preview times range form 0.7 to 1.1 and the transport delays range from 0.11 to 0.15. For both drivers in this general center region of the control space, the indicated damping and bandwidth qualities should be fairly comparable. Examination of the time histories in Figures 6.1-1 and Figure 6.7-1 corresponding to the DLC maneuver for these two drivers shows similar behavior at a nearly identical speed. Driver 357 does exhibit better damping at the end of the run than Driver 6 and this is consistent with a slightly longer preview time (0.85) identified for this driver versus the 0.7 value identified for Driver 6. As seen, identical transport delay values (0.10) were identified for these same two cases.

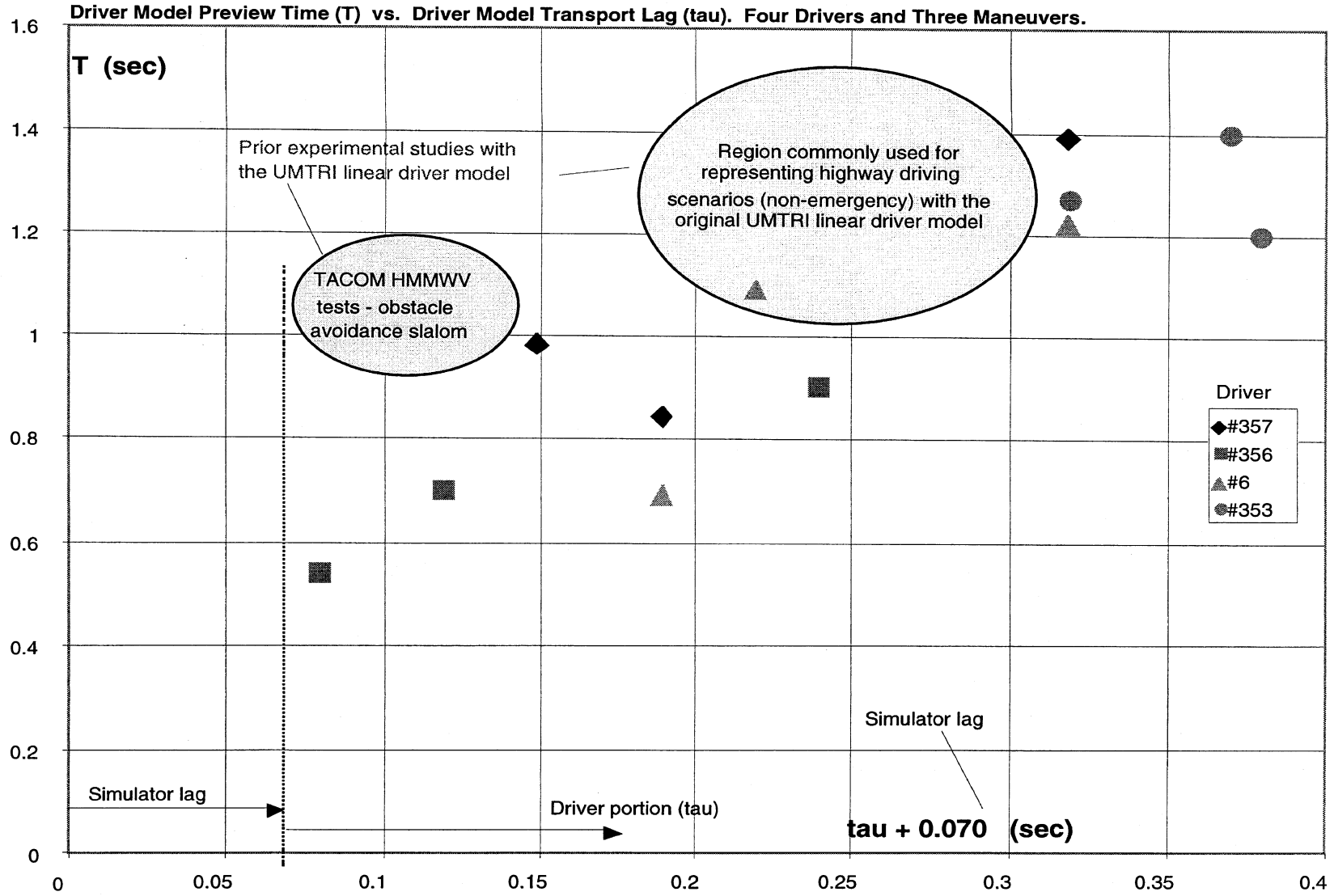

Figure 6.2-1. Drive Model Preview Parameter vs. Total Transport Delay (by Driver).

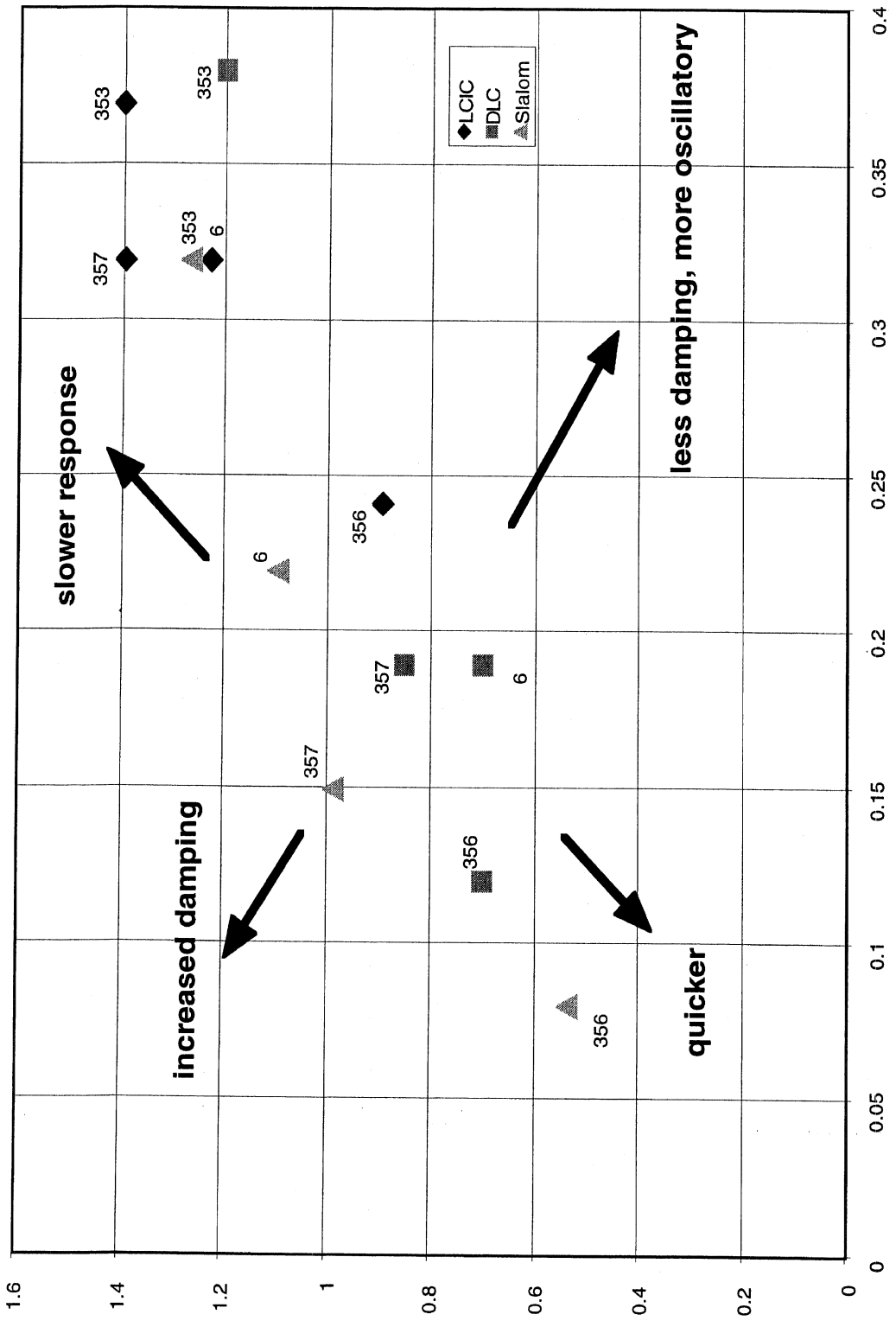

Figure 6.2-2. Drive Model Preview Parameter vs. Total Transport Delay (by Maneuver)

The remaining Slalom runs for Drivers 357 and 6 are also quite similar and were conducted at the same speed. Driver 357 displays a hint of better damping when comparing the time histories of Figures 6.1-2 and Figure 6.1-8, though the differences are quite small. The corresponding parameters appearing in Figures 6.2-1 and 6.2-2 suggest this tendency as well, though less clearly than for the aforementioned DLC case with these same two drivers. Since the overall directional damping of the closed-loop driver/vehicle system is approximately determined by lines of constant slope (upward and to the right) on this plot, it is evident that the control parameters for these two particular runs do align themselves along such an approximate line and therefore suggest only minimal differences in overall closed-loop system directional damping. The primary difference in closed-loop system behavior associated with these two parameter space locations is related to bandwidth. The parameter location for Driver 6 is closer to the origin on this plot and thereby exhibits a higher closed-loop bandwidth capability. However, the relatively low-frequency forcing function imposed by the Slalom course geometry on the closed-loop driver/vehicle system does not especially challenge the bandwidth capabilities of either driver/vehicle system, thereby explaining the nearly identical Slalom responses.

Overall, the model parameter pairs that appear in the control space of Figures 6.2-1 and 6.2-2 do not seem to suggest any particular "skill clustering" that might provide clues about possible relationships between these particular parameters and driver skill level. Though, processing of additional simulator driver data may alter this current observation.

Lastly, if the control parameters appearing in Figures 6.2-1 or 6.2-2 are fitted with a simple linear regression, the resulting graph is seen below in Figure 6.2-3. (This could be viewed as a series of independent experiments consisting of different driving maneuvers and drivers.) In any event, a linear-like trend is indicated that suggests a relationship between driver preview time and driver transport delay for these particular near-limit maneuvers. The relationship suggests that as driver transport delay increases/decreases by some amount X, that driver preview time correspondingly increases/decreases by 2.6 X in order to provide comparable closed-loop system performance in these near-limit maneuvers. For example, Drivers 356, 357, and 6 all complete the DLC and Slalom maneuvers with more or less the same level of success, though they each employ different combinations of T and τ to accomplish the same driving tasks. Driver 356 uses the least preview and delay; Driver 357 uses more of each; and Driver 6 uses about the same as Driver 357 in the DLC maneuver and more of each for the Slalom maneuver.

In addition to the linear relationship between the driver preview and transport delay, a preview threshold (or floor) also exists suggesting a minimal amount of required preview time in order to successfully complete these maneuvers, even with zero transport delays in the driver. The indicated threshold for these data is about 0.6 seconds (τ=0 in the regression of Figure 6.2-3.) The control behavior of Driver 356 pretty much defines this lower limit where near-zero transport delays are associated with preview times of about 0.6 seconds.

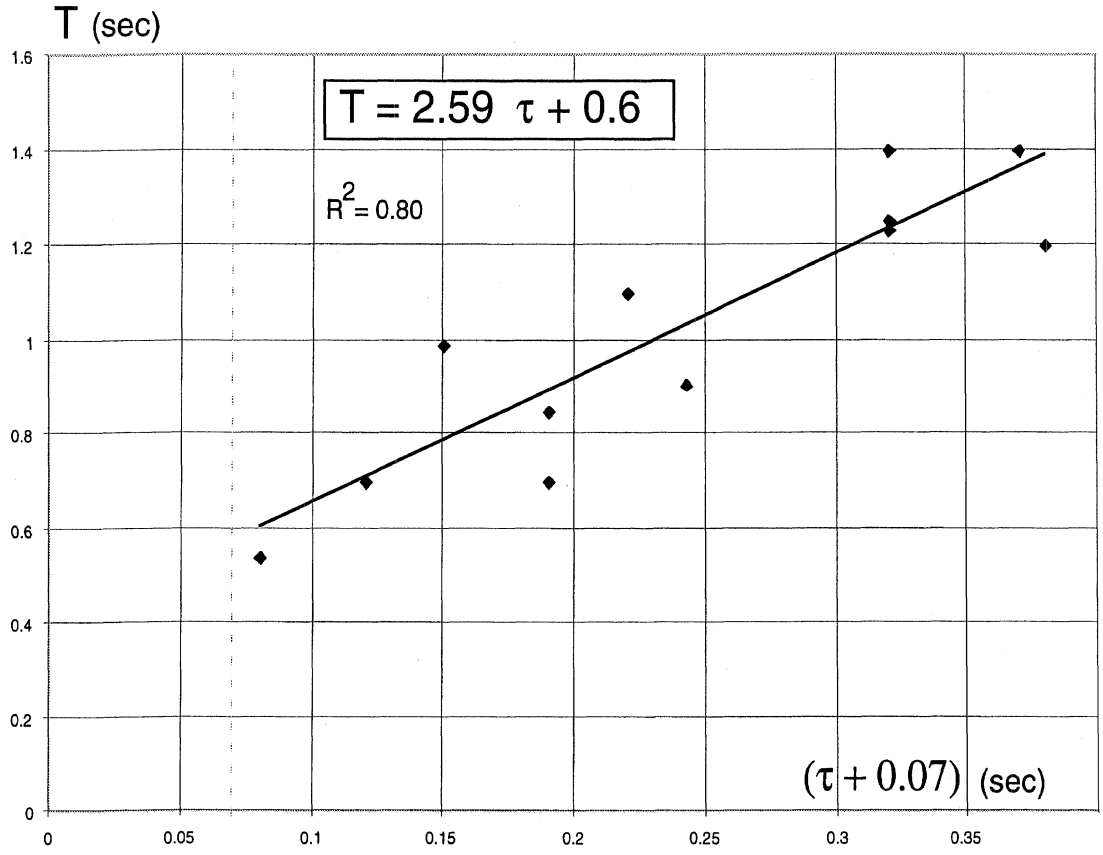

Figure 6.2-3. Driver Model Preview Parameter vs. Total Transport Delay Regression.

6.3 Discussion

The preview threshold value likely varies with the controlled vehicle's lateral acceleration capability or quickness. This vehicle property acts essentially as a low pass filter that inhibits drivers from tracking paths of higher frequencies. Slower responding vehicles impose a greater path filtering effect than do faster responding vehicles. Consequently, similar closed-loop measurements performed with vehicles having significantly different directional dynamics are likely to produce different threshold values for these same regression analyses. (i.e., a sports car may produce a threshold value more like 0.3 than the 0.6 seen value here for the pickup truck).

The linear trend line that is observed here is interesting and seems to suggest an approximate line of near-constant directional damping for the closed-loop driver/vehicle systems. Locations on the line further away from the origin are associated with lower bandwidth capabilities for path following. Locations along the line closer to the origin have higher bandwidth capabilities. Consequently, road geometries having higher frequency content that require more rapid lateral movement would most likely elicit driver control strategies that lie more toward the origin. In contrast, road geometries having smaller path curvatures would permit longer driver preview times and transport delay values to prevail, while maintaining the same relative level of closed-loop directional

damping. If such lines of *preferred damping* are indeed part of a natural closed-loop control strategy employed by drivers instinctively, then different path-following requirements can be accommodated by simple coordinated adjustment of a driver's preview time and transport delay characteristics so as to maintain an approximately constant level of closed-loop system damping. That is, a regression line similar to that seen in Figure 6.2-3 may offer a simple conceptual model that helps explain how drivers coordinate their attentiveness to control activity (as represented by the transport delay parameter) with their required preview time or look-ahead distance (as imposed by the geometry of the upcoming road scene). Shorter preview times imply more attention to control activity, and vice versa.

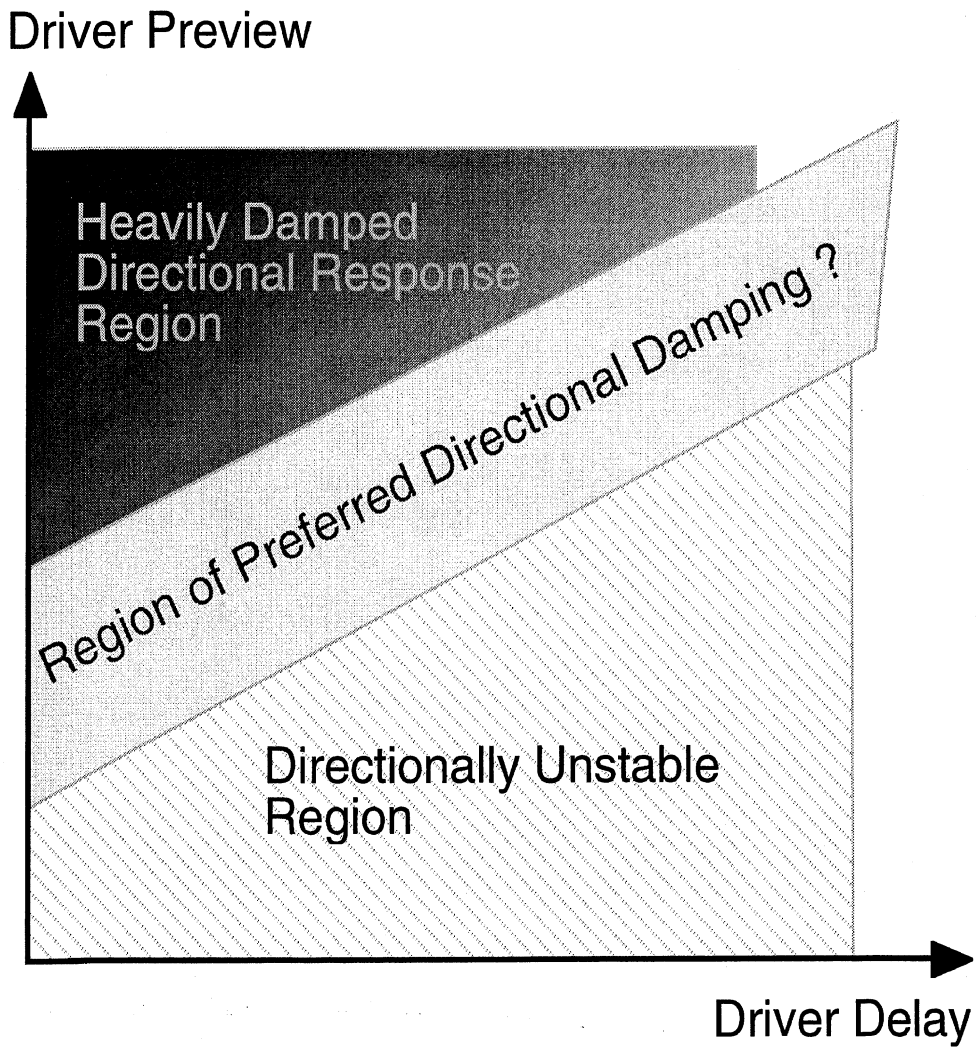

Figure 6.3-1. Possible Relationship Between Driver Preview and Transport Lags Suggested by the Model Validation of Initial Simulator Data.

These observations are of course particular to these data and associated simulator tests and may not provide more broadly applicable insight into driver steering behavior during near-limit maneuvering with actual vehicles. On the other hand they may. Further

controlled tests, particularly full-scale track tests, would be helpful in verifying and/or clarifying these initial observations that are based here only on driver responses from a limited-motion driving simulator.

7.0 Conclusions and Recommendations

A number of conclusions and recommendation can be offered based on the research conducted under this project work. The following *conclusions* are noted.

- The nonlinear GM driver steering model developed under this work significantly extends analysis and predictive capabilities well into the nonlinear/near-limit handling regime of driver/vehicle systems. Side-by-side comparisons with its linear model predecessor clearly indicate noteworthy improvements in steering responsiveness and accuracy when encountering nonlinear operating conditions and/or sudden changes in operating conditions requiring on-the-fly adaptive control behavior. Comparisons between the nonlinear GM driver model response predictions and its linear model counterpart during simulated encounters with a low friction surface and a tire blowout event illustrate many of these differences, as noted in Section 4.

- In addition to the extended nonlinear performance, the development work has also added certain new model features that include *variable driver preview*, driver *speed control* preferences based on upcoming road curvature changes, *sensory input processing* of vehicle response signals, *path selection/adjustment* options, and a simplified *situational awareness* element. [Section 3]

- Validation of the driver model against a subset of driving simulator data collected for GM by a third party has shown basic agreement with the simulator measurements. Driver model predictions for two "expert" category drivers, one "typical" category driver, and one "novice" category" driver have, for the most part, indicated very reasonable agreement. [Sections 5 and 6]

- The validation conducted under this work is really a validation of the driver model for representing a specific set of driving simulator data. It should not be necessarily assumed that agreement, or lack of agreement, within the comparisons presented in Section 6 provide a sound basis, as yet, for recommending or rejecting the developed model for predicting real world driver-vehicle interactions. Only full scale driver-vehicle measurements provided by test track experiments can unambiguously yield that level of certainty.

- A better model and understanding of driver path-selection capabilities, particularly as it relates to driver skill is needed. The relatively simple characterization within this version of the driver model allows either a smoothed version of the road centerline to be implemented or a quasi- "racing line" approximation based on a set of left and right boundary path inputs. Either case is simply a mechanism for allowing the program user to modulate the basic path input specification. However, drivers are commonly more complex and variable in their path selection strategies than that currently represented within the model and improvements to this model element would prove helpful for future usage.

- As noted in Section 5, the level of discrimination between the different driver skill levels seen in Figure 5.3-1 is not terribly large (other than for the 15-year-old driver # 360).

Nine of the twelve drivers are grouped within about 2 m/sec of each other in terms of average speed (over 64 runs per subject). In addition, less than one cone strike per run separates eleven of the twelve drivers from one another in terms of steering accuracy. Consequently, efforts to associate skill level with relatively subtle differences in the closed-loop performance of the different drivers indicated by these simulator data are presently inconclusive.

- A desired goal of this driver modeling project was to relate driver skill level to properties of the driver model and thereby help automate certain parameter settings in response to program users specifying a general driver skill category (e.g., novice, typical, or expert). Based on the simulator data and validation effort to date, the processed results are presently insufficient to declare strong associations between various model parameters and estimated levels of driver skill existing within the simulator subject pool of drivers. This is not to say that the goal is not achievable, but rather, that the existing set of data do not seem to indicate any strong relationships that can be identified. There are several possibilities for this observation. First, the range of speed differences between different driver skill groups seen in the plot of Figure 5.3-1 and noted above is quite small. In addition, small changes in vehicle trajectories can result in one or more additional cone strikes in these particular tests, thereby easily altering the skill region between drivers of different skill levels. Consequently, the simulator test data employed within this study do not appear to produce highly discriminatory time history responses and path trajectories for drivers of different skill levels. This observation may be a result of examining too small a sample of data, or a deficiency in the selected tests themselves, or a byproduct of the artificial and safe simulator environment that produces more uniform responses relative to what happens in a more realistic, full-motion, on-road driving environment.

- Finally, it is noted that the new GM driver model adds a number of new features that significantly broaden the capabilities for representing driver steering behavior. These capabilities include such items as variable preview, speed control, and path selection behavior. Many of these need to be evaluated through future usage and comparison with appropriate test data. Their presence in the model though does now allow computer-based investigations into the potential influence of these capabilities/behavior on closed-loop driving performance.

Accompanying *recommendations* for future follow-on research by GM aimed at enhancing and further validating the developed driver model are also offered here (in descending order of likely importance).

- Additional full-scale test track experiments conducted by GM itself (or an equivalent independent third party) are recommended in order to conduct a "real world" validation of the developed model. This effort would hopefully mirror many of the same test procedures conducted in the simulator tests, subject of course to practical limitations present in a test track environment. Measurements from these tests would provide a source of reliable, driver/vehicle response data that includes all genuine vehicle motion and visual

experiences normally present to any driver in an actual driving environment. The new measurements would provide a source of high quality or benchmark data against which the existing simulator data and the GM driver model could be more properly evaluated.

- Subsequent processing of these recommended full-scale test track data should be conducted similarly to the procedures used for the simulator data in this project. A direct comparison can then be made against the simulator data analyses conducted under this work in order to verify and substantiate findings and observations noted in this report. Depending on the outcome of that comparison, the existing database of simulator data should be either re-emphasized or de-emphasized in future GM analyses and driver model enhancement efforts.

- Consideration should be given to acquiring use of an eye mark recorder device (or comparable instrument) for use in a subset of future driver/vehicle tests in order to measure *where* and *how* drivers look during the course of different driving scenarios, particularly in obstacle avoidance or sudden emergency maneuvering conditions. These data would also help considerably in refining and improving the initial simplified model of variable preview behavior currently implemented under this project work.

- A subset of human factors research aimed at better understanding how drivers allocate and share control task activities during different types of demanding path-following or obstacle avoidance maneuvering is recommended. Results from this type of research could help GM better understand possible internal control strategies employed by drivers for attention allocation/de-allocation during path-following tasks of varying difficulty. The discussion of Section 6.3 speculates on this issue in the limited context of driver preview and transport delay allocation. Experiments conducted with paths of varying curvature and associated control requirements could be designed to gather a broad range of driver/vehicle response data. These resulting data could then be processed similarly to those in Section 6 in order to obtain relationships between driver preview utilization and upcoming road geometry, and, corresponding relationships between driver preview utilization and driver transport delay characteristics. The findings from this analysis could, in turn, provide a basic model for representing continuous adjustment of driver preview and transport delays as a function of upcoming road geometry characteristics within the current GM driver model.

- A similar set of experiments could be conducted for upcoming curve encounters to help identify experimentally-based parameter settings for the driver model's speed control feature.

- Research focused on path selection behavior by drivers is also recommended . As noted above and in Figures 5.4-1 and 5.4-2 where sequential test repeats show considerable trajectory and steering scatter, a better understanding of the mechanisms by which drivers select paths around obstacles and through curved road segments would prove useful for future model enhancements. A range of driver skill levels should be a major component of the test matrix.

- Inclusion of a provision for a variable driver transport delay is recommended as a future model enhancement. The notion of 'preferred closed-loop damping' by drivers, as possibly suggested by the validation calculations in Section 6, underpins this recommendation. If activated, this feature would obtain driver transport delay values from a simple regression rule like that seen in Figure 6.2-3, based on the current preview time being utilized during the course of a maneuver. This, of course, requires the variable preview element to also be active and obtaining, in turn, its continuous values from the current upcoming road geometry (as currently implemented). This feature would therefore enable a coordinated and simultaneous scaling of the transport delay parameter with variations occurring in the driver preview time parameter, thereby better mimicking the hypothetical 'preferred damping' control behavior of drivers.

- Lastly, research on quantifying driver steering variability during both repeated and unexpected steering maneuvers (at identical speeds) could help to quantify and represent such variances in the driver model. Driver skill level should be a principal test component. The resulting data could provide useful information regarding stochastic or random-like components of driver steering responses, helping to better characterize common "wobbles" or remnant noise present in driver steering waveforms and any associations with driver skill. It is not often clear what percentage of observed differences between test measurements from the same driver, or between different drivers, is attributable to random-like behavior and what percentage is attributable to intentional control inputs provoked by a slightly different operating state.

References

1. MacAdam, C. C. (1980). "An Optimal Preview Control For Linear Systems," *Journal of Dynamic Systems, Measurement, and Control, Trans ASME,* vol. 102, pp. 188-190.

2. MacAdam, C. (1981). "Application of an Optimal Preview Control for Simulation of Closed-Loop Automobile Driving," *IEEE Transactions on Systems, Man, and Cybernetics,* vol. SMC-11.

3. MacAdam, C. C. (1988). Development of Driver/Vehicle Steering Interaction Models for Dynamic Analysis. Technical Rept. (Final), UMTRI-8853, Michigan Univ. Ann Arbor, Transportation Research Inst. Sponsor: U.S. Army Tank-Automotive Research and Development Command, Warren MI.

4. Macadam, C. C., et al. (1990). "Crosswind Sensitivity of Passenger Cars and the Influence of Chassis and Aerodynamic Properties on Driver Preferences," *Vehicle System Dynamics,* vol. 19, pp. 201-236.

5. McRuer, D. T., et al. (1968). "New Approaches to Human-Pilot/Vehicle Dynamic Analysis." Tech. Report AFFDL-TR-67-150, WPAFB.

6. Weir, D., DiMarco, R. J., and McRuer, D. T. (1977). "Evaluation and Correlation of Driver/Vehicle Data, Vol II." Final Technical Report, NHTSA, DOT-HS-803-246.

7. McRuer, D. T., Allen, R. W., and Klein, R. H. (1977). "New Results in Driver Steering Control Models." *Human Factors*, 19, 4. pp 381-397.

8 MacAdam, C. C. , (1985). "Computer Model Predictions of the Directional Response and Stability of Driver Vehicle Systems During Anti-Skid Braking." *Proceedings of the IMech E Conference on Antilock Braking Systems for Road Vehicles*, Ed. P. Newcomb. London, U.K., IMech E.

9. MacAdam, C. C., and Fancher, P. S. (1985). "A Study of the Closed-Loop Directional Stability of Various Commercial Vehicle Configurations." *Proceedings of the 9th IAVSD Symposium of the Dynamics of Vehicles on Roads and Tracks*, Ed. O. Nordstrom. Linkoping, Sweden, Swets & Zeitlinger B.V. - Lisse.